GENETIC AND GENOMIC ANALYSES OF KERNEL DEVELOPMENT IN *ZEA MAYS*

A Dissertation

Presented to the Faculty of the Graduate School

of Cornell University

in Partial Fulfillment of the Requirements for the Degree of

Doctor of Philosophy

by

Elizabeth Mary Takacs

January 2012

GENETIC AND GENOMIC ANALYSES OF KERNEL DEVELOPMENT IN *ZEA MAYS*

Elizabeth Mary Takacs, Ph.D.

Cornell University 2012

Two different aspects of maize kernel development are investigated. First, transcriptomic analyses of the landmark stages in embryo development were performed using laser microdissection and RNA-sequencing to investigate the ontogeny of shoot apical meristem (SAM). The SAM gives rise to all above ground vegetative tissues and forms during embryogenesis. To date this is the first study conducted to survey the maize SAM transcriptome when it forms during embryo development. Transcriptomic analyses of a developing embryo before a SAM forms, after a SAM is established, and when the SAM is initiating a foliar leaf reveals the following: (1) how a meristem is formed; (2) how a newly formed meristem differs from a mature meristem that is initiating foliar leaves; (3) the differences between the first three lateral organs (the scutellum, the coleoptile, and foliar leaf) elaborated during embryogenesis; (4) what distinguishes initiation of juvenile from an adult leaf; and (5) the differences between the SAM initiating a foliar leaf and a lateral meristem initiating a husk leaf. Second, embryo and endosperm development is investigated using the *defective kernel* mutant *discolored1* (*dsc1*). Detailed phenotypic analyses of *dsc1* mutant kernels reveal that *DSC1* encodes a protein that is required to maintain the differentiation of both the embryo and the endosperm during kernel development. The *DSC1* gene encodes an ADP-RIBOSYLATION FACTOR-GTPASE ACTIVATING PROTEIN (ARF-GAP) that co-localizes with the *trans*-Golgi network/early endosomes and the plasma membrane in

transient expression assays in *N. benthamiana* leaves. DSC1 functions in endomembrane trafficking and the cargo that it transports is required for maintaining differentiated embryo and endosperm structures during kernel development.

BIOGRAPHICAL SKETCH

Elizabeth Mary Takacs was born in Santa Clara, California, in 1979, to William S. and Martha E. Takacs. She has two brothers (Bill and Matt) and one sister (Katie). Elizabeth graduated from Mountain Pointe High School in Phoenix, Arizona, in 1998. Following high school she attended the University of Arizona in Tucson, Arizona, and in 2002, earned a Bachelor's of Science in Molecular and Cellular Biology. In the fall of 2002, Elizabeth accepted a position as a research assistant in Dr. David Stern's laboratory at the Boyce Thompson Institute for Plant Research. She started graduate school in the fall of 2005, where she began her doctoral research on maize kernel development in Dr. Michael Scanlon's laboratory at Cornell University.

To my parents and Steve

ACKNOWLEDGEMENTS

First, I would like to thank Dr. Michael J. Scanlon for being my doctoral research advisor and mentor. I am entirely grateful for all that he has taught me regarding maize developmental biology. He gave me the opportunity to research two very different and exciting projects pertaining to kernel development. Thank you to my advisory committee members, Dr. David B. Stern and Dr. Jian Hua, for providing me with guidance, giving me insightful commentary, and supporting my research endeavors.

In addition, thank you Dr. Marja Timmermans, Dr. Gary Muelbaur, Dr. Jianming Yu, Dr. Patrick Schnable, and Dr. Diane Janick-Buckner for serving as my “unofficial committee” overseeing the maize shoot apical meristem (SAM) project. I appreciate your support and discussions regarding my project on the ontogeny of the SAM. I would like to thank our other collaborators on both the ontogeny of the SAM and the *DISCOLORED1* projects including: Dan Nettleton (Iowa State University), Jie Li (Iowa State University), Qi Sun (Cornell University), Lalit Ponnala (Cornell University), Masaharu Suzuki (University of Florida), and Robert Meeley (Pioneer Hi-bred International). Next, thank you to my lab mates for your support and help in the lab. I would like to thank the National Science Foundation and Cornell University for funding this research.

Lastly, I would like to thank my parents, Bill and Martha; Steve; my siblings, Bill, Matt, and Katie; my extended family; and my friends for giving me unconditional love and support in my educational endeavors.

TABLE OF CONTENTS

LIST OF FIGURES

LIST OF FIGURES

LIST OF TABLES

PREFACE

Collaborators contributed to the work presented in Chapter Two and Chapter Three. In Chapter Two, Ontogeny of the Shoot Apical Meristem, cDNA libraries were constructed and Illumina RNA-sequencing was performed at the Cornell University Life Sciences Core Laboratories Center. Alignment and quantification of RNA-seq reads was performed by Lalit Ponnala and Qi Sun at the Cornell Biology Service Unit, and Jie Li and Dan Nettleton at Iowa State University performed statistical analysis of the RNA-sequencing data, which included quantification of transcript accumulation, normalization of the biological replications, and pairwise and six-way comparisons of the samples to determine P values, q values, and fold-changes. Marja Timmermans (Cold Spring Harbor Laboratory), Gary Muehlbauer (University of Minnesota), Patrick Schnable (Iowa State University), Jiaming Yu (Kansas State University), and Diane Janick-Buckner (Truman State University) contributed to discussions regarding experimental design, data analysis, data presentation, and manuscript revisions. In Chapter Three, DISCOLORED1 (DSC1) is an ADP-RIBOSYLATION FACTOR-GTPase ACTIVATING PROTEIN (ARF-GAP) required to maintain differentiation of maize kernel structures, Masaharu Suzuki (University of Florida) identified the full length *DSC1* transcript and Robert Meeley (Pioneer Hi-Bred International, Inc) provided three additional *dsc1* mutant alleles. All remaining experiments were performed by myself.

CHAPTER 1

INTRODUCTION

Introduction

Maize is an important agronomic crop mostly due to the abundant endosperm found within the kernel (i.e., the caryopsis). At maturity, the kernel consists of the diploid embryo and the triploid endosperm surrounded by the pericarp, or the ovary wall, fused to the seed coat (Figure 1.1a, b). Angiosperm development of the kernel begins following double fertilization, when two identical generative sperm nuclei are released into the female gametophyte through the pollen tube. The nucleus of one sperm cell fuses with the nucleus in the egg cell producing the zygote that will develop into the embryo. The mature maize embryo comprises all of the structures that will give rise to the seedling, including the root and shoot apical meristem, the scutellum, the coleoptile, the coleorhiza, and up to six leaf primordia (Figure 1.1a, b; Abbe and Stein, 1954). The other sperm cell nucleus fuses with the two polar nuclei of the central cell forming a triploid nucleus that will ultimately give rise to four distinct endosperm structures: the aleurone; the starchy endosperm; the basal endosperm transfer layer (BETL); and the embryo surrounding region (ESR). Constituting the bulk of the seed (~85%), the maize endosperm is a highly specialized nutritive structure. The embryo and the endosperm are genetically identical except for ploidy level. The embryo has a one to one maternal to paternal ratio, whereas the endosperm has a two to one maternal to paternal ratio. Seed abortion can result if the two to one maternal to paternal genomic ratio during endosperm development is not maintained or established at fertilization (reviewed in Raghavan, 2003). Although the endosperm and the embryo are clonally distinct, seed development and germination rely on the interaction between these two compartments.

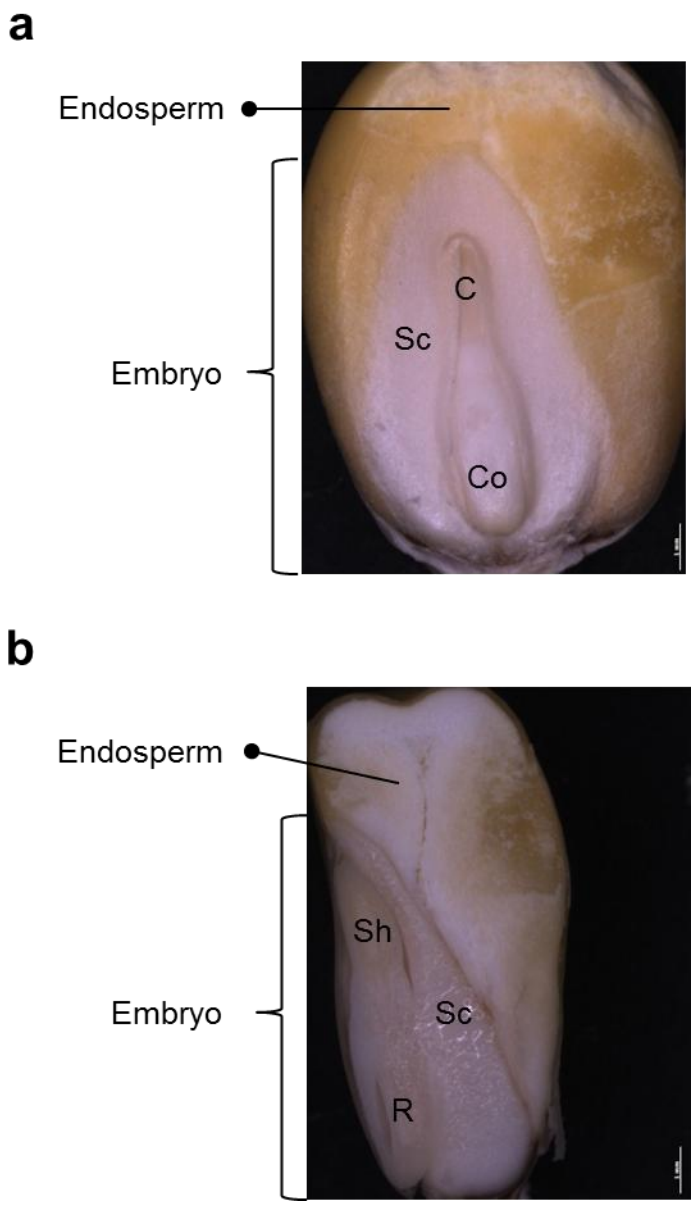

Figure 1.1 The mature maize kernel.

(a) Frontal view of a kernel with the pericarp removed.
(b) Sagittal view of a kernel cut in half.

C, coleoptile; Co, coleorhiza; R, root; Sc, scutellum; Sh, shoot.

Embryo development

Maize embryogenesis does not proceed with a stereotypical pattern of cell division. However, clonal sector analysis of cells from distinct regions of the maize embryo illustrates that cell fate is predictable (Poethig *et al.,* 1986). Development of the maize embryo is divided into distinct stages using morphological and transcriptional markers and is described in detail below (Abbe and Stein, 1954).

Defining the apical-basal axis

Polarity is established following the first zygotic division, which is asymmetric and transverse, creating a small apical cell and a large basal cell (Randolph, 1936). Subsequent divisions of the apical cell will produce cytoplasmically dense cells composing the embryo proper, whereas subsequent divisions of the basal cell will produce the highly vacuolated cells of the suspensor. Together the embryo proper and the suspensor form the radially symmetric proembryo (Figure 1.2a, b; Abbe and Stein, 1954). The proembryo stage occurs before formation of the shoot apical meristem (SAM). However, clonal sector analysis reveals that the SAM will arise from the progeny of only one of the two cells formed from the first longitudinal division of the apical cell (Poethig *et al.,* 1986). Furthermore, cell lineages giving rise to the SAM and the first lateral organ initiated during embryogenesis (the scutellum) are not delineated until after at least two longitudinal apical cell divisions have taken place (Poethig *et al.,* 1986).

Transcriptional markers that define the apical and basal regions of the maize proembryo specify regions of the proembryo that will ultimately give rise to the shoot, the root, and the epidermis. Transcripts of two members of the *WUSCHEL-RELATED*

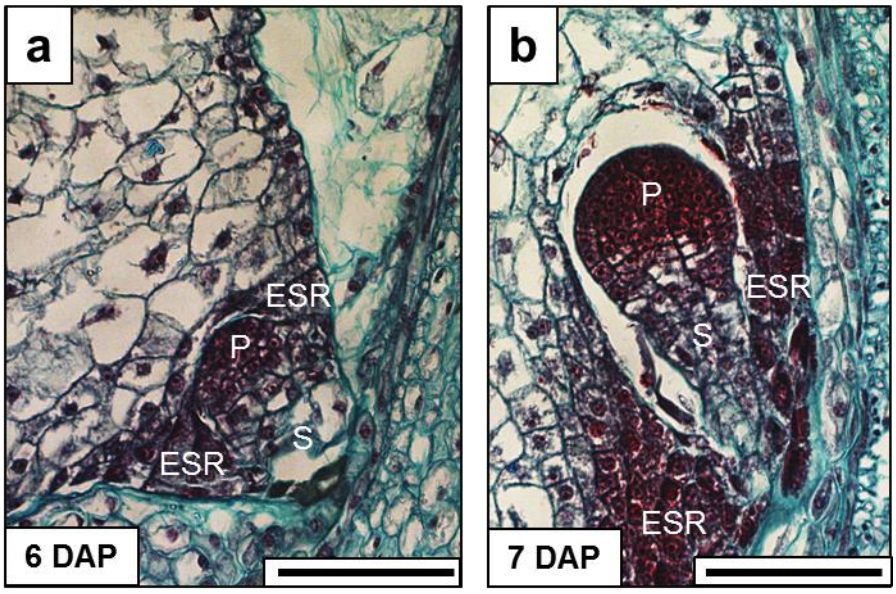

Figure 1.2 The proembryo.

The proembryo harvested at (a) 6 DAP and (b) 7 DAP is comprised of an apical embryo proper and a basal suspensor.

DAP, days after pollination; P, embryo proper; S, suspensor; ESR, embryo surrounding region.
Scale bars represent 100 μm.

HOMEOBOX (*WOX*) transcription factor gene family (*WOX2A* and *WOX5B*) accumulate in the apical domain of the proembryo (Nardmann *et al.,* 2007). Here, *WOX2A* transcripts detected on the germinal face of the embryo proper specify where the meristem will form, whereas *WOX5B* transcripts accumulate centrally at the base of the embryo proper where the root will form (Nardmann *et al.,* 2007). The GRAS (GIBBERELLIN-INSENSITIVE (GAI), REPRESSOR of GA1-3 (RGA), and SCARECROW (SCR)) transcription factor *Zea mays SCR* is another marker that eventually specifies root structures. Accumulation of *ZmSCR* transcripts is observed in the embryo proper (Lim *et al.,* 2005). Transcripts that will specify the epidermis at later stages of development include four members of the *HOMEODOMAIN LEUCINE-ZIPPER IV* (*HD-ZIP IV*) gene family (*Zea mays OUTER CELL LAYER1* (*OCL1)*, *OCL3*, *OCL4*, and *OCL5;* Ingram *et al.,* 1999; Ingram *et al.,* 2000; Javelle *et al.,* 2011). Both *OCL4* and *OCL5* transcripts accumulate in the protoderm (the outermost cell layer) forming a cap over the embryo proper (Ingram *et al.,* 2000; Javelle *et al.,* 2011). In contrast, *OCL3* transcripts accumulate in the suspensor (Ingram *et al.,* 1999; Ingram *et al.,* 2000; Javelle *et al.,* 2011). Interestingly, the transcript accumulation pattern of *OCL1* overlaps with both *OCL4* and *OCL5* in the protoderm and with *OCL3* in the suspensor (Ingram *et al.,* 1999; Javelle *et al.,* 2011). An additional protoderm marker is *LIPID TRANSFER PROTEIN2* (*LTP2*), which has a similar transcript accumulation pattern as *OCL1, OCL4,* and *OCL5* in the protoderm of the embryo proper (Ingram *et al.,* 1999; Javelle *et al.,* 2011).

Establishing the shoot apical meristem

The next stage in embryo development, the transition stage, marks the formation

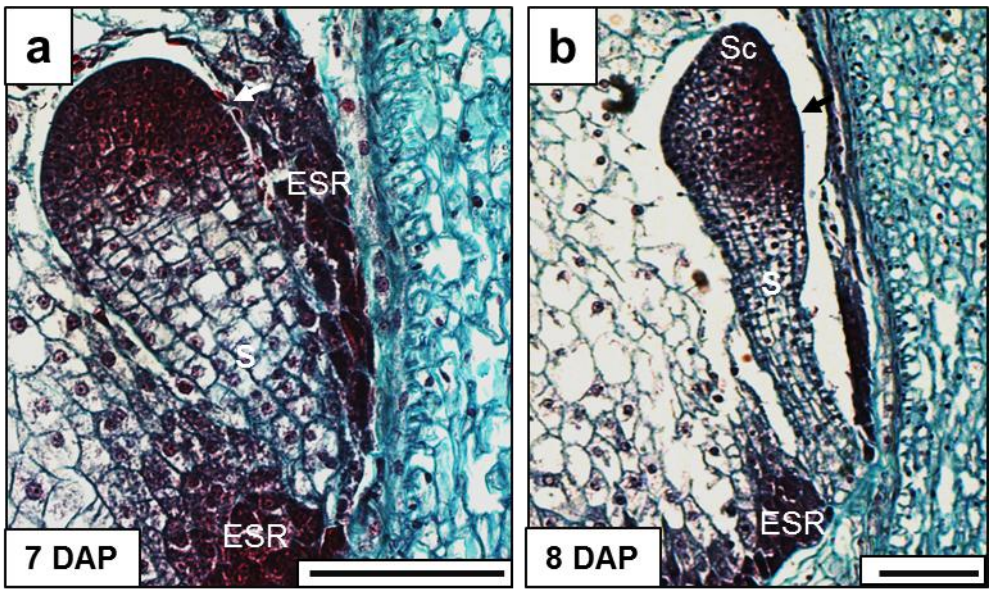

Figure 1.3 The transition stage embryo.

(a) At 7 DAP the cells located on the abgerminal face of the embryo begin to elongate, whereas cells at the site of meristem formation are proliferating and cytoplasmically dense.
(b) At 8 DAP the prominent hood of the scutellum can be detected.

DAP, days after pollination, Sc, scutellum; S, suspensor; ESR, embryo surrounding region. Arrows point to the shoot apical meristem.
Scale bars represent 100 μm.

of the SAM (Figure 1.3a, b). The SAM is responsible for making all of the above ground vegetative tissues of the plant. It has two functions: (1) to maintain a population of stem cells; and (2) to initiate lateral organs. The SAM is composed of two clonally distinct stratified cell layers: the tunica; and the corpus. Additionally in the maize SAM, stem cell maintenance occurs in the central zone, whereas stem cells are recruited for organogenesis in the peripheral zone. Forming on the lateral face of the transition-staged embryo, ~150 cells comprise the SAM and are organized into longitudinal files that are at least two layers deep (Poethig *et al.,* 1986). Also during the transition stage, the first lateral organ elaborated during embryo development (the scutellum) begins to emerge from the abgerminal side of the embryonic axis. The spade-shaped scutellum is unique to the grasses and has a controversial homology. It first serves to accumulate and store energy reserves during embryogenesis and later assumes a digestive function to nurture the germinating seedling. As the SAM forms and the prominent hood of the scutellum emerges from the embryonic axis, the transition stage embryo obtains bilateral symmetry (Abbe and Stein, 1954).

Accompanying the formation of the SAM and elaboration of the scutellum is the accumulation of gene transcripts associated with meristem maintenance and lateral organ boundary formation. The *CLASS I KNOTTED1-LIKE HOMEOBOX* (*KNOX*) transcription factor *KNOTTED1* (*KN1*) is expressed where stem cells are being replenished, but is absent from anlagen and lateral organ primordia (Smith *et al.,* 1992; Jackson *et al.,* 1994). Furthermore, transcript accumulation of *KN1* correlates with the position of the longitudinal cell files that form on the lateral face of the transition-staged embryo (Smith *et al.,* 1995). Transcripts of two members of the *NO APICAL*

MERISTEM/*CUP-SHAPED COTYLEDON* (*NAC*) gene families (*Zea mays NO APICAL MERISTEM1* (*ZmNAM1*) and *Zea mays CUP-SHAPED COTYLEDON3* (*ZmCUC3*)) also accumulate in cells on the lateral face of transition stage embryos (Zimmermann and Werr, 2005).

Transcripts that define the apical and basal regions during the proembryo stage acquire different accumulation patterns at the transition stage. For example, *WOX2A* transcripts accumulate in only a few cells at the periphery of the newly formed meristem (Nardmann *et al.,* 2007). Accumulation patterns of *OCL4* and *OCL5* transcripts shift from encasing the entire embryo proper to concentrating at either the germinal or abgerminal face of the embryo, respectively (Ingram *et al.,* 2000; Javelle *et al.,* 2011). Finally, *LTP2* transcripts accumulate in the outer cell layer of the prominent scutellar hood but not the tunica of the SAM (Ingram *et al.,* 1999; Javelle *et al.,* 2011).

In addition to markers for the SAM and lateral organs, transcripts that serve as markers for the root and coleorhiza (a sheath that surrounds the root) accumulate in the basal region of the transition stage embryo. For example, the quiescent center (progenitor of root stem cells) is marked by *WOX5B* transcripts, which again accumulate in the basal region of the embryo (Nardmann *et al.,* 2007). At this stage, *ZmSCR* transcripts accumulate in a “U”-shaped cell file that overlaps with *WOX5B* transcripts at the base of the “U” (Zimmermann and Werr, 2005; Lim *et al.,* 2005). Another *NAC* gene, *Zea mays NO APICAL MERISTEM6* (*ZmNAC6*), is expressed in the basal region of the embryo below the domains defined by *WOX5B* and *ZmSCR*, but above the suspensor (Zimmermann and Werr, 2005).

Controversy surrounding the maize cotyledon

Figure 1.4 The coleoptile stage embryo.

The coleoptile is initiated from the embryonic axis on the same side as the scutellum.

DAP, days after pollination; C, coleoptile; Sc, scutellum; S, suspensor. The arrow points to the shoot apical meristem.
Scale bars represent 100 µm.

Initiation of the coleoptile, a bi-keeled leaf-like organ, marks the next stage of embryo development (Figure 1.4). The coleoptile is initiated from the abgerminal side of the shoot axis, the same side of the embryo as the scutellum, and eventually forms a connected sheath over initiated leaf primordia and the SAM. During germination, the coleoptile functions to protect the leaf structures when the shoot extends above the ground through the soil. Controversy surrounds the homology of the first two organs initiated during embryogenesis; the scutellum, and the coleoptile. Three models that describe the controversial homology of these two organs include the following: (1) the coleoptile is the cotyledon and the scutellum is a novelty (Boyd, 1931); (2) the scutellum is the cotyledon and the coleoptile is a foliar leaf (Weatherwax, 1920); and (3) the scutellum and the coleoptile comprise a single cotyledon wherein the scutellum is homologous to a distal leaf blade and the coleoptile is a proximal leaf sheath (Kaplan, 1996).

At the coleoptile stage *KN1* transcripts accumulate in the meristem but not in the initiating coleoptile. During this stage, the accumulation patterns of *ZmNAM1* and *ZmCUC3* transcripts are confined to cells above and below the SAM defining the boundary between the initiating coleoptile and the meristem (Zimmermann and Werr, 2005). Both *OCL4* and *OCL5* transcripts accumulate in the outer cell layer encompassing the entire apical region of the embryo (Ingram *et al.,* 2000; Javelle *et al.,* 2011). In addition to the outer cell layer of the embryo, *OCL1* transcripts also accumulate in a single file that defines the root epidermis (Ingram *et al.,* 1999; Javelle *et al.,* 2011). At the coleoptile stage, *OCL3* transcripts accumulate in the suspensor and in a few cells at the tip of the scutellum (Ingram *et al.,* 2000; Javelle *et al.,* 2011). No

WOX2A transcripts accumulate in the maize embryo at the coleoptile stage (Nardmann *et al.,* 2007). However, transcripts of three additional *WOX* family members (*WOX3A*, *NARROW SHEATH1*, and *NARROW SHEATH2*) accumulate at the tip of the coleoptile (Nardmann *et al.,* 2007; Nardmann *et al.,* 2004).

Foliar leaf initiation marks the end of embryo development

The SAM initiates five to six foliar leaves in the final landmark stages (L1-L6) of embryogenesis. The first leaf is initiated 180° opposite of the coleoptile; each subsequent leaf is initiated following an alternate phyllotactic pattern (Figure 1.5a-b; Abbe and Stein, 1954). The suspensor undergoes programmed cell death, disappearing by stage L3 (Abbe and Stein, 1954). Also at stage L3, the primary root (radicle) becomes apparent (Abbe and Stein, 1954). A fully developed embryo consists of the shoot and root apical meristems, the scutellum, the coleorhiza, the coleoptile, the radicle, and five to six leaf primordia (Abbe and Stein, 1954). Lateral organ initiation ceases prior to quiescence but will resume upon germination.

Molecular markers for the shoot, root, and coleorhiza present during foliar leaf initiation (L1 stage-L6 stage) include *KN1, WOX5B,* and *ZmSCR*. From the L1 to the L6 stage, *KN1* transcripts accumulate along the root shoot axis but not at sites of leaf initiation or in the quiescent center. Both *WOX5B* and *ZmSCR* have a similar transcript accumulation pattern as in the transition stage embryo. Transcripts of two additional members of the *WOX* gene family (*WOX4* and *WOX5A*) accumulate in the basal region of the embryo. *WOX4* transcripts accumulate in the hypocotyl region, whereas *WOX5A* transcripts accumulate in the suspensor below the root quiescent center (Nardmann *et al.,* 2007).

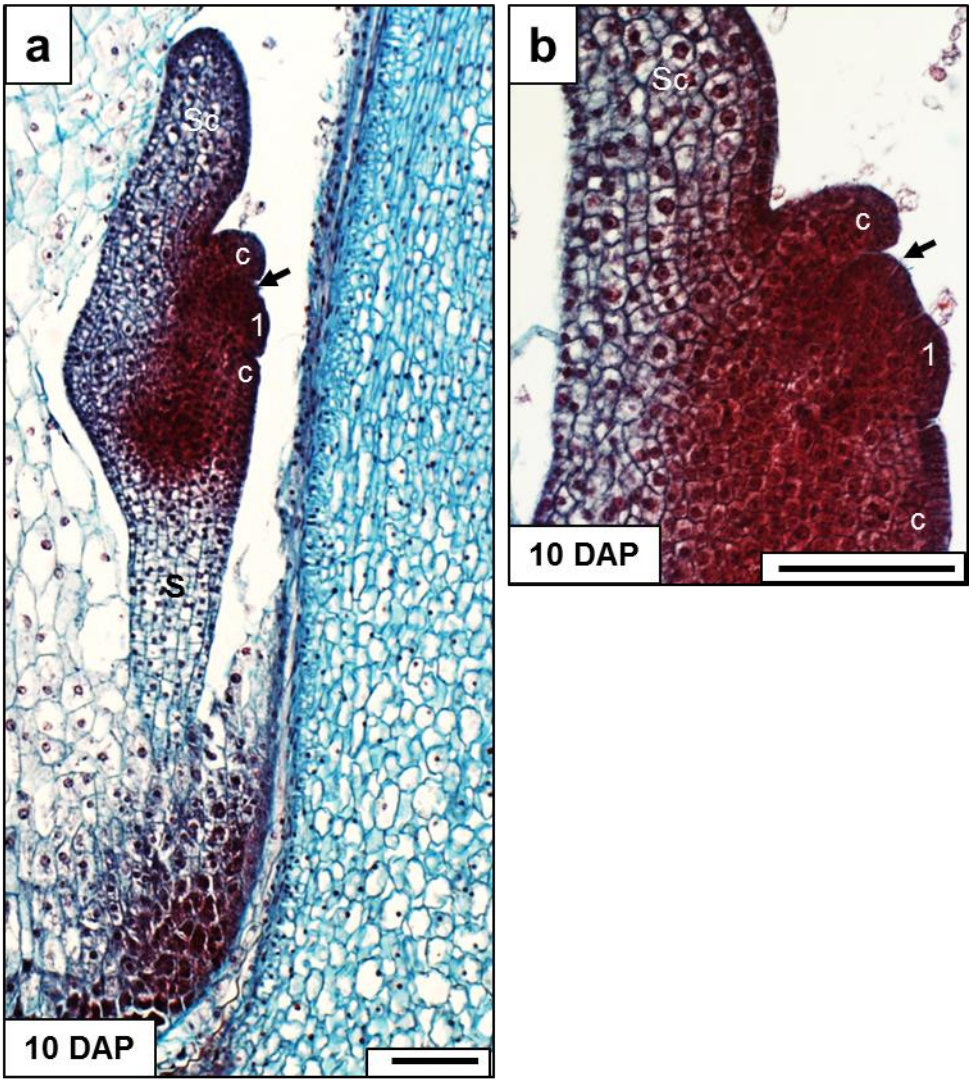

Figure 1.5 The L1 stage embryo.

(a-b) The first foliar leaf is initiated opposite of the coleoptile on the germinal face of the embryo. The embryo in (b) is magnified from (a).

DAP, days after pollination, C, coleoptile; 1, first foliar leaf; Sc, scutellum; S, suspensor. Arrows point to the shoot apical meristem.
Scale bars represent 100 µm.

Endosperm development

The maize endosperm undergoes a unique cellularization process within 72 hours of fertilization; whereupon completion the differentiation of the four endosperm structures (the ESR, the BETL, the starchy endosperm, and the aleurone) becomes apparent and/or ensues. In plants, cell fate is determined by positional cues and not cell lineage (reviewed in Szymkowiak and Sussex, 1996; Becraft and Asuncion-Crabb, 2000; Gruis *et al.,* 2006). Clonal analysis illustrates that the right and left halves of the endosperm are determined after the first mitotic division of the triploid central cell, which suggests that positional cues may originate from the embryo sac prior to the completion of endosperm cellularization (McClintock, 1978). Interestingly, the four endosperm structures do not differentiate at the same time. Differentiation of the ESR and the BETL occurs earlier than differentiation of the starchy endosperm and the aleurone cell layer. Furthermore, aleurone and starchy endosperm cells have a reversible cell fate (Becraft and Asuncion-Crabb, 2000). Following a description of endosperm cellularization, each of the four endosperm structures is discussed in detail below.

Endosperm cellularization is unique

The unique cellularization of the maize endosperm is complete by four days after pollination (DAP). First, the triploid nucleus of the central cell undergoes several rounds of mitotic divisions without cytokinesis forming a single cell with 256-512 nuclei (the syncytium; reviewed in Olsen, 2001). After mitosis ceases, a radial microtubular system extends out of the nuclear envelope defining a nucleo-cytoplasmic domain for each nucleus. Phragmoplasts form between these nucleo-cytoplasmic domains and deposit anticlinal cell walls. Next, microtubular arrays extend toward the central vacuole,

surrounding each nucleus forming an alveolus (tube-like wall structure). The alveolar nuclei undergo periclinal mitotic cell divisions depositing a cell wall between daughter cells resulting in two layers: (1) a complete outer cell layer encompassed by cell walls; and (2) an incomplete cell layer with alveoli open toward the central vacuole. Periclinal cell divisions continue in this centripetal fashion giving rise to cell files that will invade the central vacuole completing endosperm cellularization (reviewed in Olsen, 2001).

The basal endosperm transfer cell layer

The basal endosperm transfer cell layer (BETL) is a modified epithelium that forms over the vasculature of the maternal chalazal zone (Figure 1.6a, b; Brink and Cooper, 1947; Kiesselbach and Walker, 1952). BETL cells contain a well-developed endomembrane system and have secondary cell wall ingrowths (Thompson, 2001). Cell wall ingrowths extend the surface area of the plasma membrane increasing the ability of BETL cells to facilitate transport of solutes (sucrose, amino acids, and monosacharides) from the symplasm of maternal placenta into the developing endosperm (Brink and Cooper, 1947; Kiesselbach and Walker, 1952; Thompson, 2001). Transcript accumulation of *ENDOSPERM1* (*END1*) in the basal region of the syncytium suggests BETL cell fate specification occurs at this early stage of endosperm development (Gruis *et al.,* 2006). Differentiation of the BETL is complete by 16 DAP (Gao *et al.,* 1998).

Transcripts that accumulate in the BETL function in transport, transcriptional regulation, and plant defense against infection during kernel development. Two transcripts that accumulate in the BETL and function in the uptake of solutes from the pedicel into the endosperm include *CELL WALL INVERTASE1* (*INCW1*) and

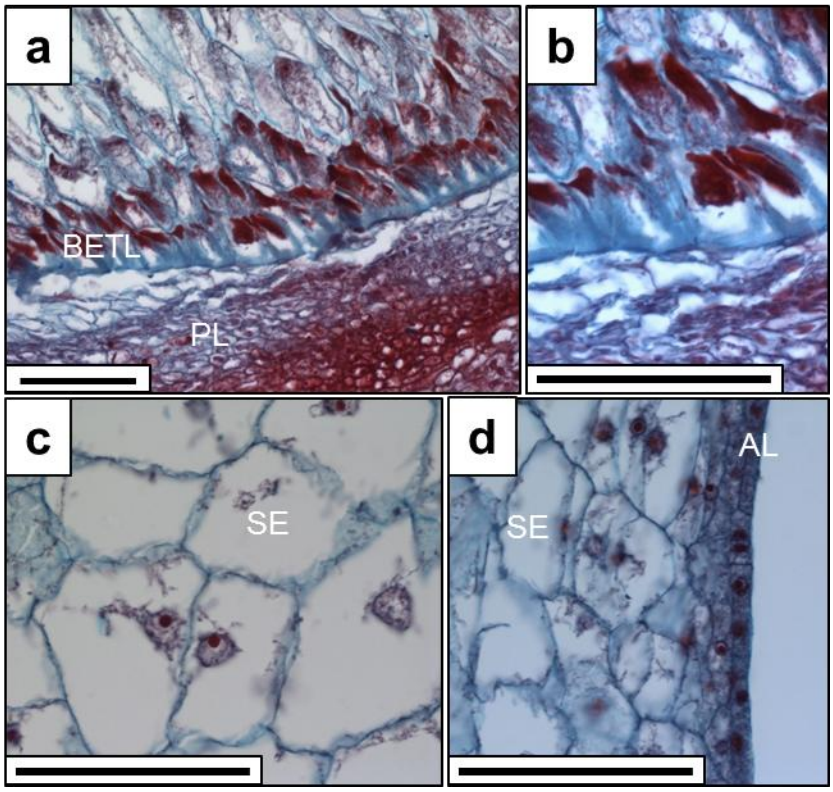

Figure 1.6 Endosperm structures.

(a-b) BETL cells have extensive cell wall ingrowths. (c) Starchy endosperm cells are large and vacuolated. (d) The aleurone cell layer forms at the periphery of the endosperm and stains more deeply than starchy endosperm cells. The cell layers between the starchy endopserm and the aleurone the sub-aleurone.

BETL, basal endosperm transfer layer; AL, aleurone; SE, starchy endosperm; PL, placenta/maternal chalazal zone.
Scale bars represent 100 μm.

MINATURE1 (*mn1*; Cheng *et al.,* 1996; Taliercio *et al.,* 1999). Both transcripts encode cell wall invertases, which function to cleave sucrose into hexose sugars (glucose and fructose; Cheng *et al.,* 1996; Taliercio *et al.,* 1999). Deficient invertase activity likely causes changes in osmotic pressure in *mn1* mutants, which results in the premature degeneration of the maternal placenta (Miller and Chorey, 1992). Furthermore, *mn1* mutants have a reduction of indole-3-acetic acid accumulation, which suggests a role for sugar signaling in regulating auxin levels (LeClere *et al.,* 2008).

The *MYB-RELATED PROTEIN1* (*MRP1*) encodes a transcription factor that functions to regulate the expression of several genes with BETL-specific transcript accumulation patterns, including *TRANSFER CELL RESPONSE REGULATOR1 (TRR1), and TRANSFER CELL RESPONSE REGULATOR2 (TRR2;* Muniz *et al.,* 2006*;* Muniz *et al.,* 2010*;* Gomez *et al.,* 2002). Both *TRR1* and *TRR2* transcripts encode atypical type-A response regulators and accumulate in the BETL from 8-14 DAP (Muniz *et al.,* 2006; Muniz *et al.,* 2010). Interestingly, TRR1 and TRR2 proteins migrate from the BETL into surrounding endosperm cells several layers deep into the kernel (Muniz *et al.,* 2006; Muniz *et al.,* 2010). Additional gene transcripts regulated by MRP1 include: two putative defense response genes (*BASAL ENDOSPERM TRANSFER LAYER1* (*BETL1*) and *BASAL LAYER-TYPE ANTIFUNGAL PROTEIN2* (*BAP2*; Hueros *et al.,* 1995; Hueros *et al.,* 1999; Serna *et al.,* 2001). BETL1 localizes to the transfer cell walls; whereas BAP2 is secreted from the BETL into the maternally derived pedicel (Hueros *et al.,* 1999; Cai *et al.,* 2002; Serna *et al.,* 2001). Finally, ectopic expression of MRP1 in the aleurone cell layer transforms aleurone cells to BETL cells, illustrating that

MRP1 transcriptional regulation is required for differentiation of the BETL (Gomez *et al.,* 2009).

The embryo surrounding region

The embryo surrounding region (ESR) is distinguishable from other cell types by the completion of endosperm cellularization and is composed of cells that are small, contain dense cytoplasm, and have an extensive network of rough endoplasmic reticulum (Kiesselbach and Walker, 1952; Schel *et al.,* 1984; Opsahl-Ferstad *et al.,* 1997). The ESR first forms a cavity wherein the proembryo develops and later forms around the base of the suspensor (Figure 1.2a, b; Figure 1.3a, b; Kiesselbach and Walker, 1952). ESR cells contain an asymmetric distribution of spherical plasma membrane infolds, an abundant ER (arranged in parallel arrays), and a high number of mitochondria oriented toward the embryo, which suggests that ESR cells are metabolically active and use exocytosis to send nutrients or signals to the developing embryo (Schel *et al.,* 1984).

Although no functional evidence exists, transcriptional evidence suggests that the ESR may mediate embryo and endosperm interactions, protect the embryo, or nurture the embryo during early kernel development. Three gene transcripts that may function in signaling from the ESR to the developing embryo include: *EMBRYO SURROUNDING REGION1* (*ESR1*); *EMBRYO SURROUNDING REGION2* (*ESR2*); and *EMBRYO SURROUNDING REGION3* (*ESR3*; Bonello *et al.,* 2002). These three *ESR* transcripts accumulate exclusively in the ESR from 4-28 DAP and encode small secreted proteins that localize to the cell walls of the ESR (Bonello *et al.,* 2002). All three ESR proteins share a conserved motif with CLAVATA3 (CLV3) and belong to the CLAVATA3/ESR-

related (CLE) family of intercellular signaling proteins (Bonello *et al.,* 2002). In *Arabidopsis*, CLV3 is a ligand that binds to the receptor-like kinase complex CLAVATA1/CLAVATA2 (Fletcher *et al.,* 1999). Another transcript that accumulates exclusively in the ESR, *EMBRYO SURROUNDING REGION6* (*ESR6*), has a putative function in defense and encodes an excreted defensin protein that ultimately accumulates in placental cells late in kernel development. In a final example, the gene transcript *INVERTASE INHIBITOR HOMOLOG1* (*INVINH1*) accumulates exclusively in the ESR and encodes a protein that regulates the activity of cell wall invertases at the apoplast (Bate *et al.,* 2004). As described in the previous section on the BETL, invertases function in cleaving sucrose into hexoses, which act as carbon sources for dividing cells. Endosperm cells initially divide more rapidly than embryo cells post-fertilization. To enable the embryo to develop at a slower rate, INVINH1 may block the hexose supply from the endosperm to the embryo (Bate *et al.,* 2004).

The starchy endosperm

The starchy endosperm, which constitutes the majority of the endosperm, stores energy reserves in the form of starch and prolamin proteins (Figure 1.6c; Duvik, 1961). Following endosperm cellularization, the starchy endosperm undergoes endoreduplication (reviewed in Larkins *et al.,* 2001) and eventually programmed cell death (Young and Gallie, 2000). Endoreduplication (i.e., when cells replicate nuclear DNA without chromatin condensation, chromatid separation, or cytokinesis) occurs at ~12 DAP or when the mitotic divisions of the endosperm begin to cease (reviewed in Larkins *et al.,* 2001). The putative function of endoreduplication is to increase gene expression without increasing cell number (reviewed in Larkins *et al.,* 2001). The

programmed cell death of the starchy endosperm occurs in two waves (Young and Gallie, 2000). Cells located in the center of the kernel undergo programmed cell death first at ~16 DAP, followed by cells located at the upper end of the kernel near the silk scar at 20 DAP. From 24 DAP to 40 DAP, programmed cell death proceeds from the upper end of the kernel to the lower end of the kernel (Young and Gallie, 2000). The predicted function of this programmed cell death is to make the storage proteins and starch reserves within starchy endosperm cells available to the germinating seedling (Young and Gallie, 2000).

The aleurone

The aleurone is a single cell file encompassing the starchy endosperm (Figure 1.6d). Aleurone cells differentiate from starchy endosperm cells and have a reversible fate: they can re-differentiate back into starchy endosperm cells late in development in the absence of a persistent differentiation signal (Becraft and Asuncion-Crabb, 2000). As mentioned above, ectopic expression of MRP1 can induce BETL specification of aleurone cells (Gomez *et al.,* 2009). This cell fate is also reversible; when expression of MRP1 ceases, the induced BETL cells revert to an aleurone cell fate (Gomez *et al.,* 2009). During normal endosperm development aleurone cells maintain an aleurone cell identity and do not re-differentiate back into starchy endosperm cells. The cells that constitute the aleurone contain lytic vacuoles, protein storage vacuoles, anthocyanins, a large number of mitochondria, and have a developed endoplasmic reticulum (Jones, 1969; Morrison *et al.,* 1975). During germination the cell wall degrading proteolytic and hydrolytic enzymes found in the aleurone cells convert the storage proteins and starch granules produced in the starchy endosperm into sugars and amino acids for the

growing embryo (Young and Gallie, 2000). Aleurone cells remain living in the mature endosperm before undergoing programmed cell death just after germination (Fath *et al.,* 2000).

Several genes have been identified that are implicated to function in cell-to-cell signaling that specifies aleurone cell fate. Most notably, *DEFECTIVE KERNEL1* (*DEK1*) and *CRINKLY4* (*CR4*) transcripts encode proteins that maintain aleurone cell specification (Becraft *et al.,* 1996; Lid *et al.,* 2002). Mutations in *DEK1* or *CR4* give rise to kernels that have no aleurone cell layer or patches of starchy endosperm cells invading the aleurone layer cell file, respectively (Becraft *et al.,* 1996; Lid *et al.,* 2002). Both *DEK1* and *CR4* encode receptors that function at the plasma membrane; DEK1 encodes a trans-membrane domain protein with a cytoplasmic calpain protease loop and CR4 encodes a tumor necrosis factor receptor-like receptor kinase (Becraft *et al.,* 1996; Lid *et al.,* 2002). In addition to transcripts that maintain aleurone cell fate, several transcripts are implicated to restrict aleurone cell fate and include *SUPERNUMERY ALEURONE1* (*SAL1*), *EXTRA CELL LAYER1* (*XCL1*), and *THICK1* (*THK1;* Kessler *et al.,* 2002; Shen *et al.,* 2003; Yi *et al.,* 2011). Mutations at these loci (*SAL1, XCL1,* and *THK1*) give rise to kernels that have multiple aleurone cell layers (Kessler *et al.,* 2002; Shen *et al.,* 2003; Yi *et al.,* 2011). *SAL1* encodes an E vacuolar protein sorting that functions in endomembrane trafficking, and *THICK1* (*THK1*) was identified as acting downstream of *DEK1* (Lid *et al.,* 2002; Yi *et al.,* 2011).

Purpose

A genomics and a genetics approach are utilized to better understand maize kernel development. First, embryogenesis is investigated with emphasis on the

ontogeny of the shoot apical meristem. Although several studies have surveyed the transcripts in fourteen day old maize shoot apical meristems (Emrich *et al.,* 2007; Ohtsu *et al.,* 2007; Brooks *et al.,* 2009; Nogueira *et al.,* 2009; Jia *et al.,* 2009), no transcriptomic study has analyzed SAM ontogeny during embryogenesis. Transcriptional analysis using laser microdissection and RNA-sequencing of the SAM during embryogenesis will allow us to investigate not only how to make a meristem, but how a newly formed meristem differs from a mature meristem. This will help to identify transcripts that are implicated to function in both the apical-basal patterning of the maize embryo and establishing a meristem during embryogenesis. Using this transcriptional data set we can also investigate how the first three lateral organs (the scutellum, the coleoptile, and the first foliar leaf) are elaborated during embryogenesis to address the controversy surrounding the homology of the scutellum and the coleoptile. Additional analyses with the transcriptional data set investigate the differences between initiation of leaves made in the embryo versus seedlings post germination and what distinguishes a lateral meristem from a shoot apical meristem. Taken together, the transcriptional data set of the ontogeny of the SAM will serve as a tool to better understand different aspects of embryo development.

In addition performing a global analysis of maize embryo development, a genetics approach using the *defective kernel* mutation *discolored1* will be used to address how differentiation of embryo and endosperm structures is maintained during maize kernel development (Scanlon *et al.,* 1994; Scanlon and Myers 1998). Although hundreds of *defective kernel* mutations have been identified, few genes underlying these loci have been identified or analyzed in detail (Neuffer and Sheridan, 1980;

Scanlon *et al.,* 1994; Fu *et al.,* 2002). Previously *dsc1* was mapped to chromosome 4 and transposon-tagging was used to obtain a genomic fragment of *dsc1*, which has provided us an opportunity to further investigate DSC1 function during kernel development (Scanlon *et al.,* 1994; Scanlon and Myers, 1998).

REFERENCES

Abbe, E.C. and Stein, O.L. The growth of the shoot apex in maize: embyrogeny. *Am. J. Bot.* **41**(4), 285-293 (1954).

Bate, N., Niu, X., Wang, Y., Reimann, K., and Helentjaris, T. An invertase inhibitor from maize localizes to the embryo surrounding region during early kernel development. *Plant Physiol.* **134**, 246-254 (2004).

Becraft, P.W. and Asuncion-Crabb, Y. Positional cues specify and maintain aleurone cell fate in maize endosperm development (2000).

Becraft, P.W., Stinard, P.S., and McCarty, D.R. CRINKLY4: a TNFR-like receptor kinase involved in maize epidermal differentiation. *Science* 273, 1406-1409 (1996).

Bonello, J.F., Sevilla-Lecoq, S., Berne, A., Risueno, M.C., Dumas, C., and Rogowsky, P.M. ESR proteins are secreted by the cells of the embryo surrounding region. *J. Exp. Bot.* **53**, 1559-1568 (2002).

Boyd, L. Evolution in the monocotyledonous seedling, a new interpretation of the grass embryo. *Trans. Bot. Soc. Edinburgh* **30**, 286-302 (1931).

Brink, R.A., and Cooper, D.C. The endosperm in seed development. *Bot. Rev.* 13(9), 479-541 (1947).

Brooks III, L., Strable, J., Zhang, X., Ohtsu, K., Zhou, R., Sarkar, A., Hargreaves, S., Elshire, R.J., Eudy, D., Pawlowska, T., Ware, D., Janick-Buckner, D., Buckner, B., Timmermans, M.C.P., Schnable, P.S., Nettleton, D., and Scanlon, M.J. Microdissection of shoot meristem functional domains. *PLoS Genet.* **5**(5)**,** e1000476 (2009).

Cai, G., Faleri, C., Del Casino, C., Hueros, G., Thompson, R.D., and Cresit, M. Subcellular localization of BETL-1, -2, and -4 in *Zea mays* L. endosperm. *Sex. Plant Reprod.* **15**, 85-98 (2002).

Cheng, W.H., Taliercio, E.W., and Chourey, P.S.The *Minature1* seed locus of maize encodes a cell wall invertase required for normal development of endosperm and maternal cells in the pedicel. *Plant Cell* **8**, 971-983 (1996).

Duvik, D.N. Protein granules of maize endosperm cells. *Cereal Chem.* **38**, 374-385 (1961).

Emrich, S.J., Barbazuk, W.B., Li, L., and Schnable, P.S. Gene discovery and annotation using LCM-454 transcriptome sequencing. *Genome Res.* **17**, 69-73 (2007).

Fath, A., Bethke, P., Lonsdale, J., Meza-Romero, R., and Jones, R. Programmed cell death in cereal aleurone. *Plant Mol. Biol.* **44**, 255-266 (2000).

Fletcher, J.C., Brand, U., Running, M.P., Simon, R., and Meyerowitz, E.M. Signaling of cell fate decisions by CLAVAT3 in Arabidopsis shoot meristems. *Science* **283**, 1911-1914 (1999).

Fu, S., Meeley, R., and Scanlon, M.J. *empty pericarp2* encodes a negative regulator of the heat shock response and is required for maize embryogenesis. *Plant Cell* **14**, 3119-3132 (2002).

Gao, R., Dong, S., Fan, J., and Hu, C. Relationship between development of endosperm transfer cell and grain mass in maize. *Biol. Plant* **41**, 539-546 (1998).

Gomez, E., Royo, J., Guo, Y., Thompson, R.D., and Hueros, G. Establishment of cereal endosperm expression domains: identification and properties of a maize transfer cell-specific transcription factor, *ZmMRP-1. Plant Cell* **14**, 599-610 (2002).

Gomez, E., Royo, J., Muniz, L.M., Sellam, O., Pau, W., Gerentes, D., Barrero, C., Lopez, M., Perez, P., and Hueros, G. The maize transcription factor myb-related protein-1 is a key regulator of the differentiation of transfer cells. *Plant Cell* **21**, 2022-2035 (2009).

Gruis, D., Guo, H., Selinger, D., Tian, Q., and Olsen, O-A. Surface position, not signaling from surrounding maternal tissues, specifies aleurone epidermal cell fate in maize. *Plant Physiol.* **141**(3), 898-909 (2006).

Hueros, G., Varotto, S., Salamini, F., and Thompson, R.D. Molecular characterization of *BET1,* a gene expressed in the endosperm transfer cells of maize. *Plant Cell* **7**, 747-757 (1995).

Hueros, G., Gomez, E., Cheikh, N., Edwards, J., Weldon, M., Salamini, F., and Thompson, R.D. Identification of a promoter sequence from the *BETL1* gene cluster able to confer transfer-cell-specific expression in transgenic maize. *Plant Physiol.* **121**, 1143-1152 (1999).

Ingram, G.C., Magnard, J-L., Vergne, P., Dumas, C., and Rogowsky, P.M. *ZmOCL1*, an HDGL2 family homeobox gene, is expressed in the outer cell layer throughout maize development (1999).

Ingram, G.C., Boisnard-Lorig, C., Dumas, C., and Rogowsky, P.M. Expression patterns of genes encoding HD-ZipIV homeodomain proteins define specific domains in maize embryos and meristems. *Plant J.* **22**(5), 401-414 (2000).

Jackson, D., Veit, B., and Hake, S. Expression of maize KNOTTED1 related homeobox genes in the shoot apical meristem predicts patterns of morphogenesis in the vegetative shoot. *Development* **120**, 405-413 (1994).

Javelle, M., Vernoud, V., Rogowsky, P.M., and Ingram, G.C. Epidermis: the formation and functions of a fundamental plant tissue. *New Phytologist* **189**, 17-39 (2011).

Jia, Y., Lisch, D.R., Ohtsu, K., Scanlon, M.J., Nettleton, D., Schnable, P.S. Loss of RNA-dependent RNA Polymerase2 (RDR2) function causes widespread and unexpected changes in the expression of transposons, genes, and 24-nt small RNAs. *PLoS Genet.* **5**(11)**,** e1000737 (2009).

Jones, R.L. The fine structure of barley aleurone cells. *Planta* **85**, 359-375 (1969).

Kaplan, D.R. Early plant development: from seed to seedling to established plant. In *Principles of Plant Morphology, Chapter 5.* Berkeley, CA: Copy Central, University of California, Berkeley, 1996.

Kessler, S., Seiki, S., and Sinha, N. *Xcl1* causes delayed oblique periclinal cell division in developing maize leaves, leading to cellular differentiation by lineage instead of position. *Development* **129**, 1859-1869 (2002).

Kiesselbach, T.A., and Walker, E.R. Structure of certain specialized tissue in the kernel of corn. *Amer. J. Bot.* 39(8), 561-569 (1952).

Larkins, B.A., Dilkes, B.P., Dante, R.A., Coelho, C.M., Woo, Y-M., and Liu, Y. Investigating the hows and whys of DNA endoreduplication. *J. Exp. Bot.* **52**(355), 183-192 (2001).

LeClere, S., Schmelz, E.A., and Chourey, P.S. Cell wall invertase-deficient *minature1* kernels have altered phytohormone levels. *Phytochem.* **69**, 692-699 (2008).

Lid, S.E., Gruis, D., Jung, R., Lorentzen, J.A., Ananiev, E., Chamberlin, M., Niu, X., Meeley, R., Nichols, S.E., and Olsen, O-A. The *defective kernel1* (*dek1*) gene required for aleurone cell development in the endosperm of maize grains encodes a membrane protein of the calpain gene superfamily. *Proc. Natl. Acad. Sci. USA* **99,** 5460-5465 (2002).

Lim, J., Jung, J.W., Lim, C.E., Lee, M-H., Kim, B.J., Kim, M., Bruce, W.B., and Benfey, P.N. Conservation and diversification of *SCARECROW* in maize. *Plant Mol. Biol.* **59**, 619-630 (2005).

McClintock, B. Development of the maize endosperm as revealed by clones. *In: The clonal basis of development.* S. Sutelny, I.M. Sussex, eds. Academic, New York, New York pp217-237 (1978).

Miller, M.E., and Chourey, P.S. The maize invertase-deficient *miniature-1* seed mutation is associated with aberrant pedicel and endosperm development. *Plant Cell* **4**, 297-305 (1992).

Morrison, I.N., Kuo, J., and O'Brien, T.P. Histochemistry and fine chemistry of developing wheat aleurone cells. *Planta* **123**, 1050-116 (1975).

Muniz, L., Royo, J., Gomez, E., Barrero, C., Bergareche, D., and Hueros, G. The maize transfer cell-specific type-A response regulator *ZmTCRR-1* appears to be involved in intercellular signaling. *Plant J.* **48**, 17-27 (2006).

Muniz, L.M., Royo, J., Gomez, E., Baudot, G., Paul, W., and Hueros, G. Atypical response regulators expressed in the maize endosperm transfer cells link canonical two component systems and seed biology. *BMC Plant Biol.* **10**, 84 (2010).

Nardmann, J., Zimmerman, R., Durantini, D., Kranz, E., and Werr, W. *WOX* gene phylogeny in *Poaceae*: a comparative approach addressing leaf and embryo development. *Mol. Biol. Evol.* **24**(11), 2474-2484 (2007).

Nardmann, J., Ji, J., Werr, W., and Scanlon, M.J. The maize duplicate genes *narrow sheath1* and *narrow sheath2* encode a conserved homeobox gene function in a lateral domain of shoot apical meristems. *Development* **131**, 2827-2839 (2004).

Neuffer, M.G., and Sheridan, W.F. Defective kernel mutants of maize. *I. Genetic and lethality studies*. *Genetics* **95**, 929-944 (1980).

Nogueira, F.T.S., Chitwood, D.H., Madi, S., Ohtsu, K., Schnable, P.S., Scanlon, M.J., Timmermans, M.C.P. Regulation of small RNA accumulation in the maize shoot apex. *PLoS Genet.* **5**(1)**,** e1000320 (2009).

Ohtsu, K., Smith, M.B., Emrich, S.J., Borsuk, L.A., Zhou, R., Chen, T., Zhang, X., Timmermans, M.C.P., Beck, J., Buckner, B., Janick-Buckner, D., Nettleton, D., Scanlon, M.J., and Schnable, P.S. Global gene expression analysis of the shoot apical meristem of maize (*Zea mays* L.). *Plant J.* **52**, 391-404 (2007).

Olsen, O-A. Endosperm development: cellularization and cell fate specification. *Annu. Rev. Plant Physiol. Plant Mol. Biol.* **52**, 233-267 (2001).

Opsahl-Ferstad, H-G., Le Deunff, E., Dumas, C., and Rogowsky, P.M. *ZmEsr*, a novel endosperm-specific gene expressed in a restricted region around the maize embryo. *Plant J.* **12**(1)**,** 235-246 (1997).

Poethig, R.S., Coe Jr., E.H., and Johri, M.M. Cell lineage patterns in maize embryogenesis: A clonal analysis. *Developmental Biol.* **117**, 392-404 (1986).

Raghavan, V. Some reflections on double fertilization, from its discovery to the present. *New Phytologist* **159**, 565-583 (2003).

Randolph, L.F. The development of morphology of the caryopsis in maize. *J. Agric. Res.* **53**, 318-333 (1936).

Scanlon, M.J., Stinard, P.S., James, M.G., Myers, A.M., and Robertson, D.S. Genetic analysis of 63 mutations affecting maize kernel development isolated from Mutator stocks. *Genetics* **136**, 281-294 (1994).

Scanlon, M.J. and Myers, A.M. Phenotypic analysis and molecular cloning of *discolored-1* (*dsc1*) a maize gene required for early kernel development. *Plant Mol. Biol.* **37**, 483-493 (1998).

Schel, J.H.N., Kieft, H., and Van Lammeren A.A.M. Interactions between embryo and endosperm during early developmental stages of maize caryopses (*Zea mays*). *Can. J. Bot.* **62**, 2842-2853 (1984).

Serna, A., Maitz, M., O'Connell, T., Santandrea, G., Thevissen, K., Tienens, K., Hueros, G., Faleri, C., Cai, G., Lottspeich, F., and Thompson, R.D. Maize endosperm secretes a novel antifungal protein into adjacent maternal tissue. *Plant J.* **25**, 687-698 (2001).

Shen, B., Li, C., Min, Z., Meeley, R.B., Tarczynski, M.C., and Olsen, O-A. *sal1* determines the number of aleurone cell layers in maize endosperm and encodes a class E vacuolar sorting protein. *Proc. Natl. Acad. Sci. USA* **100(**11), 6552-6557 (2003).

Smith, L.G., Greene, B., Veit, B., and Hake, S. A dominant mutation in the maize homeobox gene, Knotted-1, causes its ectopic expression in leaf cells with altered fates. *Development* **116**, 21-30 (1992).

Smith, L.G., Jackson, D., and Hake, S. Expression of *knotted1* marks shoot meristem formation during maize embryogenesis. *Developmental Genet.* **16**, 344-348 (1995).

Szymkowiak, E.J., and Sussex, I.M. what chimeras can tell us about plant development. *Annu. Rev. Physiol. Plant Mol. Biol.* **47**, 351-376 (1996).

Taliercio, E.W., Kim, J.Y., Mahe, A., Shanker, S., Choi, J., Cheng, W.H., Prioul, J.L., and Chourey, P.S. Isolation, characterization and expression analyses of two cell wall invertase genes in maize. *J. Plant Physiol.* **155**, 197-204 (1999).

Thompson, R.D., Hueros, G., Becker, H., and Maitz, M. Development and functions of seed transfer cells. *Plant Sci.* 160, 775-783 (2001).

Weatherwax, P. Position of the scutellum and homology of coleoptile in maize. *Bot. Gaz.* **69**, 179-182 (1920).

Yi, G., Lauter, A.M., Scott, M.P., and Becraft, P.W. The *thick aleurone1* mutant defines a negative regulation of maize aleurone cell fate that functions downstream of *defective kernel1*. *Plant Physiol.* **156**(4), 1826-1836 (2011).

Young, T.E., and Gallie, D.R. Programmed cell death during endosperm development. *Plant Mol. Biol.* **44**, 283-301 (2000).

Zimmermann, R., and Werr, W. Pattern formation in the monocot embryo as revealed by *NAM* and *CUC3* orthologues from *Zea mays* L. *Plant Mol. Biol.* **58**, 669-685 (2005).

CHAPTER 2

ONTOGENY OF THE MAIZE SHOOT APICAL MERISTEM[1]

1 Takacs, E.M., Li, J., Ponnala, L., Janick-Buckner, D., Yu, J, Muehlbauer, G.J., Timmermans, M.C.P., Schnable, P.S., Sun, Q., Nettleton, D., and Scanlon, M.J. authors contributing to manuscript.

Abstract

The maize shoot apical meristem (SAM) forms early in embryogenesis and functions during stem cell maintenance and organogenesis to generate all the above ground tissues of the plant. Laser microdissection of discrete domains from developing maize embryos and seedlings was combined with RNA-seq analyses for transcriptomic analyses of SAM ontogeny and function. Analysis of transcript accumulation before and after SAM initiation indicates that lateral organ specification precedes stem cell maintenance in maize. Compared to the newly initiated SAM, the mature SAM is enriched for transcripts that function in transcriptional regulation, hormonal signaling, and transport. The scutellum, coleoptile and leaf 1 comprise the first three lateral organs elaborated from maize embryos; transcriptional profiling provides insight into their homology and to the identity of the single maize cotyledon. Comparisons of shoot meristems during initiation of juvenile leaves, adult leaves, and husk leaves illustrate differences in phase-specific (juvenile versus adult) and meristem-specific (SAM versus lateral meristem) transcript accumulation. Novel molecular markers of key events in maize embryogenesis are described, and comprehensive transcriptional data from six stages in maize shoot meristem development are publicly released for use in future studies.

Introduction

Plant shoots develop new leaves, stems, and buds throughout the life cycle via the maintenance of an organogenic population of stem cells within the stem cell niche or shoot apical meristem (SAM). These dual SAM functions of stem cell maintenance and organogenesis are ultimately responsible for the production of all above ground plant

tissues. Angiosperm SAMs display histological stratification into the clonally distinct tunica (outer) and corpus (inner) cell layers, and are subdivided into the stem cells of the central zone (CZ) and the organogenic peripheral zone (PZ). The maize SAM forms during embryogenesis and persists until it transitions into an inflorescence meristem that ultimately forms the pollen-bearing tassel. Despite the vital importance of the SAM during plant shoot development, little is known about its ontogeny.

Although maize embryos do not display stereotypical patterns of cell division, fate mapping confirms that cells occupying specific positions in the developing embryo correlate with predictable cell fates (Poethig *et al.,* 1986). Additionally, stage-specific morphological (Abbe and Stein, 1954) and transcriptional landmarks (Nardmann and Werr, 2009) are described to identify key events in maize embryogenesis, including before SAM formation, during the transition to SAM initiation, and after the SAM is competent to form lateral organs. For example, transcript accumulation of the homeobox transcription factor *KNOTTED1* (*KN1*) is utilized as a marker for maize stem cell maintenance that is not detected in lateral organ primordia or anlagen (Smith *et al.,* 1992; Jackson *et al.,* 1994). The pre-meristematic proembryo contains no lateral organs and comprises a radially symmetrical embryo proper and a basal suspensor that do not accumulate *KN1* transcripts (Figure 2.1a, g and Table 2.1; Smith *et al.,* 1995). Two morphological events accompany the transition stage embryo: (1) formation of the SAM, marked by *KN1* expression, on the lateral face of the embryo; and (2) elaboration of the scutellum from the abgerminal face of the embryo (Figure 2.1b, h). A grass-specific lateral organ of controversial homology, the scutellum is specialized to absorb nutrients from the endosperm during seedling germination. During the coleoptilar stage,

Figure 2.1 SAM formation and organ initiation.

TBO stained embryos at key stages in embryo development (a-d) and the SAM (e) and lateral meristem (f) from 14 day old seedlings. Transcript accumulation of *KN1* during embryogenesis (g-j) and in the SAM (k) and lateral meristem (l) of a 14 day old seedling. Before and after LM of maize embryos (m-p,s-v) and SAM (q,w) and lateral meristem (r,x) from 14 day old seedlings.

1, leaf 1; c, coleoptile; p, embryo proper; s, suspensor; sc, scutellum. Arrows point to meristem.
Scale bars represent 100 μm.

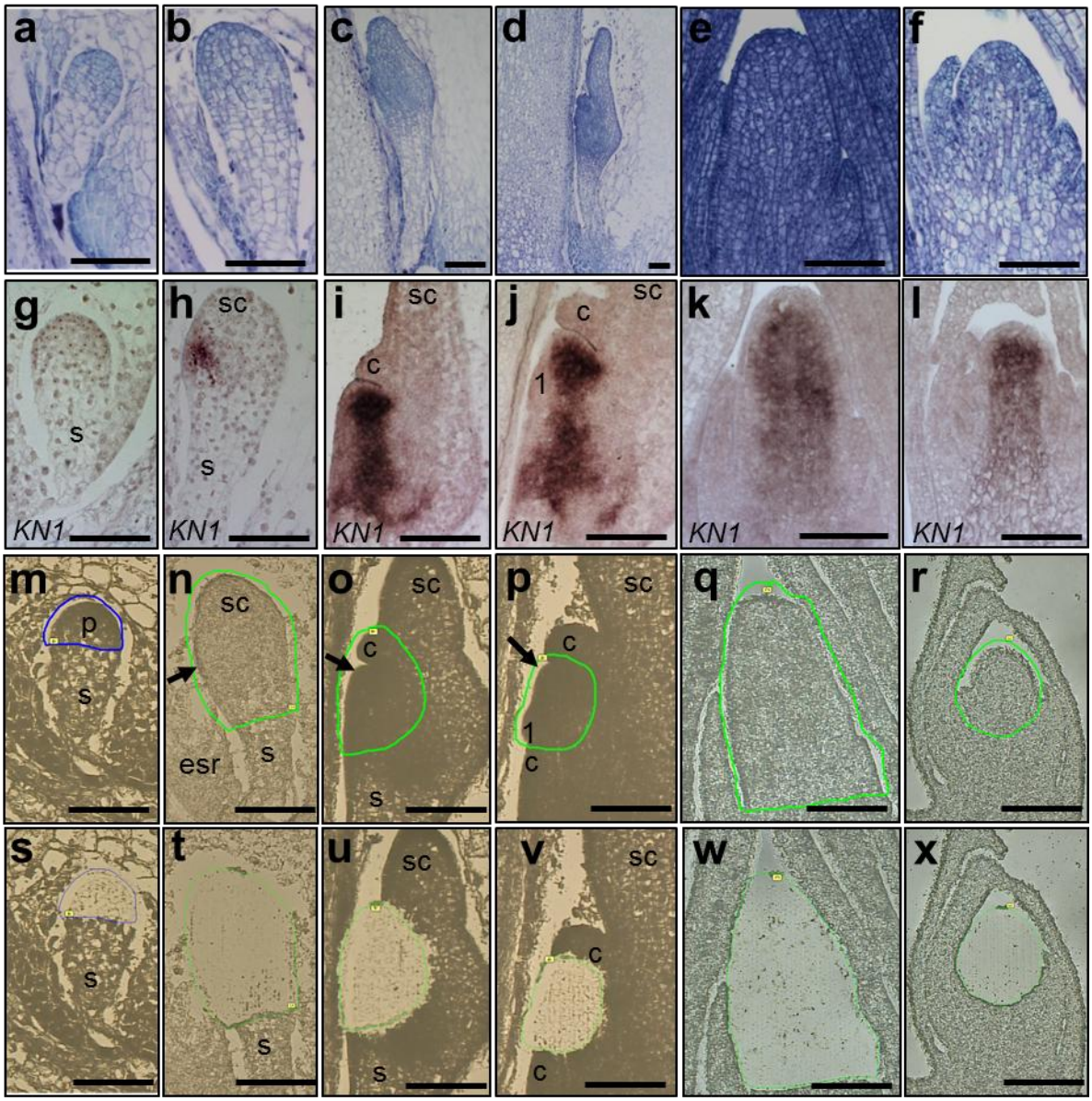
a
b
c
d
e
f
g
h
i
j
k
l
m
n
o
p
q
r
s
t
u
v
w
x
sc
c
1
s
p
esr
KN1
proembryo
transition phase
coleoptile stage
L1 stage
L14 stage
lateral meristem

Table 2.1 Primers used in this study.

Gene name	Accession	Forward primer	Reverse primer
KNOTTED1	GRMZM2G017087	ACAAGGTGGGGGCACCA	TCGGTCTCTCCTCCGCTA
Zea mays YABBY16	GRMZM2G054795	CTCATCCAATAACTCCAACAAAG	GATTTTGCATAGGGTTCTTCTTC
Zea mays YABBY14	GRMZM2G005353	CGACCTCACCGCACGGTCT	GAGCTCCCTCCTGAGTTTGC
ZEA MAYS LEAFY COTYLEDON1	GRMZM2G011789	GGACTCCAGCAGCTTCCT	GTACGCGTAAGGCAGGTAGT
TAPETUM DETERMINANT1-LIKE	GRMZM2G176390	GACAATGGTGCTTTAAGAAACG	GAGTTGGAGTACTGGAAGGAGAC
RAN BINDING PROTEIN2	GRMZM2G094353	GAACAGGAAGCCAGGAGACT	CAGTGCAAGTAGTTTTCGTAGGT
POLLEN OLE E I	GRMZM2G040517	CCTTGAAGGACCACTGTGC	GTACATGAGCGCAGTCTTGG
LIPID TRANSFER PROTEIN1	GRMZM2G101958	CAGCTAGCTCTAGCAAAGCA	TTGCAAACAAAAAGAGGTGA
LIPID TRANSFER PROTEIN2	GRMZM2G083725	GCAGCCAAGCAAATAAAAGT	ACAAGTCACCATGAAACACG
ARABIDOPSIS LSH1 AND ORYZA G11	GRMZM2G087267	TCTCCTCAACCCACCATATT	GTGCGGGATCAAGAAGTG
UNKNOWN1	GRMZM2G038497	CTGTACCTGCAGAACTGCTACAT	CCCATCAACTAAAACTAGACAAACA
UNKNOWN2	GRMZM2G073192	GCTGCAGCTTTACCGATTCC	CTTACAAGCTCACCATCCAAAG
ARABIDOPSIS LSH1 AND ORYZA G12	GRMZM2G034385	GGTACGAGTCGCAGAAGC	ATCTGGTGCTCGTAGTGGTG
LIPID TRANSFER PROTEIN3	GRMZM2G093997	CAACTCTTTCTCTCCTGCAA	CTACGTACTTGGTGCAGTCG

a bi-keeled leaf-like coleoptile initiates from the abgerminal side of the newly ramified meristem, and ultimately forms a protective sheath surrounding the embryonic shoot (Figure 2.1c). At this stage, *KN1* transcripts are detectable throughout the dome-shaped SAM but are excluded from the meristem periphery where the coleoptile emerges (Figure 2.1i).

Three distinct models have been proposed to debate the homology of the maize cotyledon (Kaplan, 1996; Boyd, 1931; Weatherwax, 1920). One model proposes that the coleoptile is the maize cotyledon and the scutellum is a novel evolutionary innovation that arose in the grasses (Boyd, 1931). A second model suggests that the scutellum comprises the cotyledon, whereas the coleoptile is a foliar leaf (Weatherwax, 1920). Others have argued that the maize cotyledon is a bimodal structure in which the scutellum forms the distal tip and the coleoptile forms the sheathing base of the single cotyledon (Kaplan, 1996). Providing evidence for the bimodal cotyledon, maize displays distichous phyllotaxy (leaves emerge from opposite sides of the stem and in two ranks) and the scutellum and coleoptile *both* initiate from the abgerminal side of the embryo (Kaplan, 1996). Formation of the first foliar leaf from the germinal flank of the domed SAM occurs during stage 1 (L1; Figure 2.1d), whereupon *KN1* transcripts accumulate in the embryonic shoot-root axis but not at sites of leaf initiation (Figure 2.1j). Once established, leaf initiation continues in a distichous phyllotactic pattern until the embryonic SAM has initiated up to five or six leaves, whereupon development is interrupted during seed quiescence. Upon germination, the SAM resumes its dual functions of stem cell maintenance and leaf initiation (Figure 2.1e, k). Similar to the SAM, lateral shoot meristems undergo vegetative growth, first initiating a bi-keeled

prophyll followed by foliar husk leaves, before transitioning into an inflorescence meristem or undergoing senescence (Figure 2.1f, l).

Previous studies have analyzed transcripts encoded in various hand-dissected and laser-microdissected (LM) shoot apices from fourteen day old seedlings using microarray analysis, as well as 454-based and Illumina-based RNA-sequencing (RNA-seq; Emrich *et al.,* 2007; Ohtsu *et al.,* 2007; Brooks *et al.,* 2009; Nogueira *et al.,* 2009; Jia *et al.,* 2009). However as yet, no transcriptomic analyses of maize SAM ontogeny during embryogenesis are described. LM of specific domains during landmark developmental stages in embryogenesis is combined with RNA-seq technology to generate a transcriptional profile of the developing maize SAM and embryonic lateral organs. Five main questions are addressed in this study. First, how is a meristem first established and when are the dual meristematic functions of stem cell maintenance and organogenesis initiated? Second, what distinguishes a newly formed embryonic meristem from a meristem that is mature and initiating foliar leaves? Third, what are the transcriptomic differences during initiation of the first three embryonic lateral organs - the scutellum, coleoptile, and leaf 1? Fourth, what transcriptional profiles distinguish embryonic leaves from leaves made from the adult-staged SAM following seedling germination? Fifth, what are the differences between the SAM and lateral meristems?

Results and Discussion

LM and RNA-seq of SAM ontogeny

LM enables the isolation of discrete domains within microscopic samples for use in transcriptomic analyses (Nelson *et al.,* 2006; Scanlon *et al.,* 2009). Six samples were microdissected from developing embryos and fourteen day old seedlings, including: (1)

the cells comprising the embryo proper of the proembryo (Figure 2.1m, s); (2) the organizing SAM and emerging scutellar hood of the transition stage embryo (Figure 2.1n, t); (3) the SAM and the initiating coleoptile of the coleoptile stage embryo (Figure 2.1o, u); (4) the SAM and leaf primordium of a stage 1 embryo (Figure 2.1p, v); (5) the SAM and P1 leaf of a fourteen day-old seedling (L14; Figure 2.1q, w); and (6) the lateral meristem and the newly initiated husk leaf from the fourteen day-old seedling (Figure 2.1r, x). Two biological replicates were obtained per sample; replicates comprised cells from three to eight separate embryos or seedlings (Table 2.2). Total RNA isolated from the microdissected cells was subjected to two rounds of linear amplification to generate microgram quantities of RNA amenable to RNA-seq analyses (described in Brooks *et al.,* 2009). Amplified RNA was used to construct cDNA libraries and Illumina-based RNA-seq generated a total of 130 million 44 base pair sequence reads that were aligned to the maize genome (Methods; Schnable *et al.,* 2009). A summary of the total number of reads per biological replicate and their alignment to the maize gene space is presented in Table 2.2 (Methods). Read counts for each transcript were normalized to account for variation in library size across the twelve samples and are reported as reads mapped per million mapped sequences (RPM; Methods). Pairwise comparisons between each of the six samples and a comparison across the entire sample set were performed to identify differentially accumulated transcripts taking into account false discovery rates (FDR; Methods). For all comparisons, an adjusted P value (*q*-value ≤ 0.05) was used to identify up-regulated transcripts (Methods).

Transcripts from a total of 20,610 genes are represented in the combined RNA-seq data sets (Figure 2.2). There is little variation in the total number of genes

Table 2.2 LM and RNA-seq alignment summary.

Sample	Number of replicates captured	Total area of tissue captured (µm2)	Total # of sequences (million)	Percent of unambiguous sequence alignments to maize gene space
Proembryo 1	7	221,338	17.7	41%
Proembryo 2	7	255,205	13	51%
Transition phase 1	3	695,787	10.6	62%
Transition phase 2	3	1,036,719	12.7	88%
Coleoptile stage 1	6	810,869	20.7	67%
Coleoptile stage 2	4	432,794	21.6	66%
L1 stage 1	6	343,410	18.3	71%
L1 stage 2	3	148,276	21.5	62%
L14 stage 1	5	1,279,864	14.2	77%
L14 stage 2	6	1,652,455	18.5	78%
Lateral meristems 1	6	503,008	16.7	52%
Lateral meristems 2	8	909,404	18.2	57%

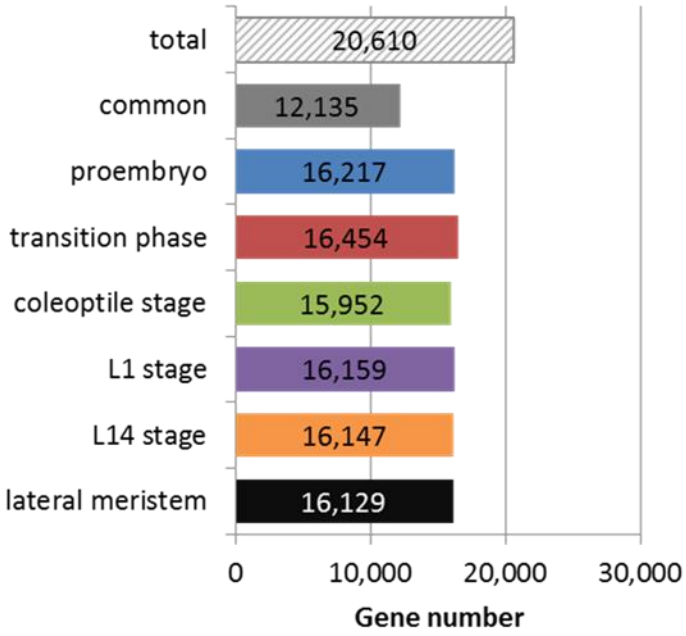

Figure 2.2 Genes represented in each of the six RNA-seq data sets.

All genes represented in each of the six samples (RPM ≥ 1).

represented among the six stages; the transition stage comprised the largest number of individual gene transcripts (16,454) while the coleoptile stage had the fewest (15,952; Figure 2.2). Six-way comparisons of the transcriptional datasets identified 12,135 genes that are common to each sample (Figure 2.2). Previous studies in maize and *Arabidopsis* guided the selection of candidate genes predicted to function during shoot development, which were surveyed for transcriptional patterns across the six samples. The 226 selected candidate genes were dispersed into seven developmental categories, including: stem cell maintenance; lateral organ initiation; dorsiventral patterning; chromatin structure and remodeling; hormonal signaling; apical-basal patterning; and cell division and growth. A heat map was generated based on the relative transcript accumulation of each candidate gene during the six SAM developmental stages, revealing dynamic changes in transcriptional pattern before and after formation of the meristem, after the nascent meristem becomes functionally mature, during elaboration of three distinct lateral organ types (i.e., the scutellum, the coleoptile, and the leaf), and during initiation of juvenile, adult, and husk leaves (Figure 2.3). These summary data confirm that the combined strategies of LM and RNA-seq can successfully detect transcriptional differences on a global scale.

Establishing a meristem

To identify SAM-specific gene transcripts, transcript accumulation in the pre-meristematic proembryo was compared to all samples microdissected after SAM formation (i.e., the transition stage, the coleoptile stage, the L1 stage, the L14 stage, and lateral meristems). A total of 4,145 gene transcripts were up-regulated in comparisons of the proembryo to meristem containing samples (Figure 2.4a; Methods).

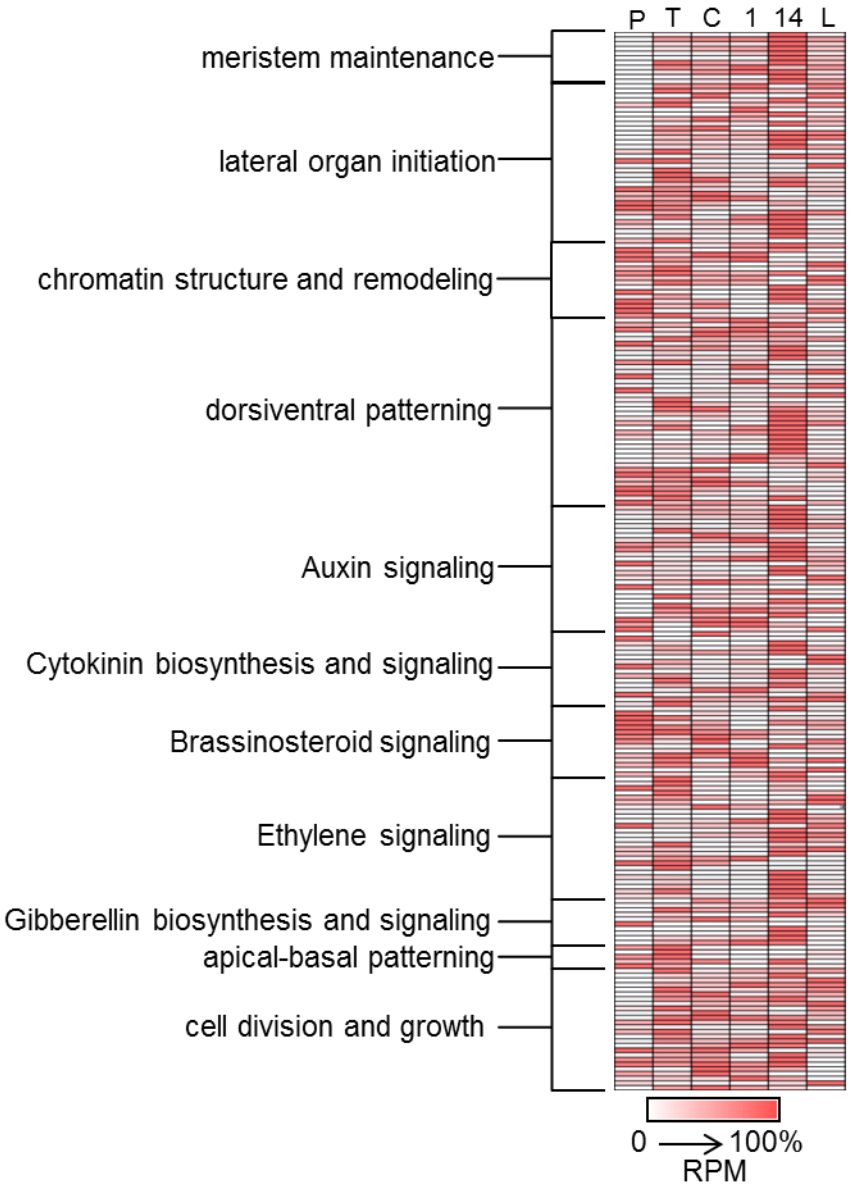

Figure 2.3 Relative transcript accumulation of 226 candidate genes.

Heat map based on the relative transcript accumulation of 226 candidate genes sorted according to implicated function.

P, proembryo; T, transition phase; C, coleoptile stage; 1, L1 stage; 14, L14 stage; L, lateral meristem.

Figure 2.4 Genes up-regulated before and after meristem formation.

(a) 4,145 genes with two-fold or more transcript accumulation (q-value ≤ 0.05) in the pre-meristematic proembryo compared to the five samples with meristems. (b) 742 differentially expressed genes present after the meristem forms distributed into modified MapMan categories.

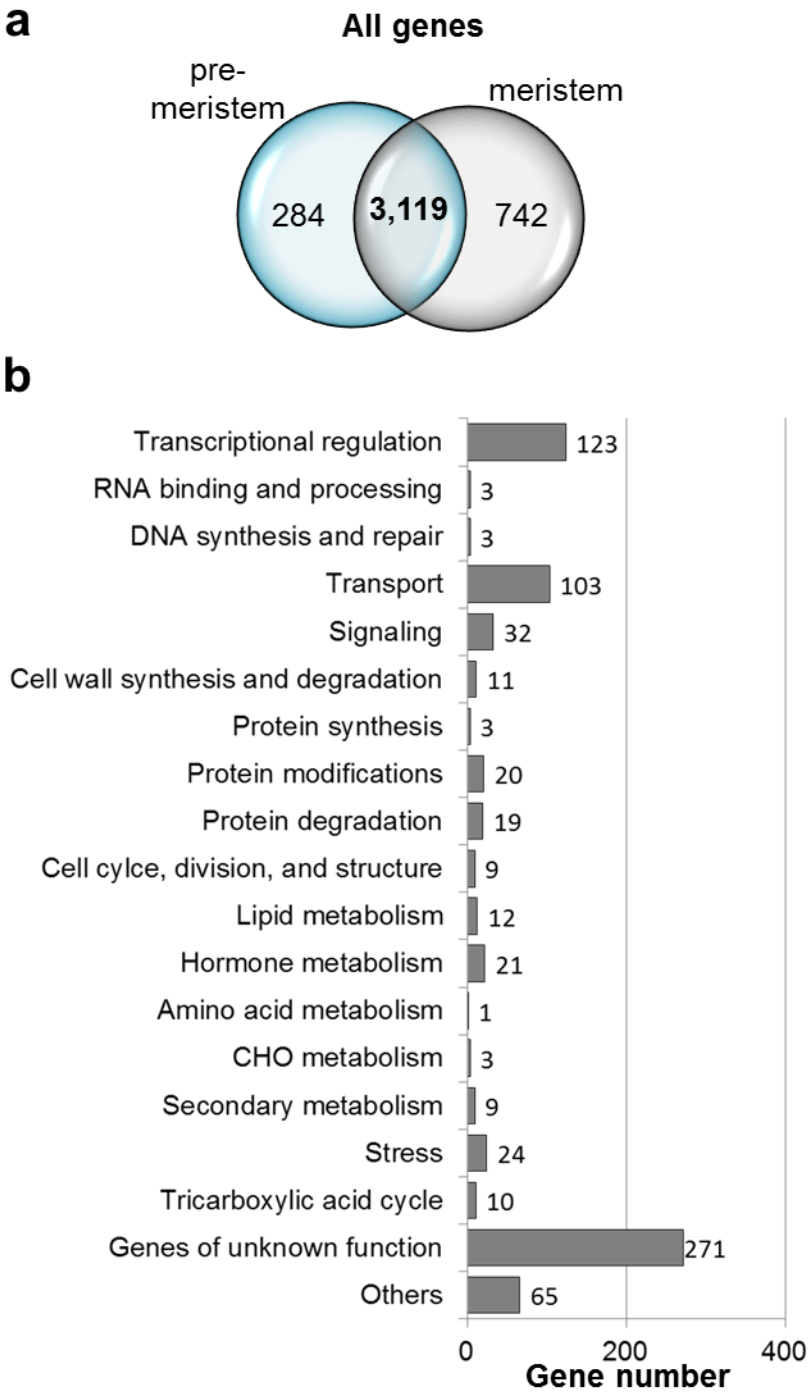
a
All genes
pre-meristem
meristem
284
3,119
742
b
Transcriptional regulation
123
RNA binding and processing
3
DNA synthesis and repair
3
Transport
103
Signaling
32
Cell wall synthesis and degradation
11
Protein synthesis
3
Protein modifications
20
Protein degradation
19
Cell cylce, division, and structure
9
Lipid metabolism
12
Hormone metabolism
21
Amino acid metabolism
1
CHO metabolism
3
Secondary metabolism
9
Stress
24
Tricarboxylic acid cycle
10
Genes of unknown function
271
Others
65
0
200
400
Gene number

Of the 4,145 gene transcripts represented, 284 are exclusively present in the proembryo, whereas 742 are unique to samples containing a meristem (Figure 2.4a). These 742 meristem-specific genes were distributed into MapMan categories and more than half of the predicted gene products fell into three categories: transcriptional regulation (123), genes that function in transport (103), and genes of unknown function (271; Figure 2.4b; Thimm *et al.,* 2004). Nineteen genes implicated to function in transcriptional regulation were exclusively detected in the pre-meristematic proembryo, whereas 123 were found only in samples containing a meristem (Figure 2.5a). These 123 meristematic genes that function in transcriptional regulation were sorted into gene families of known predicted function (Figure 2.5b).

Transcription factors implicated to function in stem cell maintenance include six *CLASS I KNOTTED1-LIKE HOMEOBOX* (*KNOX*) genes and three *BEL-LIKE* (*BELL*) *HOMEOBOX* genes; CLASS I KNOX and BELL proteins form heterodimers that regulate stem cell identity (Reiser *et al.,* 200; Mukherjee *et al.,* 2009; Muller *et al.,* 2001; Bellauoui *et al.,* 2001; Smith *et al.,* 2002; reviewed in Hay and Tsiantis, 2010). At least two gene transcripts encoding WUSCHEL-RELATED HOMEODOMAIN (WOX) proteins (WOX2A and WOX9B) were up-regulated in the proembryo. However, in *Arabidopsis WOX2* and *WOX9* (also known as *STIMPY*) are also expressed before SAM initiation and specify the apical-basal axis of the embryo (Haecker *et al.,* 2004; Brueuniger *et al.,* 2008; Wu *et al.,* 2007). Previous reports in maize revealed that *WOX2A* transcripts accumulate in the apical cap of the proembryo before localizing to the germinal face of the transition stage embryo (Nardmann *et al.,* 2007). The accumulation of *WOX2A* and *WOX9B* transcripts in the pre-meristematic maize proembryo is consistent with a

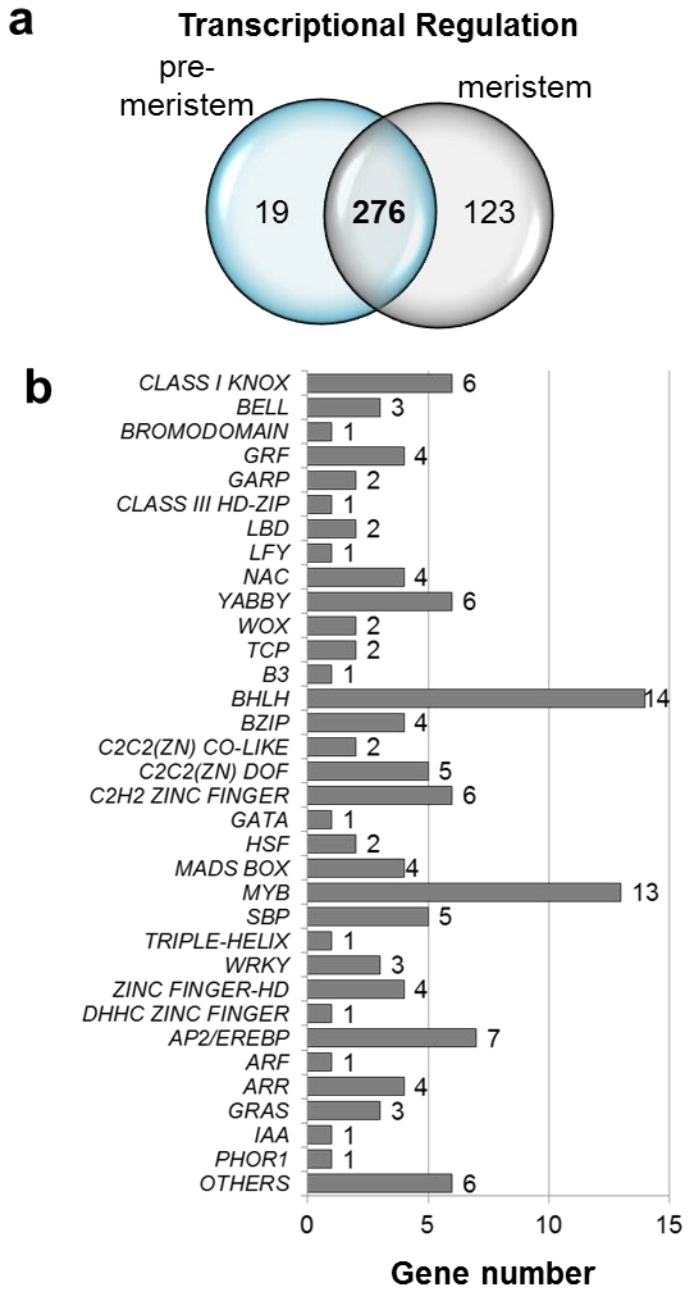

Figure 2.5 Transcriptional regulation when the meristem forms.

(a) 418 genes differentially expressed before and after the meristem forms.
(b) 123 differentially expressed genes present after the meristem forms sorted into their respective gene family.

conserved function of these WOX paralogs in establishing apical-basal domains in the maize embryo, prior to SAM initiation.

Transcripts encoding transcription factors implicated to function during organogenesis and that are not detected in the proembryo include members of the *WOX* (2; Nardmann *et al.,* 2007; Santa-Catarina *et al.,* 2011), *YABBY* (6; Juarez *et al.,* 2004; Sarojam *et al.,* 2010), *GROWTH REGULATING FACTOR* (*GRF*; 4; Zhang *et al.,* 2008; Kim *et al.,* 2003), and *NO APICAL MERISTEM/CUP-SHAPED COTYLEDON* (*NAC*; 4; Zimmerman and Werr, 2005; Vroeman *et al.,* 2003; Aida *et al.,* 1999) gene families. Previous studies in *Arabidopsis* and maize demonstrated that *yabby* genes are expressed in leaf and floral anlagen, and in the marginal tips of leaf and floral primordia (Siegfried *et al.,* 1999; Juarez *et al.,* 2004). Consistent with these previous findings, transcript accumulation of *Zea mays YABBY14* (*ZYB14*), *Zea mays YABBY9* (*ZYB9*), and *Zea mays YABBY10* (*ZYB10*) was up-regulated in samples containing a meristem as compared to the proembryo stage (Juarez *et al.,* 2004). Furthermore, transcripts of the *Arabidopsis FILAMENTOUS FLOWER* (*FIL*; also known as *ABNORMAL FLORAL ORGAN* and *YABBY1*) and *YABBY3* (*YAB3*) accumulate in late globular and heart stage embryos, indicating that these YABBY paralogs also mark the initiating cotyledons (Siegfried *et al.,* 1999). Transcripts of another YABBY homologue, which we have designated *Zea mays YABBY16* (*ZYB16*; GRMZM2G054795), accumulate in the developing scutellum at the apex of the maize proembryo (Figure 2.6a). In addition, *ZYB16* transcripts are retained in the scutellar tip, in the initiating coleoptile, and in the anlagen of initiating leaves at later stages in embryogenesis (Figure 2.6b-d). These data suggest that the scutellum displays a pattern of *ZYB16*

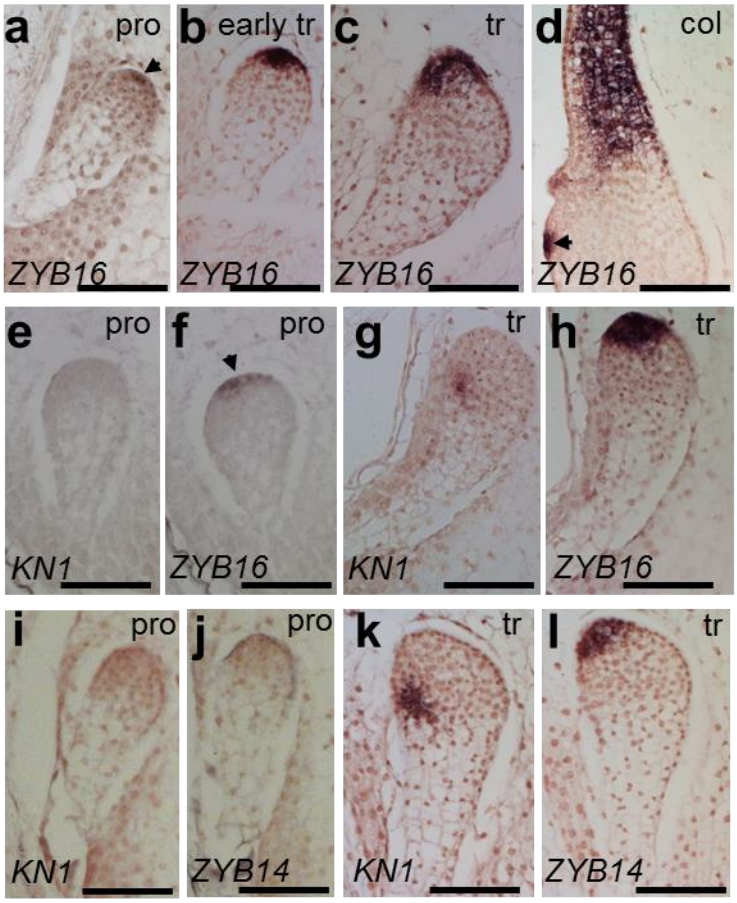

Figure 2.6 Lateral organ initiation precedes stem cell maintenance.

In situ hybridizations using *ZYB16* (a-d,f,h), *KN1* (e,g, i, k), and *ZYB14* (j,l) probes.

Pro, proembryo; tr, transition phase; col, coleoptile stage.
Scale bars are set to 100μm.

transcript equivalent to that of other lateral organs in the maize shoot, which is consistent with models ascribing leaf homology to the scutellum (Kaplan, 1996). Moreover, *in situ* hybridizations performed using *KN1* and *ZYB16* probes on consecutive embryo sections of both proembryo-(Figure 2.6e, f) and transition-staged samples (Figure 2.6g, h) confirm that the onset of *ZYB16* transcript accumulation precedes that of *KN1*. In contrast, control hybridizations reveal that both *KN1* and *ZYB14* transcripts first accumulate during the transition stage (Figure 2.6i-l). Taken together, these data suggest that the dual functions of the maize SAM are not simultaneously activated during SAM ontogeny. Lateral organ initiation, as indicated by accumulation of *ZYB16* transcripts, precedes stem cell maintenance in the maize SAM.

Morphological and molecular maturation of the maize SAM

Significant morphological differences are recognized in a newly-formed transition stage shoot meristem and a mature, L14 stage SAM that has initiated multiple foliar leaves. At the transition stage the meristem is flattened and composed of ~150 cells organized in longitudinal files at least two cell layers deep, which correlates with the transcript accumulation of the stem cell marker *KN1* in these embryos (Figure 2.1b, h; Poethig *et al.,* 1986; Smith *et al.,* 1992; Jackson *et al.,* 1994). Lateral organs are not initiated from the early transition stage SAM; the scutellum forms during the proembryo stage (above) whereas the coleoptile does not initiate until the late transition/coleoptilar stage (Abbe and Stein, 1954). In contrast, the L14 stage SAM attains a post-like architecture comprising multiple cell layers organized into distinct functional zones and is actively initiating leaves (Figure 2.1e, k). To investigate the transcriptional changes that correlate with these morphological differences during SAM maturation, the

transcriptome of the L14 stage SAM was compared to that of the newly formed transition stage SAM. This comparison identified 1,706 gene transcripts that were up-regulated (Figure 2.7a). A Fisher's exact test revealed that transcripts implicated to function in protein synthesis are enriched in newly-initiated SAMs; whereas in L14 stage SAMs transcripts that function in hormone metabolism, transport, and transcriptional regulation are up-regulated (Figure 2.7b; Methods; Thimm *et al.*, 2004).

Enrichment of protein synthesis in transition stage SAMs is consistent with previous findings that enhanced ribosome function is required to establish a shoot meristem (Weijers *et al.,* 2001; Tzafrir *et al.,* 2004; reviewed in Byrne, 2009). Transcripts encoding the maize RIBOSOMAL PROTEIN S5A and S5B (RPS5A, also known as *Arabidopsis* MINUTE-LIKE1 (AML1); RPS5B) are both up-regulated in transition-staged embryos compared to the L14 stage SAMs. Development of *aml1* mutant embryos is arrested at the globular stage in *Arabidopsis*, before the meristem is established (Weijers *et al.,* 2001). Additionally as compared to the L14 stage SAM, the transition stage SAM contains more up-regulated gene transcripts that are implicated to function in protein targeting (14:5), amino acid synthesis (19:9), and DNA synthesis and repair (24:11). These data suggest that an increase in DNA and protein metabolic activity immediately precedes the proliferative growth displayed during later stages of SAM ontogeny.

The dual functions of stem cell maintenance and lateral organ initiation occur concomitantly in mature L14 stage SAMs, as is reflected in predicted functions of the 109 transcripts implicated to function in transcriptional regulation that are up-regulated

Figure 2.7 Transcriptomic comparisons of a newly formed meristem to a mature meristem.

(a) 1,706 genes with two-fold or more transcript accumulation (*q*-value ≤ 0.05) when comparing the transition stage to the L14 stage. (b) 1,706 up-regulated genes sorted into modified MapMan categories (Thimm *et al*., 2004).

Total number of genes in each functional category is displayed in the bar. Asterisk following gene number indicates enrichment of that functional category using Fisher's exact test (*p*-value ≤ 0.01, FDR 6%).

a

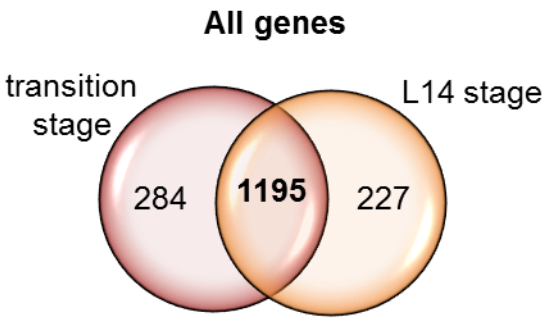
All genes
transition stage
L14 stage
284
1195
227

b

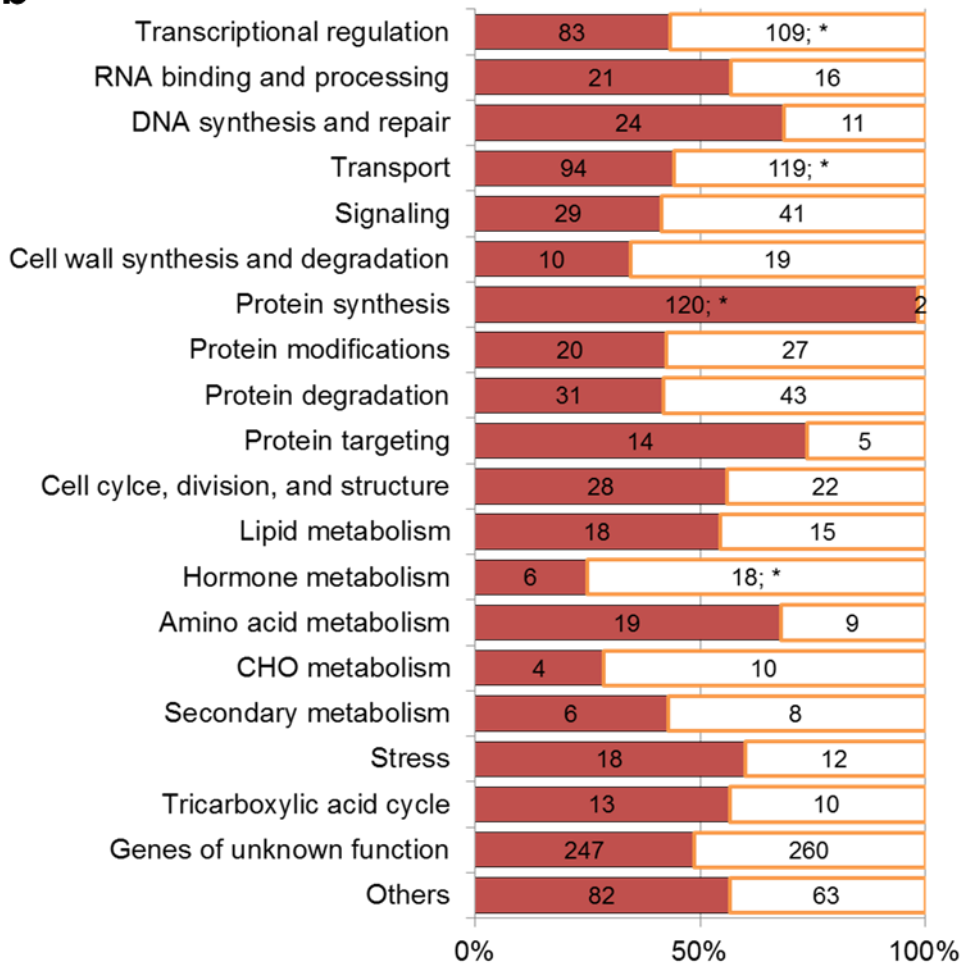
Transcriptional regulation 83 109; *
RNA binding and processing 21 16
DNA synthesis and repair 24 11
Transport 94 119; *
Signaling 29 41
Cell wall synthesis and degradation 10 19
Protein synthesis 120; * 2
Protein modifications 20 27
Protein degradation 31 43
Protein targeting 14 5
Cell cylce, division, and structure 28 22
Lipid metabolism 18 15
Hormone metabolism 6 18; *
Amino acid metabolism 19 9
CHO metabolism 4 10
Secondary metabolism 6 8
Stress 18 12
Tricarboxylic acid cycle 13 10
Genes of unknown function 247 260
Others 82 63
0%
50%
100%

at this stage. Among these are four transcripts encoding known stem cell regulators, including three *CLASS I KNOX* genes and a GATA domain protein homologous to HANABA TARANU in *Arabidopsis* (Figure 2.8a, b; Reiser *et al.,* 2000; Mukherjee *et al.,* 2009; reviewed in Hay and Tsiantis, 2010; Zhao *et al.,* 2004). Up-regulated transcripts encoding proteins that function in organogenesis and cell proliferation of lateral organs include *WUSHEL-RELATED HOMEOBOX3A* (*WOX3A*), the *YABBY* gene *DROOPING LEAF2* (*DL2*), the lateral organ boundary gene *INDETERMINATE GAMETOPHYTE1* (*IG1*), and two *GRF-LIKE* transcripts (Nardmann *et al.,* 2007; Nardmann *et al.,* 2004; Zhang *et al.,* 2007; Yamaguchi *et al.,* 2004; Evans 2007; Zhang *et al.,* 2008; Kim *et al.,* 2003). In addition to three *AUXIN RESPONSE FACTOR* (*ARF*) class transcription factors, several transcripts that encode hormone biosynthetic proteins are also up-regulated in stage 14 SAMs, including seven gibberellin metabolic transcripts implicated to function in lateral organ growth and development. These data suggest that compared to the transition stage, the stage 14 meristem contains a wider diversity of transcripts implicated in both lateral organ initiation and stem cell maintenance.

Elaboration of the first three lateral organs during embryogenesis

Three different types of lateral organs are elaborated in maize embryos: the scutellum; the coleoptile; and five to six foliar leaves. A three-way comparison was made between the transition stage, the coleoptile stage, and the L1 stage to determine the transcriptional differences correlated with the development of these morphologically distinct organs. A total of 532 transcripts were up-regulated in the three-way comparison. Of these up-regulated transcripts, 517 sort into three main clusters based upon relative transcript abundance during the three embryonic stages. These include:

Figure 2.8 Transcriptional regulation in a newly formed meristem versus a mature meristem.

(a) 192 genes implicated to function in transcriptional regulation are differentially expressed between a newly formed meristem and a mature meristem. (b) The 192 genes are distributed into their respective gene family.

a

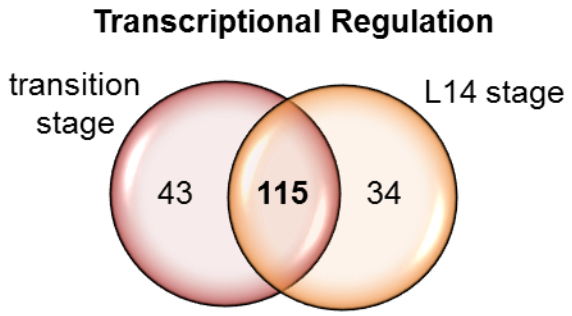
Transcriptional Regulation
transition stage
L14 stage
43
115
34

b

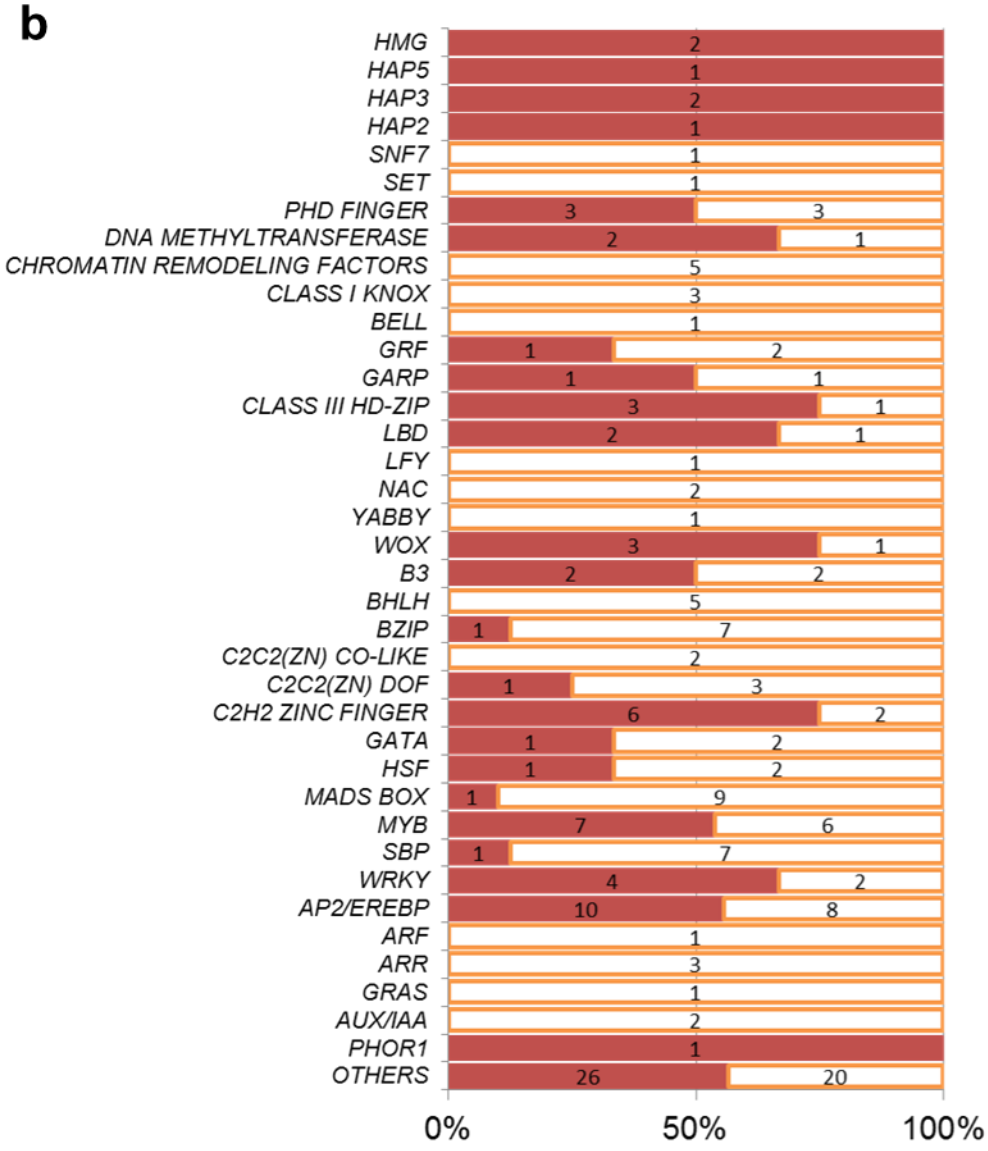
HMG 2
HAP5 1
HAP3 2
HAP2 1
SNF7 1
SET 1
PHD FINGER 3 3
DNA METHYLTRANSFERASE 2 1
CHROMATIN REMODELING FACTORS 5
CLASS I KNOX 3
BELL 1
GRF 1 2
GARP 1 1
CLASS III HD-ZIP 3 1
LBD 2 1
LFY 1
NAC 2
YABBY 1
WOX 3 1
B3 2 2
BHLH 5
BZIP 1 7
C2C2(ZN) CO-LIKE 2
C2C2(ZN) DOF 1 3
C2H2 ZINC FINGER 6 2
GATA 1 2
HSF 1 2
MADS BOX 1 9
MYB 7 6
SBP 1 7
WRKY 4 2
AP2/EREBP 10 8
ARF 1
ARR 3
GRAS 1
AUX/IAA 2
PHOR1 1
OTHERS 26 20
0%
50%
100%

(1) transcripts up-regulated in the transition stage versus both the coleoptile and L1 stages; (2) transcripts up-regulated in the transition stage versus the L1 stage; and (3) transcripts up-regulated in the L1 stage versus the transition stage (Figure 2.9; Figure 2.10). The 517 genes from the respective clusters were distributed into 25 modified MapMan annotated functional categories (Figure 2.9; Thimm *et al.,* 2004). Sixty-three transcripts implicated to function in transcriptional regulation were present in the three main clusters, many of which have specific functions in embryo development (Figure 2.11).

Several transcripts encoding transcription factors implicated to function during apical-basal patterning of the embryo were up-regulated during the transition stage, including *WOX2A*, *WOX5B*, and *NUTCRACKER* (*NUC*; Haeker *et al.,* 2004; Levesque *et al.,* 2006; Nardmann *et al.,* 2007). Whereas WOX2 functions in the apical embryo domain, *WOX5* and *NUC* homologs accumulate in the basal regions of developing embryos, where they eventually specify distinct root domains (Nardmann *et al.,* 2007; Haeker *et al.,* 2004; Levesque *et al.,* 2006). These root-specific transcription factors were probably detected in our transition staged samples because these microdissected domains included both the apical and basal regions of the embryo (Figure 2.1n, t); whereas from later stages only shoot domains were isolated. Up-regulated during development of both the scutellum and the coleoptile, the *HEME ACTIVATOR PROTEIN3* (*HAP3*) class transcription factor *Zea mays LEAFY COTYLDEON1* (*ZmLEC1*) functions during lipid metabolism in maize, whereas homologs in *Arabidopsis* also specify cotyledon development (Mu *et al.,* 2008; Shen *et al.,* 2010). Fatty acid biosynthesis is especially proliferative during embryogenesis, wherein oil bodies are

Figure 2.9 All genes up-regulated during the elaboration of the scutellum, the coleoptile, and the first foliar leaf.

Three main clusters comprised of 517/532 genes up-regulated in the three-way comparison of the transition stage, coleoptile stage, and L1 stage embryos. Distribution of genes according to cluster into modified MapMan bins.

T, transition stage; C, coleoptile stage; L1, Stage L1.

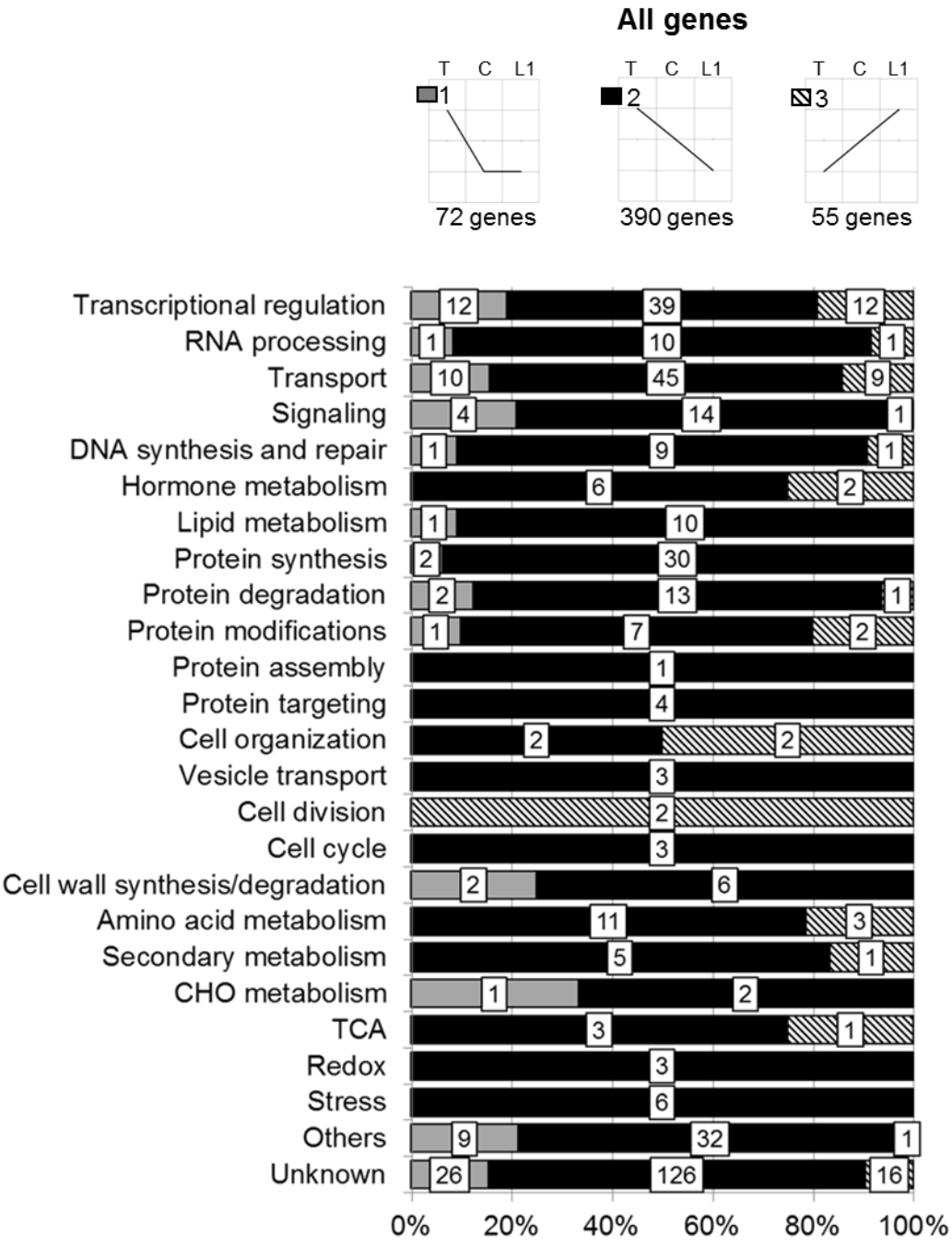
All genes
T C L1
1
72 genes
T C L1
2
390 genes
T C L1
3
55 genes
Transcriptional regulation
RNA processing
Transport
Signaling
DNA synthesis and repair
Hormone metabolism
Lipid metabolism
Protein synthesis
Protein degradation
Protein modifications
Protein assembly
Protein targeting
Cell organization
Vesicle transport
Cell division
Cell cycle
Cell wall synthesis/degradation
Amino acid metabolism
Secondary metabolism
CHO metabolism
TCA
Redox
Stress
Others
Unknown
0%
20%
40%
60%
80%
100%

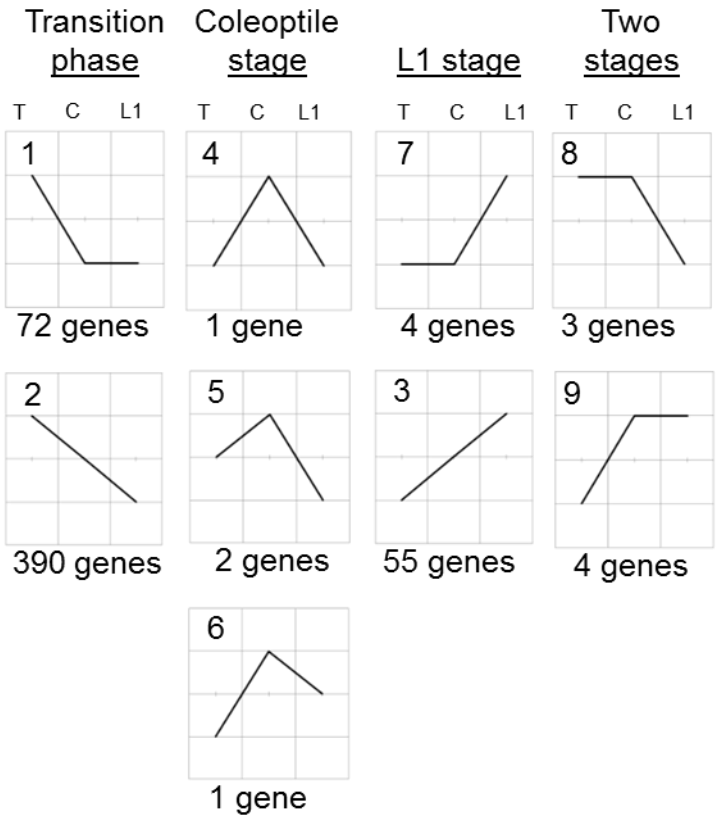

Figure 2.10 Gene clusters from elaboration of lateral organs during embryogenesis.

532 genes up-regulated from the three-way comparison of scutellum, coleoptile, and leaf initiation were sorted into twelve clusters. Clusters include up-regulated in one stage over the two remaining stages (clusters 1, 4, and 7), up-regulated in one stage over one of the remaining stages (clusters 2, 5, 6, and 3), or in two stages over the remaining stage (clusters 8 and 9).

Figure 2.11 Transcriptional regulation during the elaboration of the scutellum, the coleoptile, and the first foliar leaf.

The 63 genes that are implicated to function in transcriptional regulation from the three main clusters distributed into gene families.

T, transition stage; C, coleoptile stage; L1, Stage L1.

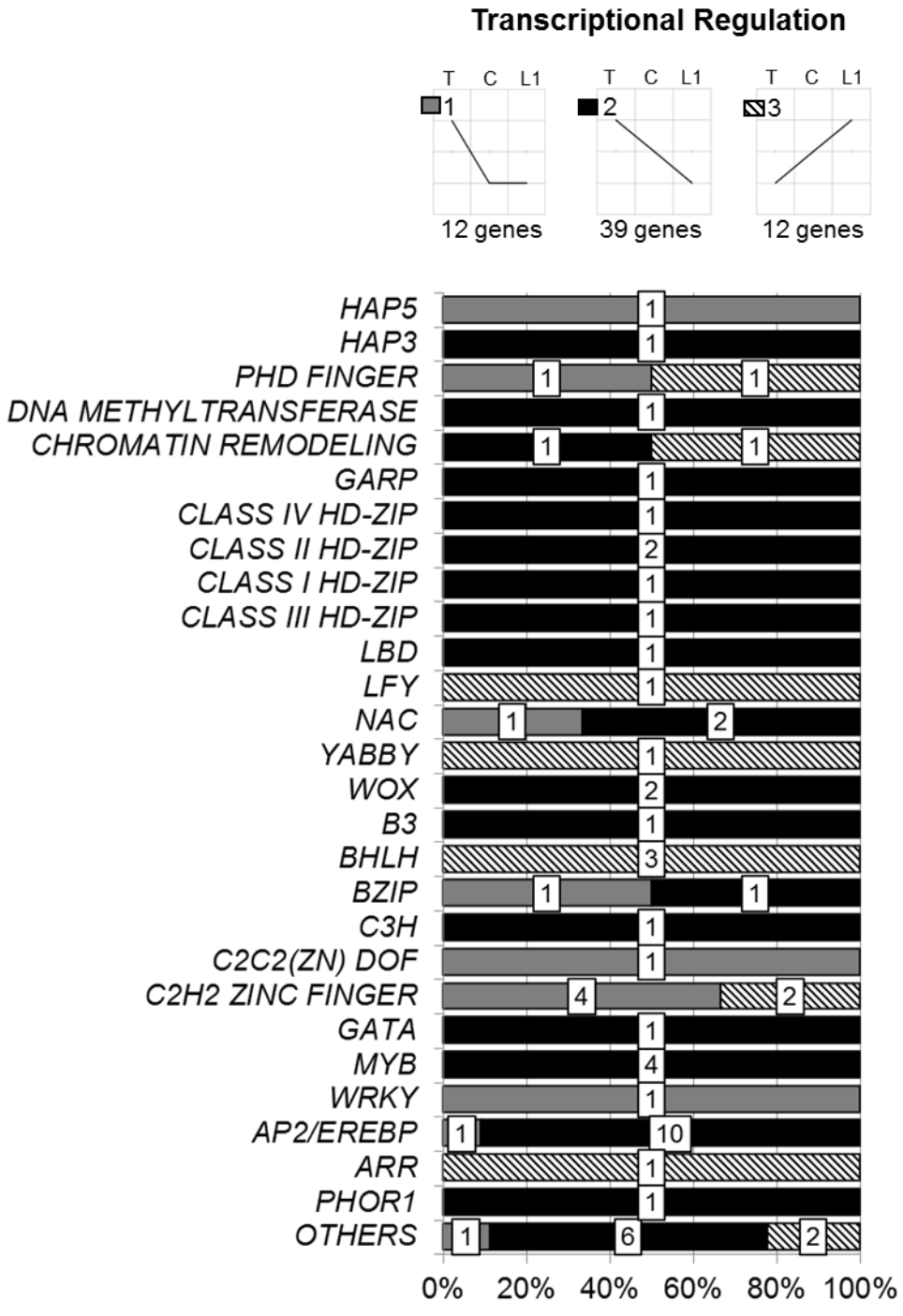
Transcriptional Regulation
T C L1
1
2
3
12 genes
39 genes
12 genes
HAP5
HAP3
PHD FINGER
DNA METHYLTRANSFERASE
CHROMATIN REMODELING
GARP
CLASS IV HD-ZIP
CLASS II HD-ZIP
CLASS I HD-ZIP
CLASS III HD-ZIP
LBD
LFY
NAC
YABBY
WOX
B3
BHLH
BZIP
C3H
C2C2(ZN) DOF
C2H2 ZINC FINGER
GATA
MYB
WRKY
AP2/EREBP
ARR
PHOR1
OTHERS
0% 20% 40% 60% 80% 100%

stored as energy reserves that will subsequently be utilized during germination. *ZmLEC1* is expressed throughout the apical cap in the proembryo and early transition stage (Figure 2.12a, b; Zhang *et al.,* 2002), but is restricted to the scutellar tip and base during the late transition stage (Figure 2.12c) before eventually localizing to the emerging coleoptile (Figure 2.12d). At the L1 stage, *ZmLEC1* transcripts accumulate at the germinal side of the scutellar hood, and at the boundary between the apical embryo and the basal suspensor (Figure 2.12e). As in *Arabidopsis*, no *ZmLEC1* transcripts are detected in foliar leaves (Figure 2.12e-g; Suzuki *et al.,* 2008; Shen *et al.,* 2010; Lotan *et al.,* 1998). Accumulation of *ZmLEC1* in both the scutellum and coleoptile, but not in maize embryonic foliar leaves, is likewise consistent with models wherein the scutellum and the coleoptile comprise the apical and basal zones of the single maize cotyledon.

Interestingly only four transcripts are exclusively up-regulated in the coleoptile stage versus the transition and/or L1 stages. One such transcript encodes the maize BASIC HELIX-LOOP-HELIX transcription factor PHYTOCHROME-INTERACTING FACTOR3-LIKE5 (PIL5); the PIL5 homolog in *Arabidopsis* functions to inhibit seed germination (cluster 5, Figure 2.10; Oh *et al.,* 2007). The relatively few transcripts exclusively up-regulated during the coleoptile stage indicate that the coleoptile transcriptome is inherently similar to that of *both* the scutellum and the foliar leaf. These data are consistent with models ascribing the dual identity of the coleoptile as a component of the cotyledon that also functions as a leaf-like organ.

Several gene transcripts up-regulated at the L1 stage versus the transition stage are implicated to have specific functions in foliar leaves, such as transcripts predicted to encode transcription factors regulating leaf size and leaf-cell proliferation (i.e.,

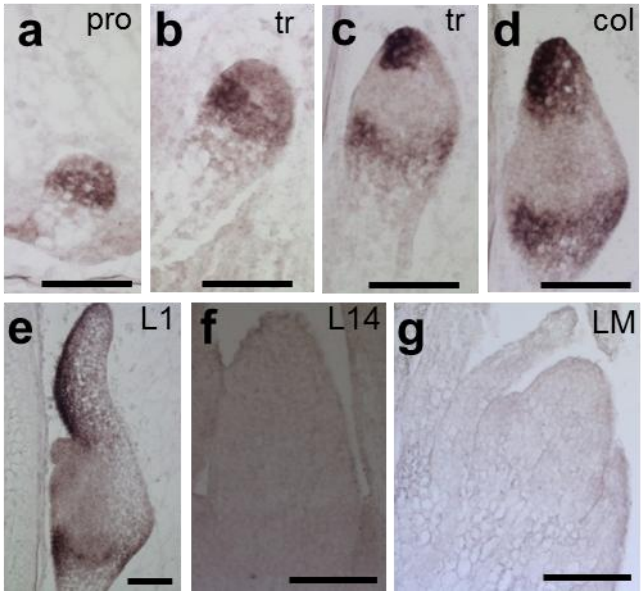

Figure 2.12 Cotyledon marker *ZmLEC1.*

In situ hybridizations illustrate the accumulation of *ZmLEC1* transcripts during embryogenesis (a-e) and in fourteen day old seedlings (f,g).

Pro, proembryo; tr, transition phase; col, coleoptile stage; L1, leaf 1 stage; L14; 14 day old seedling SAM; LM, lateral meristem.
Scale bars represent 100μm.

SPATULA, *AINTEGUMENTA*, and *ENHANCED DOWNY MILDEW2*; Ichihashi *et al.,* 2010; Mizukami and Fischer, 2000; Tsuchiya and Eulgem, 2010). Additional examples include the YABBY-like transcription factor implicated to function during leaf midrib formation (*DROOPING LEAF1* (*DL1*)), and homologs of the microRNA biogenesis gene (*SERRATE*; Yamaguchi *et al.,* 2004; Clarke *et al.,* 1999; Laubinger *et al.,* 2008). Interestingly, *DL* transcripts accumulate in young leaf primordia, but not in the coleoptile or scutellum of rice embryos (Yamaguchi *et al.,* 2004), which indicates that the grass coleoptile attains some, but not all, foliar-leaf attributes.

Among the differentially accumulated transcripts identified in embryonic lateral organs are several that exhibit tissue/organ specific expression and are useful markers of embryo development, including: (1) the scutellum-specific *TAPETUM DETERMINANT1-LIKE* (*TDL1*; GRMZM2G176390); (2) the vasculature-specific *RAN-BINDING PROTEIN2* (*RANBP2*; GRMZM2G094353); (3) the coleorhiza-specific *POLLEN OLE E I-LIKE* (*OLE*; GRMZM2G040517); and (4) two epidermis-specific maize *LIPID TRANSFER PROTEINS* (*LTP*1*; GRMZM2G101958 and *LTP*2*; GRMZM2G083725). Transcripts of *TDL1* are first detected in the tip of the developing scutellar hood at the transition stage (Figure 2.13b) and in the outer cell layer of the scutellum in the coleoptile stage and L1 stage embryos (Figure 2.13c). No *TDL1* transcripts accumulate in the proembryo, or in the fourteen day old seedling SAM and lateral meristem (Figure 2.13a, d, e). *RANBP2* transcripts accumulate in the developing vasculature of all lateral organs elaborated in the embryo and in fourteen day old seedlings (Figure 2.13f-j). Transcripts of *OLE* accumulate in the basal region of transition-staged embryos, opposite that of the apical expression described for the

Figure 2.13 Differentially accumulated transcripts during the elaboration of embryonic organs.

In situ hybridizations illustrate transcript accumulation of *TDL1* (a-e), *RANBP2* (f-j), *OLE* (k-o), *LTP*1* (p-t), and *LTP*2* (u-z).

Pro, proembryo; tr, transition phase; col, coleoptile stage; L1, leaf 1 stage; L14; 14 day old seedling SAM; LM, lateral meristem; 24 DAP, embryo harvested 24 days after pollination.
Scale bars represent 100μm.

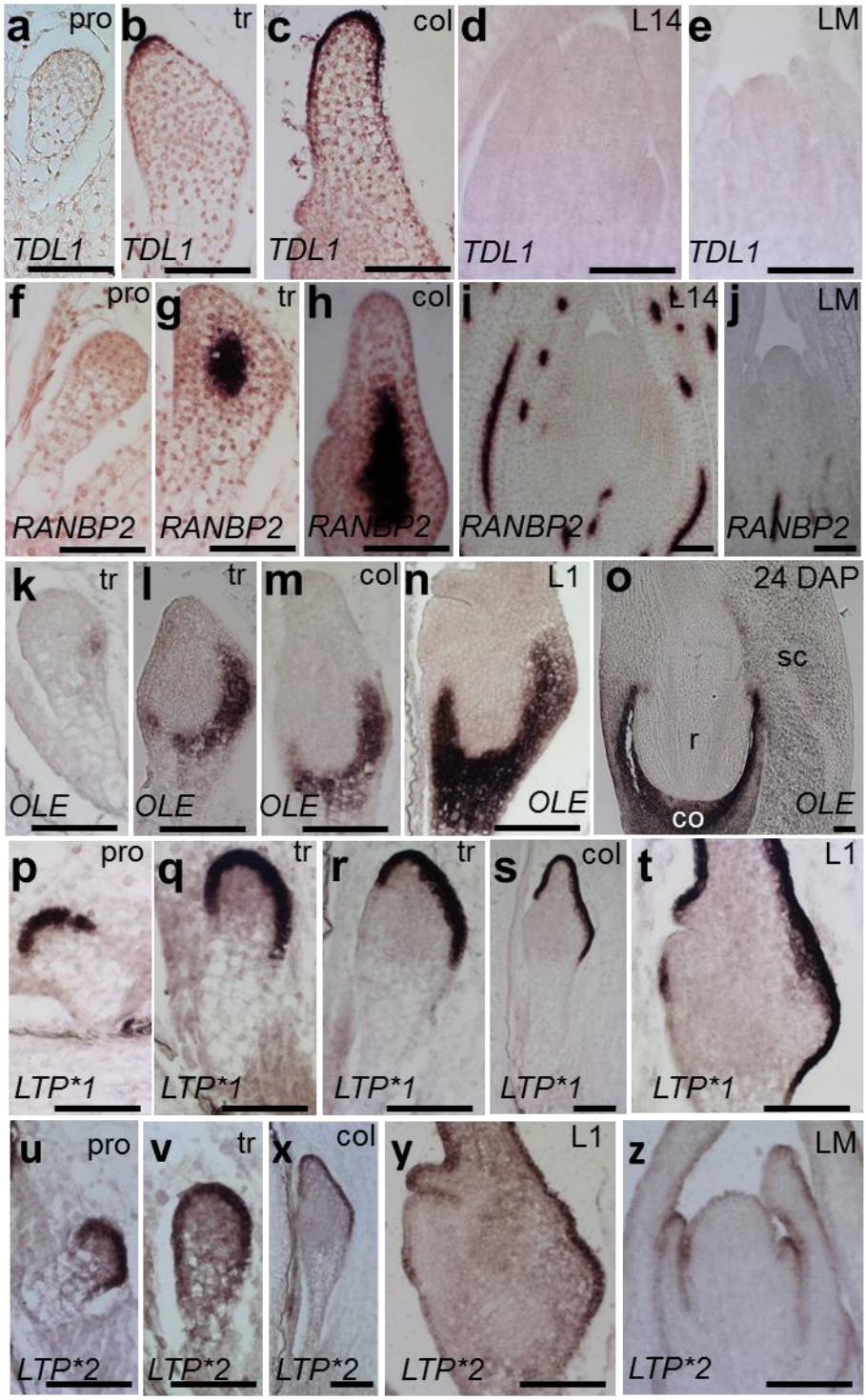
a pro
TDL1
b tr
TDL1
c col
TDL1
d L14
TDL1
e LM
TDL1
f pro
RANBP2
g tr
RANBP2
h col
RANBP2
i L14
RANBP2
j LM
RANBP2
k tr
OLE
l tr
OLE
m col
OLE
n L1
OLE
o 24 DAP
sc
r
co
OLE
p pro
LTP*1
q tr
LTP*1
r tr
LTP*1
s col
LTP*1
t L1
LTP*1
u pro
LTP*2
v tr
LTP*2
x col
LTP*2
y L1
LTP*2
z LM
LTP*2

scutellum marker *ZYB16* (Figure 2.13k, l; Figure 2.6c). As development proceeds, *OLE* transcripts are restricted to the basal region of the embryo that eventually defines the coleorhiza, a sheathing structure that surrounds the maize primary root (Figure 2.13m-o). The two protodermal markers, *LTP*1* and *LTP*2*, are expressed in the apical regions of the proembryo and early transition-staged embryo (Figure 2.13p, q, u, v), where after these *LTP* transcripts accumulate in the emerging scutellum of the late transition-staged embryo (Figure 2.13r). Subsequently, *LTP*1* and *LTP*2* localize to the epidermal cell layer of embryonic lateral organs (Figure 2.13s, t, x-z).

Other useful developmental markers identified in our RNA-seq analyses include the homolog of an *Arabidopsis LIGHT-DEPENDENT SHORT HYPOCOTYLS 1* and *ORYZA LONG STERILE LEMMA1* (*ALOG*) transcript *ALOG*1* (GRMZM2G087267) that is implicated during specification of organ boundaries, and two gene transcripts of unknown predicted function, designated as *UNKNOWN*1* (*UNK*1*; GRMZM2G038497) and *UNKNOWN*2* (*UNK*2*; GRMZM073192). In maize embryos, *ALOG*1* transcripts demarcate the boundary between all lateral organs and the developing SAM (Figure 2.14a-e). *UNK*1* transcripts first accumulate in a few cells at the site of organ initiation and then become localized to the adaxial side of the emerging lateral organ (Figure 2.14f-j). In contrast, *UNK*2* transcripts are detected in the emerging tips of all embryonic lateral organs (Figure 2.14k-o). The similar accumulation patterns of these three transcripts during elaboration of the scutellum, coleoptile, and first foliar leaf further supports the model ascribing leaf homology to the scutellum and the coleoptile.

Comparative transcriptomic analyses of juvenile, adult, and husk foliar leaves

Juvenile and adult foliar leaves of maize exhibit significant morphological

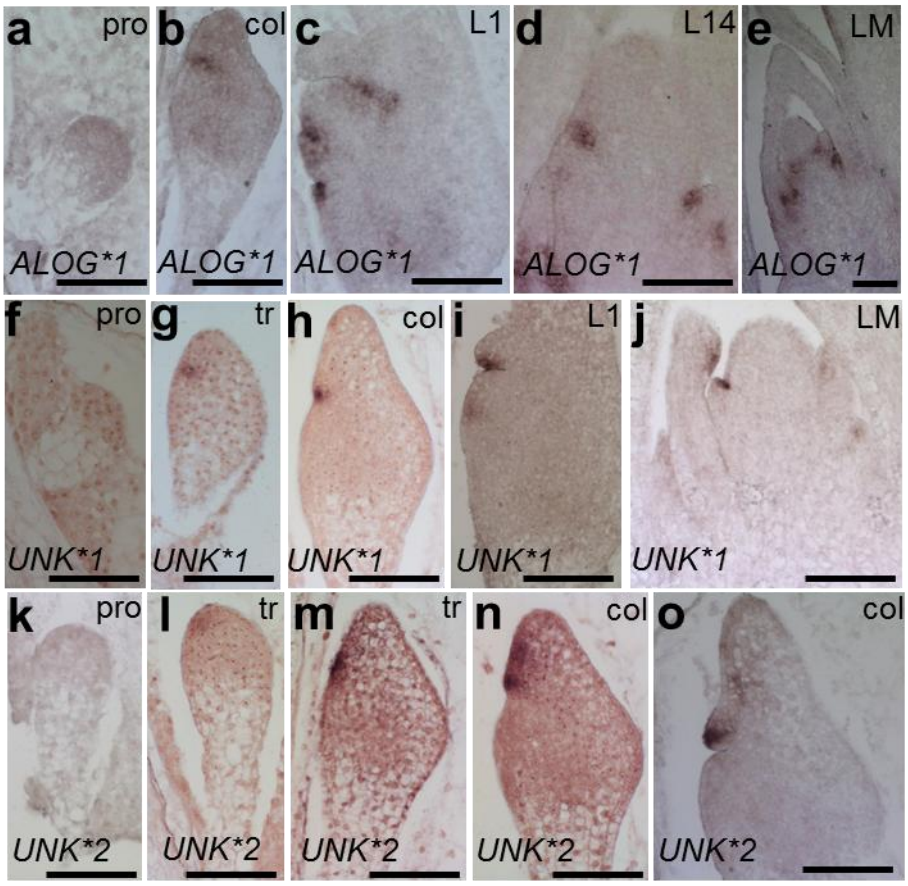

Figure 2.14 Developmental markers identified in RNA-seq analyses.

In situ hybridizations illustrate transcript accumulation of *ALOG*1* (a-e), *UNK*1* (f-j), and *UNK*2* (k-o).

Pro, proembryo; tr, transition phase; col, coleoptile stage; L1, leaf 1 stage; L14; 14 day old seedling SAM; LM, lateral meristem.
Scale bars represent 100μm.

differences. Juvenile leaves are short and narrow, accumulate epicuticular waxes but no epidermal hairs, and lateral meristems of juvenile nodes form long vegetative shoots tipped by a male inflorescence (tassel; Poethig, 1988; Poethig, 1990; Moose and Sisco, 1994). In contrast, adult leaves are long and broad, have epidermal hairs but accumulate little epicuticular waxes, and adult lateral meristems form short branches that initiate husk leaves and form a female inflorescence (ear) (Poethig, 1988; Poethig, 1990; Moose and Sisco, 1994). Furthermore, leaves initiated from both the SAM and from juvenile lateral meristems differ in many ways from husk leaves formed from adult-staged lateral meristems. Compared to foliar leaves, husk leaves have a lower vein density (Langdale *et al.,* 1988), accumulate RUBISCO in mesophyll as well as bundle sheath cells (Pengelly *et al.,* 2011), and make a greater contribution to grain filling (Fujita *et al.,* 1994; Sawada *et al.,* 1995).

A complex interactive network of phase-specific transcription factors and regulatory small RNAs control vegetative and reproductive phase change in plants (Chuck *et al.,* 2007; Moose and Sisco, 1996; Lauter *et al.,* 2005; Hultquist and Dorweiler, 2008). To examine the transcriptional differences among juvenile-staged SAMs, adult-staged SAMs, and lateral shoot meristems on a genomic scale, the SAM and youngest leaf primordium were microdissected from L1-stage embryos and L14 staged seedlings, and lateral meristems were isolated from L14 stage seedlings. RNA-seq analyses and pairwise comparisons of these three microdissected samples identified a total of 5,103 up-regulated transcripts. Twelve major patterns (clusters) of transcript accumulation were identified in the three-way comparisons (Figure 2.15). Cluster six is the largest and comprises 1,121 transcripts that were up-regulated at the

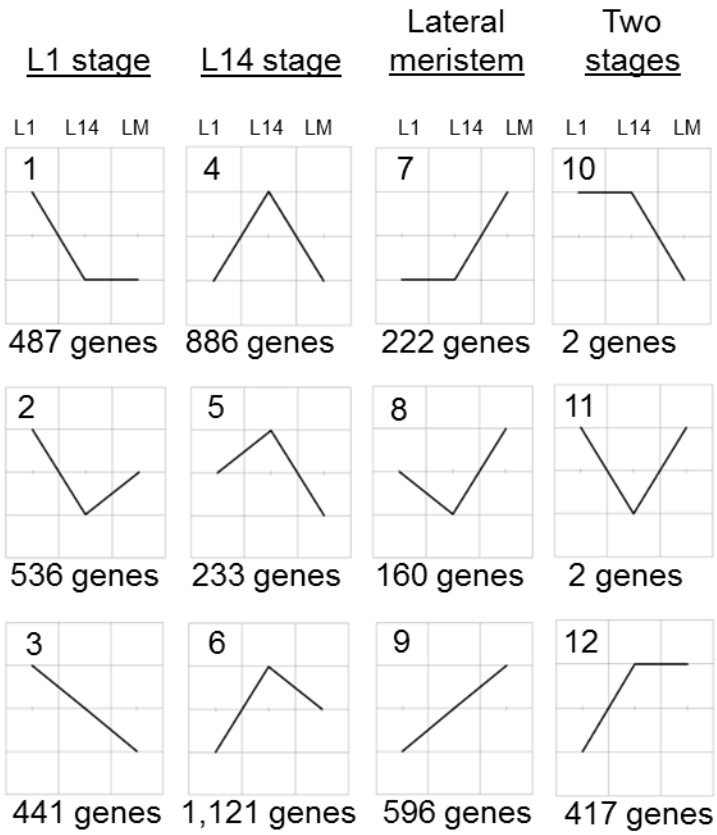

Figure 2.15 Clusters of up-regulated genes during vegetative leaf initiation of a juvenile, adult, and husk leaf.

12 clusters were generated based on the transcript accumulation of the 5,103 up-regulated genes when making the three-way comparison of the L1 stage, L14 stage, and lateral meristem.

L1, Stage L1; L14, Stage L14; LM, lateral meristem.

L14 stage compared to the L1 stage. Other large clusters include: (a) cluster 4 (886 transcripts), which comprises transcripts up-regulated at the L14 stage compared to both the L1 stage and lateral meristem; (b) cluster 9 (596 transcripts), comprising transcripts up-regulated in the lateral meristem compared to the L1 stage; and (c) cluster 2 (536 transcripts), which comprises transcripts up-regulated in the L1 stage as compared to the L14 stage. A Fisher's exact test was performed to identify enriched functional groups within the twelve gene clusters (Figure 2.16). Functions enriched during the initiation of a juvenile leaf include: RNA processing and binding (cluster two); DNA synthesis, repair, and chromatin remodeling (cluster three); protein synthesis and targeting (clusters one and two); and the tricarboxylic acid cycle (TCA; cluster one). The only category exclusively enriched in the lateral meristem is unknown function (cluster nine), which reflects the relative paucity of studies conducted on lateral meristem development in maize. Consistent with differences in cell wall composition between juvenile and adult foliar leaves, transcripts implicated in cell wall synthesis and degradation are enriched in both the L14 stage SAM and lateral meristems (cluster twelve; Abedon *et al.,* 2006).

Transcription factors implicated to function in vegetative phase change were differentially expressed between juvenile and adult leaves. As previously described, eight *SQUAMOSA-PROMOTER BINDING PROTEIN-LIKE* (*SPL*) transcripts, targeted by the juvenile-stage regulatory RNA miR156, were up-regulated in the L14 stage and lateral meristems (Chuck *et al.,* 2007; Strable *et al.,* 2008; Hultquist and Dorweiler, 2008). In addition, *GLOSSY15* (*GL15*), an AP2-like transcription factor that promotes the adult leaf identity, is up-regulated in fourteen day old seedlings (Lauter *et al.,*

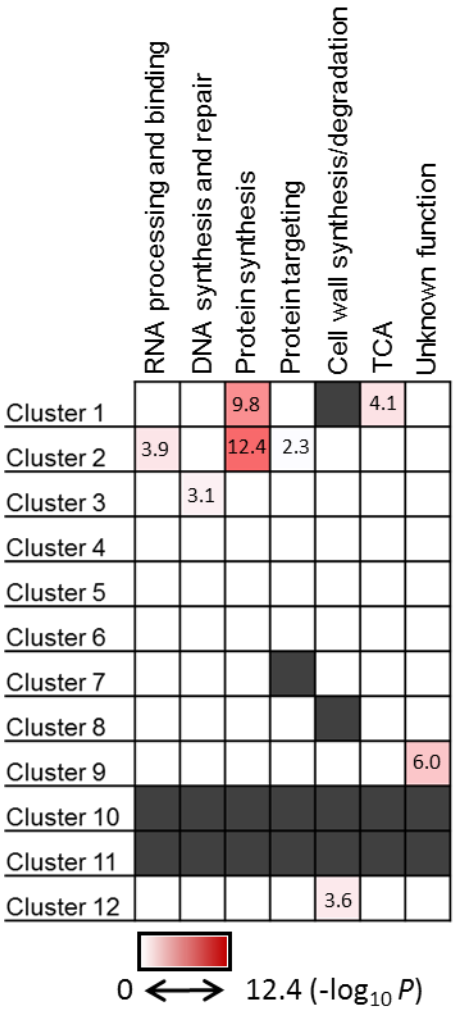

Figure 2.16 Functional category enrichment of gene clusters during vegetative leaf initiation of a juvenile, adult, and husk leaf.

Functional category enrichment of the twelve clusters presented in Figure 2.15.

-$\log_{10}P$ value, FDR5% is included for significant enrichment. White is non-significant. Red is significant enrichment. Gray is no genes present in the category for that cluster.

2005; Evans *et al.,* 1994; Moose and Sisco, 1996). Transcriptional profiles of husk leaves are more similar to L14 stage than L1 stage leaves as illustrated by the 417 gene transcripts that were up-regulated in both the L14 stage SAM and the lateral meristem versus the L1 stage SAM (cluster twelve). This is consistent with previous studies showing that, once initiated, vegetative phase change is comprehensive and affects all subsequently elaborated organs of the maize shoot (Poethig, 1990).

Two transcripts up-regulated during husk leaf initiation (*ALOG*2* GRMZM2G034385 and *LTP*3*) were analyzed by *in situ* hybridization. *ALOG*2* transcripts accumulate in the lateral organ boundaries of all three samples, suggesting a conserved function in defining foliar and husk leaves (Figure 2.17a-c). However *LTP*3* transcripts accumulate in the outer cell layer of young leaf primordia and in the tunica of the lateral meristems, but are excluded from the L1 stage and L14 stage SAMs (Figure 2.17d-f). Although the lateral meristem and the L14 stage SAM are both initiating vegetative leaves, a total of 1,505 transcripts were up-regulated (clusters 4, 5, 6, 7, 8, 10, and 11), which reflects distinct developmental genetic mechanisms within these shoot meristems.

Conclusion

From the time the SAM forms during embryogenesis, to when it is mature and initiating leaves, its transcriptome undergoes dynamic changes. Analysis of transcript accumulation before and after a meristem is present identified *ZYB16*, a gene implicated to function in lateral organ initiation. Expression of *ZYB16* before *KN1* suggests the SAM function to initiate lateral organs precedes the function to maintain stem cells. Transcriptomic analysis of a newly formed SAM reveals that the embryo is

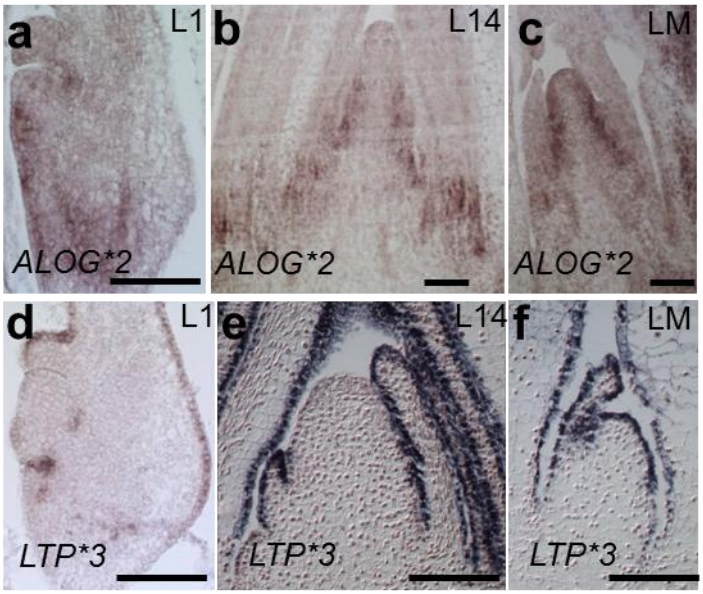

Figure 2.17 Differentially accumulated transcripts during vegetative leaf initiation of a juvenile, adult, and husk leaf.

In situ hybridizations using the following probes: (a-c) *ALOG*2* and (d-f) *LTP*3*.

L1, leaf 1; L14, leaf 14; LM, lateral meristem.
Scale bars represent 100 μm.

still establishing apical and basal domains and is accumulating storage products to utilize during germination; whereas a mature meristem is enriched for transcripts that function in transcriptional regulation, hormone signaling and metabolism, and transport. Examination of the transcript accumulation in lateral organs elaborated during embryogenesis has provided support that the maize cotyledon is a leaf-like bimodal structure composed of both the scutellum and the coleoptile. Finally, the three-way comparison between the initiation of juvenile, adult, and husk leaves reveals significant phase-specific and meristem-specific transcriptional differences. Novel molecular markers were identified that specify the cotyledon, the scutellum, the vasculature, the coleorhiza, initiating lateral organs, lateral organ boundaries, and the protoderm derived tissues. Finally, all data is publicly available at Maize Genetics and Genome database.

Methods

Plant growth conditions and sample preparation

To prepare shoot apical meristem (SAM) and lateral meristems from fourteen day old seedlings, plants from a B73 background were grown in a growth chamber with 16 hours light/25°C and 8 hours dark/22°C cycle. Seedlings harvested fourteen days after planting were dissected to remove roots and excess shoot structures as described (Scanlon *et al.,* 2009). To prepare embryo samples, plants from a B73 inbred background grown to maturity were self-pollinated. The tips of whole kernels harvested from 5 days after pollination (DAP) through 13 DAP were excised and discarded to allow the fixative to infiltrate the remainder of the kernel that contains the embryo.

Tissue fixation, embedding, sectioning, and laser microdissection (LM)

The fourteen day old SAM and lateral meristem samples and the kernel samples containing the developing embryos were fixed overnight at 4°C in Farmer's Fixative (3:1 ethanol: acetic acid) and dehydrated. After fixation, samples were prepared as described (Scanlon *et al.,* 2009). Briefly, the samples were run through an ethanol/xylenes series followed by a xylene/paraplast series before being embedded in paraplast. Embedded samples were sectioned using a rotary microtome (Model RM 2235, Leica Microsystems). The 10 µm thick sections from the fourteen day old seedling and kernel samples were mounted on VWR VistaVision HistoBond Adhesive Slides (VWR International) with DEPC-treated MQ-H2O. The slides with the sectioned samples were dried overnight at 40°C and then stored in a sealed vacuum chamber until LM was performed. LM was performed using a P.A.L.M. Laser Microbeam (P.A.L.M. Microlaser Technologies) using version 3.0.0.9 software.

RNA isolation and amplification

Total RNA was isolated from the collected cells using the Arcturus PicoPure RNA Isolation Kit (Applied Biosystems by Life Technologies). DNaseI treatement was performed during the RNA isolation using Qiagen DNaseI. RNA amplification was performed using the TargetAmp™ 2-Round Aminoallyl-aRNA Amplification Kit 1.0 (Epicentre Biotechnologies). The Bioanalyzer 2100 (Agilent Technologies) was used to determine the quality of the amplified RNA.

cDNA library preparation and Illumina RNA-seq

The cDNA libraries were prepared using the standard Illumina mRNA-seq sample prep kits (revision D, catalog number RS-930-1001) using paired-end adaptors. The samples were run in single lanes on the Illumina Genome Analyzer model GAIIx**.**

Transcript quantification of the RNA-seq data was performed using updated software as described (*Li et al.,* 2010). Reads were aligned to the maize genome assembly (RefGen version 1, http://www.maizesequence.org) and the annotated exon junctions (version 4a53, http://www.maizesequence.org) with BWA (Li *et al.,* 2009), allowing up to two mismatches. Reads assigned to each transcript were calculated by adding up reads aligned to exons and exon junctions.

Normalization and identification of differential transcript accumulation

Count data for each transcript were modeled as overdispersed Poisson random variables. The log of the Poisson mean for each count was modeled as the sum of a transcript-specific sample effect and an experimental-unit-specific offset parameter. Following Bullard *et al.,* (2010), the log of the upper quartile of the experimental-unit-specific count distribution across transcripts was used as the offset to account for variation in library size across experimental units. A separate overdispersion parameter was estimated for each transcript using the sum of the squared Pearson residuals divided by the error degrees of freedom for each transcript (12-6=6). The small fraction of overdispersion parameter estimates that were less than 1 were replaced by 1 to disallow underdispersion.

For each transcript, tests for differences between sample effects were conducted by comparing the likelihood ratio statistic divided by the estimated overdispersion parameter to an F distribution with 6 denominator degrees of freedom and either 1 or 5 numerator degrees of freedom (1 for pairwise comparison of samples and 5 for the overall test for any differences among the six samples). The p-values from these tests were converted to q-values using the method of Nettleton *et al.,* (2006). The q-values

were used to control false discovery rates as described (Storey and Tibshirani, 2003). Estimates of fold change between any pair of cell types were obtained by exponentiating the difference in sample effect estimates.

Normalized expression level is reported as reads per million mapped sequences (RPM) because LM and poly(A) tail based RNA amplification methods result in a bias of sequence alignments toward the 3' end of the transcript rather than equal distribution across the entire cDNA (Emrich *et al.,* 2007; Li *et al.,* 2010).

***In situ* hybridizations**

Dissected seedlings and the remaining portions of the kernels or seedlings were fixed in FAA, embedded, sectioned, and hybridized using gene-specific probes as previously described (Jackson, 1991). Gene specific primers designed for probe synthesis can be found in Table 2.1. Post-hybridization slides were imaged using the Zeiss AxioCam MRc5 and AxioVision Release 4.6 software.

Accession codes RNA-seq data reported here have been deposited to Maize GDB and are available online at http://www.maizegdb.org under Shoot Apical meristem at Six Stages [from the Scanlon lab-SAM Group].

Acknowledgements

Funding provided by National Science Foundation (Grant #IOS 0820610 to M.J.S.).

REFERENCES

Abbe, E.C. and Stein, O.L. The growth of the shoot apex in maize: embyrogeny. *Am. J. Bot.* **41**(4), 285-293 (1954).

Abedon, B.G., Hatfield, R.D., and Tracy, W.F. Cell wall composition in juvenile and adult leaves of maize (*Zea mays* L.). *J. Agric. Food Chem.* **54**, 3896-3900 (2006).

Aida, M., Ishida, T., and Tasaka, M. Shoot apical meristem and cotyledon formation during *Arabidopsis* embryogenesis: interaction among the *CUP-SHAPED COTYLEDON* and *SHOOT MERISTEMLESS* genes. *Development* **126**, 1563-1570 (1999).

Bellauoui, M. *et al.,* The Arabidopsis BELL1 and KNOX TALE homeodomain proteins interact through a domain conserved between plants and animals. *Plant Cell* **13**, 2455-2470 (2001).

Boyd, L. Evolution in the monocotyledonous seedling, a new interpretation of the grass embryo. *Trans. Bot. Soc. Edinburgh* **30**, 286-302 (1931).

Breuninger, H., Rikirsch, E., Hermann, M., Ueda, M., and Laux, T. Differential expression of *WOX* genes mediates apical-basal axis formation in the *Arabidopsis* embryo. *Developmental Cell* **14**, 867-876 (2008).

Brooks III, L., Strable, J., Zhang, X., Ohtsu, K., Zhou, R., Sarkar, A., Hargreaves, S., Elshire, R.J., Eudy, D., Pawlowska, T., Ware, D., Janick-Buckner, D., Buckner, B., Timmermans, M.C.P., Schnable, P.S., Nettleton, D., and Scanlon, M.J. Microdissection of shoot meristem functional domains. *PLoS Genet.* **5**(5)**,** e1000476 (2009).

Bullard, J.H., Purdom, E., Hansen, K.D., and Dudoit, S. Evaluation of statistical methods for normalization and differential expression in mRNA-Seq experiments. *BMC Bioinformatics* (2010). 11:94doi:10.1186/1471-2105-11-94

Byrne, M.E. A role for the ribosome in development. *Trends in Plant Science* **14**(9), 512-519 (2009).

Chuck, G., Cigan, A.M., Saeteurn, K., and Hake, S. The heterochronic maize mutant *Corngrass1* results from overexpression of a tandem microRNA. *Nature Genet.* **39**(4), 544-549 (2007).

Clarke, J.H., Tack, D., Findlay, K., van Montagu, M., and van Lijsebettens, M. The *SERRATE* locus controls the formation of the early juvenile leaves and phase length in *Arabidopsis. Plant J.* **20**(4), 493-501 (1999).

Emrich, S.J., Barbazuk, W.B., Li, L., and Schnable, P.S. Gene discovery and annotation using LCM-454 transcriptome sequencing. *Genome Res.* **17**, 69-73 (2007).

Evans, M.M.S., Passas, H., and Poethig, R.S. Heterochronic effects of glossy15 mutations on epidermal cell identity in maize. *Development* **120**, 1971-1981 (1994).

Evans, M.M.S. The *indeterminate gametophyte1* gene of maize encodes a LOB domain protein required for embryo sac and leaf development. *Plant Cell* **19**, 46-62 (2007).

Fujita, K., Furuse, F., Sawada, O., and Bandara, D. Effect of defoliation and ear removal on dry matter production and inorganic element absorption in sweet corn. *Soil Sci. Plant Nutr.* **40**(4), 581-591 (1994).

Haecker, A. *et al.,* Expression dynamics of WOX genes mark cell fate decisions during early embryonic patterning in *Arabidopsis thaliana. Development* **131,** 657-668 (2004).

Hay, A., and Tsiantis, M. KNOX genes: versatile regulators of plant development and diversity. *Development* **137**, 3153-3165 (2010).

Hultquist, J.F., and Dorweiller, J.E. Feminized tassels of maize *mop1* and *ts1* mutants exhibit altered levels of miR156 and specific SBP-box genes. *Planta* **229**, 99-113 (2008).

Ichihashi, Y., Horiguchi, G., Gleissberg, S., and Tsukaya, H. The bHLH transcription factor *SPATULA* controls final leaf size in *Arabidopsis thaliana. Plant Cell Physiol.* **51**(2), 252-261 (2010).

Jackson, D. *In situ* hybridization in plants. In *Molecular Plant Pathology: A Practical Approach*, D.J. Bowles, S.J. Gurr, and M. McPherson, eds. Oxford University Press, Oxford, UK, 1991.

Jackson, D., Veit, B., and Hake, S. Expression of maize KNOTTED1 related homeobox genes in the shoot apical meristem predicts patterns of morphogenesis in the vegetative shoot. *Development* **120**, 405-413 (1994).

Jia, Y., Lisch, D.R., Ohtsu, K., Scanlon, M.J., Nettleton, D., Schnable, P.S. Loss of RNA-dependent RNA Polymerase2 (RDR2) function causes widespread and unexpected changes in the expression of transposons, genes, and 24-nt small RNAs. *PLoS Genet.* **5**(11)**,** e1000737 (2009).

Juarez, M.T., Twigg, R.W., and Timmermans, M.C.P. Specification of adaxial cell fate during maize leaf development. *Development* **131**, 4533-4544 (2004).

Kaplan, D.R. Early plant development: from seed to seedling to established plant. In *Principles of Plant Morphology, Chapter 5.* Berkeley, CA: Copy Central, University of California, Berkeley, 1996.

Kim, J.H., Choi, D., and Kende, H. The AtGRF family of putative transcription factors is involved in leaf and cotyledon growth in *Arabidopsis*. *Plant J.* **36**, 94-104 (2003).

Langdale, J.A., Zelitch, I., Miller, E., and Nelson, T. Cell position and light influence C4 versus C3 patterns of photosynthetic gene expression in maize. *Embo. J.* **7**, 3643-3651 (1988).

Laubinger, S. *et al.,* Dual roles of the nuclear cap-binding complex and SERRATE in pre-mRNA splicing and microRNA processing in *Arabidopsis thaliana. Proc. Natl. Acad. Sci. USA* **105**(25), 8795-8800 (2008).

Lauter, N., Kampani, A., Carlson, S., Goebel, M., and Moose, S.P. *microRNA172* down-regulates *glossy15* to promote vegetative phase change in maize. *Proc. Natl. Acad. Sci USA* **102**(26), 9412-9417 (2005).

Levesque, M.P. Whole-genome analysis of the SHORT-ROOT developmental pathway in *Arabidopsis. PLoS Biol.* **4**(5), e143 (2006).

Li, H., and Durbin, R. Fast and accurate short read alignment with Burrows-Wheeler Transform. *Bioinformatics* **25**,1754-60 (2009).

Li, P. *et al.,* The developmental dynamics of the maize leaf transcriptome. *Nat Genet.* **42**(12), 1060-7 (2010).

Lotan, T. *et al., Arabidopsis* LEAFY COTYLEDON1 is sufficient to induce embryo development in vegetative cells. *Cell* **93**(7), 1195-1205 (1998).

Mizukami, Y., and Fischer, R.L. Plant organ size control: *AINTEGUMENTA* regulates growth and cell numbers during organogenesis. *Proc. Natl. Acad. Sci. USA* **97**(2), 942-947 (2000).

Moose, S.P., and Sisco, P.H. *Glossy15* controls the epidermal juvenile-to-adult phase transition in maize. *Plant Cell* **6**, 1343-1355 (1994).

Moose, S.P., and Sisco, P.H. Glossy15, an APETALA2-like gene from maize that regulates leaf epidermal cell identity. *Genes & Dev.* **10**, 3018-3027 (1996).

Mu, J. *et al., LEAFY COTYLEDON1* is a key regulator of fatty acid biosynthesis in Arabidopsis. *Plant Phys.* **148**, 1042-1054 (2008).

Mukherjee, K., Brocchieri, L., and Burglin, T.R. A comprehensive classification and evolutionary analysis of plant homeobox genes. *Mol. Biol. Evol.* **26**(12), 2775-2794 (2009).

Muller, J. *et al., In vitro* interactions between barley TALE homeodomain proteins suggest a role for protein-protein associations in the regulation of *Knox* gene function. *Plant J.* **27**(1), 13-23 (2001).

Nardmann, J., Ji, J., Werr, W., and Scanlon, M.J. The maize duplicate genes *narrow sheath1* and *narrow sheath2* encode a conserved homeobox gene function in a lateral domain of shoot apical meristems. *Development* **131**, 2827-2839 (2004).

Nardmann, J., Zimmerman, R., Durantini, D., Kranz, E., and Werr, W. *WOX* gene phylogeny in *Poaceae*: a comparative approach addressing leaf and embryo development. *Mol. Biol. Evol.* **24**(11), 2474-2484 (2007).

Nardmann, J., and Werr, W. Patterning of the maize embryo and the perspective of evolutionary developmental biology. In *Handbook of Maize: Its Biology.* J. Bennetzen, and S. Hake, eds. Springer New York, New York, USA, 2009.

Nelson, T., Tausta, S.L., Gandotra, N., and Liu, T. Laser microdissection of plant tissue: what you see is what you get. *Annu. Rev. Plant Biol.* **57**, 181-201 (2006).

Nettleton, D., Hwang, J.T.G., Caldo, R.A., Wise, R.P. (2006). Estimating the number of true null hypotheses from a histogram of p-values. *J. Agri., Biol., Environ.l Stat..* **11,** 337-356 (2006).

Nogueira, F.T.S., Chitwood, D.H., Madi, S., Ohtsu, K., Schnable, P.S., Scanlon, M.J., Timmermans, M.C.P. Regulation of small RNA accumulation in the maize shoot apex. *PLoS Genet.* **5**(1)**,** e1000320 (2009).

Oh, E. *et al.,* PIL5, a phytochrome-interacting bHLH protein, regulates gibberellin responsiveness by binding directly to the *GAI* and *RGA* promoters in *Arabidopsis* seeds. *Plant Cell* **19**, 1192-1208 (2007).

Ohtsu, K., Smith, M.B., Emrich, S.J., Borsuk, L.A., Zhou, R., Chen, T., Zhang, X., Timmermans, M.C.P., Beck, J., Buckner, B., Janick-Buckner, D., Nettleton, D., Scanlon, M.J., and Schnable, P.S. Global gene expression analysis of the shoot apical meristem of maize (*Zea mays* L.). *Plant J.* **52**, 391-404 (2007).

Pengelly, J.J.L. *et al.,* Functional analysis of corn husk photosynthesis. *Plant Physiol.* **156**(2), 503-513 (2011).

Poethig, R.S., Coe Jr., E.H., and Johri, M.M. Cell lineage patterns in maize embryogenesis: A clonal analysis. *Developmental Biol.* **117**, 392-404 (1986).

Poethig, R.S. Heterochronic mutations affecting shoot development in Maize. *Genetics* **119**, 959-973 (1988).

Poethig, R.S. Phase change and the regulation of shoot morphogenesis in plants. *Science* **250**, 923-930 (1990).

Reiser, L., Sanchez-Baracaldo, P., and Hake, S. Knots in the family tree: evolutionary relationships and functions of *knox* homeobox genes. *Plant Mol. Biol.* **42**, 151-166 (2000).

Santa-Catarina, C., de Oliveira, R.R., Cutri, L., Floh, E.I.S., and Dornelas, M.C. WUSCHEL-related genes are expressed during somatic embryogenesis of the basal angiosperm *Ocotea catharinesis* Mex. (Lauraceae). *Trees-Structure and Function* **25**, 1-9 (2011).

Sarojam, R. *et al.,* Differentiating Arabidopsis shoots from leaves by combined YABBY activities. *Plant Cell* **22**, 2113-2130 (2010).

Sawada, O., Ito, J., and Fujita, K. Characteristics of photosynthesis and translocation of 13C-labelled photosynthates in husk leaves of sweet corn. *Crop Sci.* **35**, 480-485 (1995).

Scanlon, M.J., Ohtsu, K., Timmermans, M.C.P., and Schnable, P.S. Laser microdissection-mediated isolation and in vitro transcriptional amplification of plant RNA. *Curr. Prot. Mol. Biol.* 25A.3.1-25A.3.15 (2009).

Schnable, P.S., *et al.,* The B73 maize genome: complexity, diversity, and dynamics. *Science* **326**, 1112-1115 (2009).

Sen, T.Z. *et al.,* MaizeGDB becomes 'sequence-centric' *Database.* 2009:Vol. 2009:bap020.

Shen, B. *et al.,* Expression of *ZmLEC1* and *WRI1* increases oil production in maize. *Plant Phys.* **153**, 980-987 (2010).

Siegfried, K.R. *et al.,* Members of the *YABBY* gene family specify abaxial cell fate in *Arabidopsis*. *Development* **126**, 4117-4128 (1999).

Smith, L.G., Greene, B., Veit, B., and Hake, S. A dominant mutation in the maize homeobox gene, Knotted-1, causes its ectopic expression in leaf cells with altered fates. *Development* **116**, 21-30 (1992).

Smith, L.G., Jackson, D., and Hake, S. Expression of *knotted1* marks shoot meristem formation during maize embryogenesis. *Developmental Genet.* **16**, 344-348 (1995).

Smith, H.M.S., Boschke, I., and Hake, S. Selective interaction of plant homeodomain proteins mediates high DNA-binding affinity. *Proc. Natl. Acad. Sci. USA* **99**(14), 9579-9584 (2002).

Storey, J. D., and Tibshirani, R. Statistical significance for genomewide studies. *Proc. Natl. Acad. Sci.* **100**, 9440-9445 (2003).

Strable, J., Borsuk, L., Nettleton, D., Schnable, P.S., and Irish, E.E. Microarray analysis of vegetative phase change in maize. *Plant J.* **56**, 1045-1057 (2008).

Suzuki, M. *et al.,* The maize *Viviparous8* locus, encoding a putative ALTERED MERISTEM PROGRAM1-like peptidase regulates abscisic acid accumulation and coordinates embryo and endosperm development. *Plant Phys.* **146**, 1193-1206 (2008).

Thimm, O. *et al.,* MAPMAN: a user-driven tool to display genomics data sets onto diagrams of metabolic pathways and other biological processes. *Plant J.* **37**, 914-939 (2004).

Tsuchiya, T., and Euglem, T. Co-option of EDM2 to distinct regulatory modules in *Arabidopsis thaliana* development. *BMC Plant Biol.* **10**, 1-14 (2010).

Tzafrir, I. *et al.,* Identification of genes required for embryo development in Arabidopsis. *Plant Physiol.* **135**, 1206-1220 (2004).

Vroeman, C.W., Mordhorst, A.P., Albrecht, C., Kwaaital, M.A.C.J., and de Vries, S.C. The *CUP-SHAPED COTYLEDON3* gene is required for boundary and shoot meristem formation in Arabidopsis. *Plant Cell* **15**(7), 1563-1577 (2003).

Weatherwax, P. Position of the scutellum and homology of coleoptile in maize. *Bot. Gaz.* **69**, 179-182 (1920).

Weijers, D. *et al.,* An *Arabidopsis* Minute-like phenotype caused by a semi-dominant mutation in a *RIBOSOMAL PROTEIN S5* gene. *Development* **128**, 4289-4299 (2001).

Wu, X., Chory, J., and Weigel, D. Combinations of *WOX* activities regulate tissue proliferation during *Arabidopsis* embryonic development. *Developmental Biol.* **309**, 306-316 (2007).

Yamaguchi, T. The *YABBY* gene *DROOPING LEAF* regulates carpel specification and midrib development in *Oryza sativa*. *Plant Cell* **16**, 500-509 (2004).

Zhang, D-F. *et al.,* Isolation and characterization of genes encoding GRF transcription factors and GIF transcriptional coactivators in Maize (*Zea mays* L.). *Plant Sci.* **175**, 809-817 (2008).

Zhang, S., Wong, L., Meng, L., and Lemaux, P.G. Similarity of expression patterns of *knotted1* and *ZmLEC1* during somatic and zygotic embryogenesis in maize (*Zea mays* L.). *Planta* **215**, 191-194 (2002).

Zhang, X. *et al.,* Laser microdissection of narrow sheath mutant maize uncovers novel gene expression in the shoot apical meristem. *PLoS Genet.* **3**(6), e101 (2007).

Zhao, Y. *et al.,* HANABA TARANU is a GATA transcription factor that regulates shoot apical meristem and flower development in Arabidopsis. *Plant Cell* **16**, 2586-2600 (2004).

Zimmermann, R., and Werr, W. Pattern formation in the monocot embryo as revealed by *NAM* and *CUC3* orthologues from *Zea mays* L. *Plant Mol. Biol.* **58**, 669-685 (2005).

CHAPTER 3

DISCOLORED1 (DSC1) is an ADP-RIBOSYLATION FACTOR-GTPase ACTIVATING PROTEIN (ARF-GAP) required to maintain differentiation of maize kernel structures[1]

1 Takacs, E.M., Suzuki, M., Meeley, R., and Scanlon, M.J. authors contributing to manuscript.

Abstract

Double fertilization evolved in the angiosperm lineage and gives rise to the clonally-distinct embryo and endosperm of the developing seed. Recessive mutations in *DISCOLORED1* (*DSC1*) gives rise to nonviable mutant kernels that are defective in both embryo and endosperm development. Here, detailed phenotypic analyses illustrate that *dsc1-R* mutant kernels are able to establish but fail to maintain differentiated embryo and endosperm structures. Development of the embryo and endosperm is normal albeit delayed, prior to the abortion and subsequent degeneration of differentiated kernel structures. Using a genomic fragment that was previously isolated by transposon tagging, the full length *DSC1* transcript is identified and shown to encode an ADP-RIBOSYLATION FACTOR-GTPase ACTIVATING PROTEIN (ARF-GAP) that co-localizes with the *trans*-Golgi network/early endosomes and the plasma membrane during transient expression assays in *N. benthamiana* leaves. A role for DSC1 function during endomembrane trafficking and the maintenance of maize kernel differentiation is discussed.

Introduction

The mature maize kernel is a single-seeded fruit composed of the triploid endosperm, the diploid embryo, and the maternally derived pericarp, pedicel, and placenta. During germination the endosperm nurtures the embryo as it matures into a seedling. Development of the clonally distinct endosperm and embryo ensues following double fertilization of the female gametophyte. The fertilized central cell gives rise to the triploid endosperm, which becomes cellularized four days after pollination (DAP; reviewed in Olsen, 2001). Four distinct structures differentiate to comprise the mature

maize endosperm, and include: the basal endosperm transfer layer (BETL); the embryo surrounding region (ESR); the starchy endosperm; and the aleurone. The BETL forms at the base of the kernel and facilitates the transfer of maternally derived nutrients and photosynthates from the placenta into the developing endosperm (Brink and Cooper, 1947; Kiesselbach and Walker, 1952). Distinguishing features of the BETL are the cell wall projections that increase the surface area of the plasma membrane, and thus facilitate the transport function of these cells (reviewed in Thompson *et al.,* 2001). The ESR forms around the earliest-staged embryo (the proembryo) and has a predicted function in signaling between the developing embryo and the endosperm (Schel *et al.,* 1984; Opsahl-Ferstad *et al.,* 1997). Functioning as energy reserves, starchy endosperm cells accumulate starch and proteins that are later digested in order to nurture the germinating seedling (Duvik, 1961). Cuboidal-shaped aleurone cells form a single-cell layer that encompasses the starchy endosperm; during germination the aleurone functions to digest the stored energy reserves in the kernel (Young and Gallie, 2000). Aleurone cells are clonally related to starchy endosperm cells and can re-differentiate into starchy cells late in development in the absence of an unknown cell-to-cell signaling cascade that is required to maintain the aleurone-specific cell fate (Becraft and Asuncion-Crabb, 2000).

The diploid embryo is derived from the fertilized egg cell, and at maturity is composed of the shoot and root apical meristems, the scutellum, five to six foliar leaves protected by the sheathing leaf-like coleoptile, and a primary root protected by the sheathing coleorhiza (Abbe and Stein, 1954). Embryo development is marked by key developmental events (Kaplan and Cooke, 1997) comprising the pre-meristematic

proembryo, the establishment of the shoot apical meristem (SAM), and the elaboration of three distinct varieties of lateral organs (the scutellum, the coleoptile, and foliar leaves). Historically, these key events in maize embryo development have been described in nine stages (Abbe and Stein, 1954) and include: (1) the proembryo, before the meristem is formed; (2) the transition stage, when the SAM is established; (3) the coleoptile stage, after the SAM has formed and initiates the coleoptile; and (4) the L1-L6 stage, when the SAM initiates the first six foliar leaves (Abbe and Stein, 1954; Poethig *et al.,* 1986). During embryogenesis transcriptional markers including *KNOTTED1* (*KN1*), *RAN-BINDING PROTEIN2* (*RANBP2*), and *Zea mays YABBY14* (*ZYB14*) identify the SAM, vasculature, and lateral organs (the scutellum, the coleoptile, and foliar leaves), respectively (Smith *et al.,* 1992; Smith *et al.,* 1995; Jackson *et al.,*1994; Juarez *et al.,* 2004; Takacs *et al.,* unpublished).

DEFECTIVE KERNEL (*DEK*) mutations condition defects in both embryo and endosperm development, and thus are useful genetic tools to study kernel development (Neuffer and Sheriden, 1980; Scanlon *et al.,* 1994). Several *DEK* mutants have defects in the epidermal patterning of the embryo, and in the maintenance of the aleurone cell layer of the endosperm (Becraft and Asuncion-Crabb, 2000; Becraft *et al.,* 1996; Lid *et al.,* 2002; Shen *et al.,* 2003; Becraft *et al.,* 2002; Kessler *et al.,* 2002). Some of the genes identified underlying these *DEK* mutations (*DEFECTIVE KERNEL1* (*DEK1*), *CRINKLY4* (*CR4*), and *SUPERNUMERY ALEURONE1* (*SAL1*)) maintain differentiation of aleurone cells during kernel development by functioning in cell-to-cell signaling pathways (Becraft *et al.,* 1996; Lid *et al.,* 2002; Shen *et al.,* 2003). Both *DEK1* and *CR4* encode proteins anchored at the plasma membrane that are required to maintain

aleurone cell fate (Becraft *et al.,* 1996; Becraft and Asuncion-Crabb, 2000; Lid *et al.,* 2002). *DEK1* encodes a trans-membrane domain protein with a cytoplasmic calpain-like protease (Lid *et al.,* 2002); *CR4* encodes a tumor necrosis factor receptor-like receptor kinase (Becraft *et al.,* 1996). In contrast, *SAL1* functions to inhibit aleurone cell fate during kernel development and encodes an E class vacuolar sorting protein (Shen *et al.,* 2003), which implicates an essential role for endomembrane trafficking in endosperm differentiation.

Endomembrane trafficking sorts and delivers cargo from one membrane-bound compartment of the plasma membrane to another (reviewed in Takai *et al.,* 2001). As a result, endomembrane trafficking is responsible for mediating intracellular and intercellular transport of proteins, cell wall pectins, structural sterols, receptors, lipids, and signaling molecules (Samaj *et al.,* 2005; Cosgrove, 1997). Endomembrane trafficking is regulated in part by the cyclic activity of ARF-GTPases, which cycle between active and inactive forms that correlate with vesicle formation and dissociation, respectively (Nie and Randazzo, 2006). Active ARF-GTPases associate with GTP and are membrane-bound during vesicle formation; inactive ARF-GTPases associate with GDP in the cytosol, and function in vesicle dissociation. These cyclic activities of ARF-GTPases are regulated by ADP-RIBOSYLATION FACTOR-GUANINE EXCHANGE FACTORS (ARF-GEFs) and ADP-RIBOSYLATION FACTOR GTPase ACTIVATING PROTEINS (ARF-GAPs). ARF-GEFs have a Sec7 domain that catalyzes the exchange of GDP for GTP, whereas hydrolysis of the GTP-bound ARF is mediated by catalytic zinc-finger domains composed of four cysteine residues and an arginine finger within the ARF-GAP domain (Chardin *et al.,* 1996; Goldberg, 1999; Scheffzek *et al.,* 1998).

In one example, endomembrane trafficking is necessary to establish auxin gradients in developing *Arabidopsis* embryos. Auxin maxima establish polarity during apical-basal patterning and form at the sites of cotyledon initiation (Friml *et al.,* 2003; Feraru and Friml, 2008). The polar localization of PINFORMED (PIN) auxin efflux carrier proteins at the plasma membrane determines auxin flux and creates auxin maxima (Friml *et al.,* 2003; Wisniewska *et al.,* 2006). PIN proteins are actively recycled in vesicles from the endosome to the plasma membrane but preferentially localize at the plasma membrane. In *Arabidopsis*, ARF-GEF GNOM/EMB30 (GN) and ARF-GAP VASULAR NETWORK DEFECTIVE3/SCARFACE/ARF-GAP DOMAIN3 (VAN3) regulate the transport of vesicles carrying PIN1 as they are recycled from the plasma membrane to endosomal compartments (Geldner *et al.,* 2003; Koizumi *et al.,* 2005; Sieburth *et al.,* 2006). Null mutations at the *GN* locus are embryo lethal (Mayer *et al.,* 1993); whereas loss-of-function alleles of *VAN3* give rise to mutants that have discontinuous vasculature in cotyledons and leaves and are unable to undergo reproductive growth (Koizumi *et al.,* 2005; Seiburth *et al.,* 2006).

Previously, the maize *dek* mutant *discolored* (*dsc1*) was identified in a *Mutator* (*Mu*) transposon population and named for its shrunken brown kernel phenotype (Robertson, 1978; Scanlon *et al.,* 1994; Scanlon and Myers, 1998). The recessive *DSC1-R* mutation gives rise to nonviable kernels and was mapped to chromosome 4 (Scanlon *et al.,* 1994; Scanlon and Myers, 1998). Transposon-tagging identified a 3,808 bp *Mu1* transposon-inserted genomic DNA fragment that aligns to the 5’ UTR and the first exon of *DSC1* (AF006498; Scanlon and Myers, 1998).

Here, detailed phenotypic analyses of *dsc1* mutant kernels illustrate that *dsc1* mutant embryo and endosperm structures are developmentally delayed but do differentiate, prior to kernel abortion and tissue degeneration. The full length *DSC1* transcript encodes an ARF-GAP and accumulates in kernels harvested from 6 days after pollination (DAP) to 18 DAP, and in seedling roots and shoots. Transient expression assays in *N. benthamiana* leaves show that YFP-tagged DSC1 proteins co-localize with the *trans*-Golgi network/early endosomes and with the plasma membrane. Taken together, these data reveal that DSC1 regulates endomembrane trafficking and is required for maintenance of differentiated cell types in the maize kernel.

Results

DSC1 is required to maintain differentiation of embryo and endosperm structures

Self-pollinated plants heterozygous for the *DSC1-R* mutation segregate mutant kernels with aberrations in the embryo and the endosperm (Scanlon *et al.,* 1994; Scanlon and Myers, 1998). At 12 DAP, non-mutant kernels are yellow, whereas *dsc1-R* mutant kernels are white and remarkably smaller than non-mutant siblings (Figure 3.1a; Scanlon *et al.,* 1994; Scanlon and Myers, 1998). Dissected kernels at 18 DAP reveal that the *dsc1-R* mutant embryo is not discernable, and the reduced endosperm fails to fill the kernel space (Figure 3.1b, c; Scanlon *et al.,* 1994; Scanlon and Myers, 1998). At 25 DAP, all *dsc1-R* mutant kernels are brown, misshapen, and embryo lethal (Figure 3.1d; Scanlon *et al.,* 1994; Scanlon and Myers, 1998).

Detailed phenotypic analyses of *dsc1-R* mutant kernels harvested at different time-points following pollination show that development of both the embryo and endosperm is delayed. Despite this developmental retardation, the differentiation of

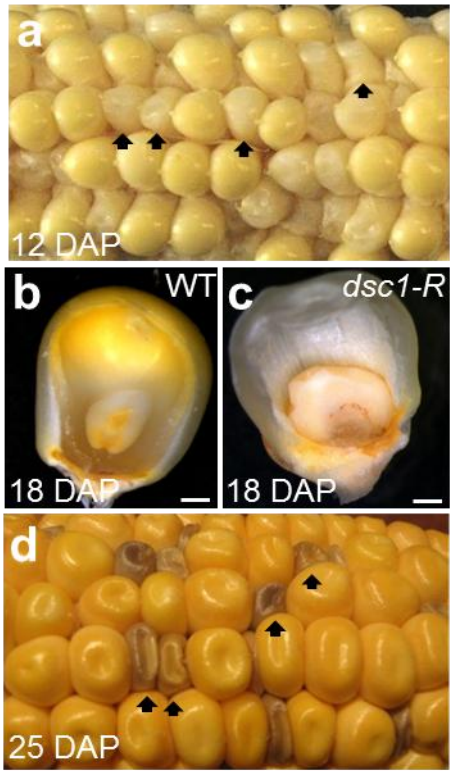

Figure 3.1 *DSC1-R* is a *DEFECTIVE KERNEL* mutation.

Ear harvested at (a) 12 DAP segregating *dsc1-R* mutant kernels. Frontal view of (b) non-mutant sibling and (c) *dsc1-R* mutant kernels harvested at 18 DAP. The outer layer is removed to reveal the embryo and endosperm inside of the pericarp Ear harvested at (d) 25 DAP segregating *dsc1-R* mutant kernels.

Arrows point to *dsc1-R* mutant kernels. DAP, days after pollination.
Scale bars represent 1 mm.

normal embryo and endosperm structures occur prior to the degradation of these kernel structures. For example, late proembryo-staged embryos are harvested from non-mutants at 8 DAP (Figure 3.2a, b), whereas 8 DAP mutant embryos comprise far fewer cells than non-mutant embryos and are still encased by the ESR (Figure 3.2g, h). Non-mutant sibling embryos harvested 12 DAP are in stage L2, having already elaborated the scutellum, the coleoptile, and the first foliar leaf (Figure 3.2c, d). In contrast, 12 DAP *dsc1-R* mutant embryos have advanced only to the early transition stage (Figure 3.2i, j). At 16 DAP, non-mutant sibling embryos have initiated up to three foliar leaves (Figure 3.2e, f), whereas *dsc1-R* mutant embryos exhibit a range of developmentally retarded and aberrant phenotypes. For example, some mutant embryos dissected at 16 DAP were in stage L1, whereas sibling mutant embryos were already degenerating and did not resemble any non-mutant embryo stage (Figure 3.2k, l). Accumulation of *KN1*, *RANBP2*, and *ZYB14* transcripts in non-mutant embryos harvested at the transition stage serve as molecular markers for the meristem, the vasculature, and the scutellum; respectively (Figure 3.3a-c; Smith *et al.,* 1995; Juarez *et al.,* 2004; Takacs *et al.,* unpublished). Equivalent transcript accumulation patterns of *KN1*, *RANBP2*, and *ZYB14* are observed in wild type and *dsc1-R* mutant embryos at the transition stage (Figure 3.3d-f). All *dsc1-R* mutant embryos harvested 20 DAP or later are degenerating and nonviable (Figure 3.4a-d). Consistent with the degenerated embryo phenotypes observed in late-staged mutant embryos, *dsc1-R* mutant embryos do not accumulate *KN1* or *ZYB14* transcripts after 16 DAP (Figure 3.4e, f).

Differentiation of the different endosperm cell types (the aleurone, the BETL, and the starchy endosperm) is also delayed in *dsc1-R* mutant kernels. Similar to the *dsc1-R*

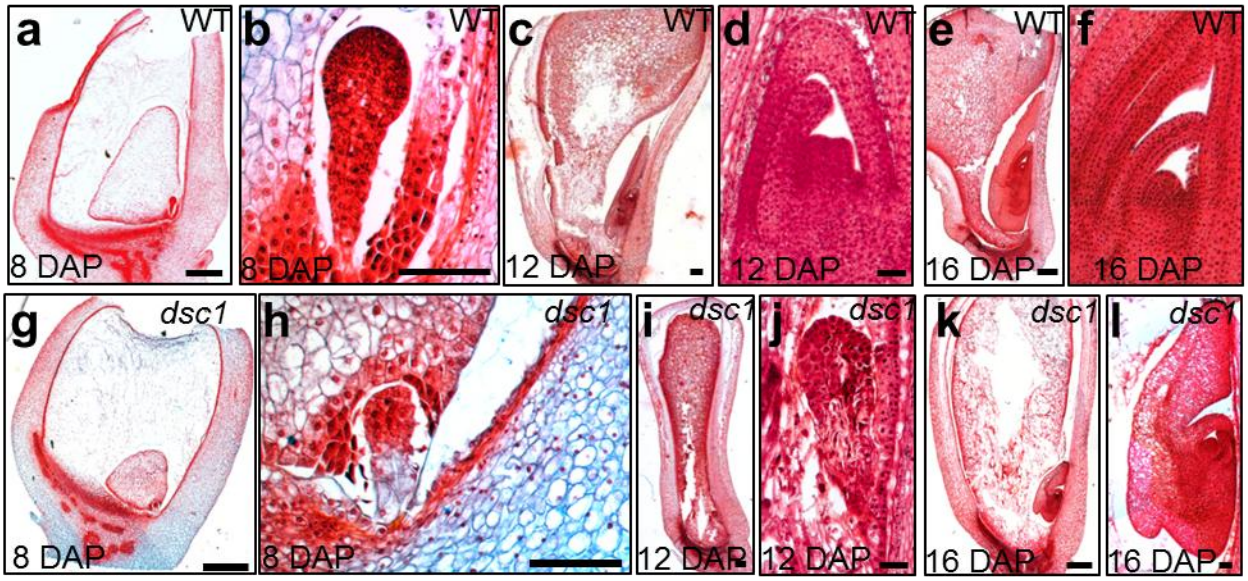

Figure 3.2 Embryogenesis is delayed in *dsc1-R* mutant embryos.

Sagittal sections of (a-f) non-mutant and (g-l) *dsc1-R* mutant embryos harvested at 8 DAP (a-b, g-h), 12 DAP (c-d, i-j), and 16 DAP (e-f, k-l) stained with Safranin-O and Fast Green. Images of embryos in (b, d, f, ,h, j, l) are magnified from the whole kernel images in (a, c, e, g, i, k), respectively.

DAP, days after pollination.
Scale bars in (a, c, e, g, i, k) represent 500 um and in (b, d, f, h, j, l) represent 100 um.

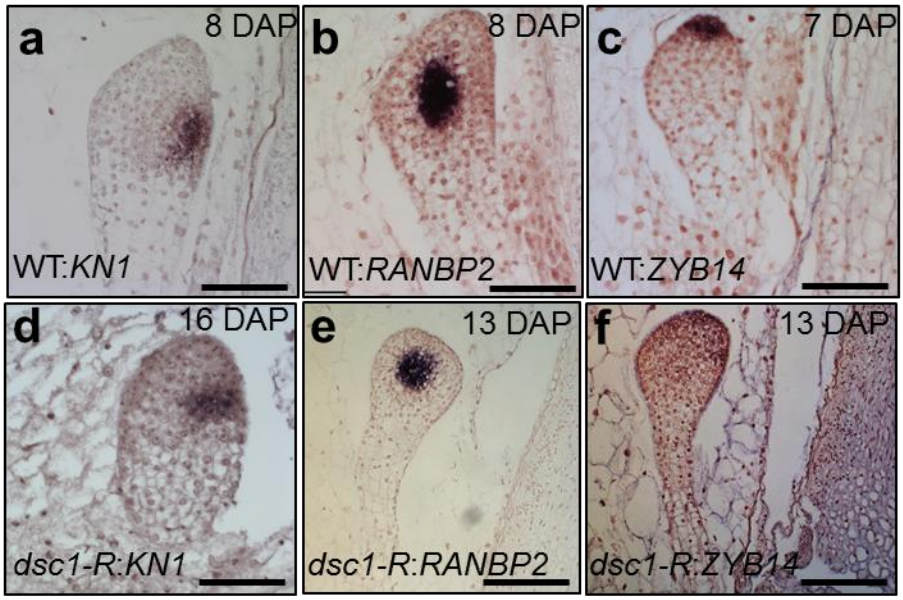

Figure 3.3 *dsc1-R* mutant embryos make differentiated structures

Sagittal sections of (a-c) non-mutant and (d-f) *dsc1-R* mutant embryos probed with *KNOTTED1* (*KN1;* a, d), *RAN BINDING PROTEIN2* (*RANBP2;* b, e), and *Zea mays YABBY14* (*ZYB14;* c, f). Non-mutant and *dsc1-R* mutant embryos were harvested at different time-points to show the same stage of embryo development.

DAP, days after pollination.
Scale bars represent 100 um.

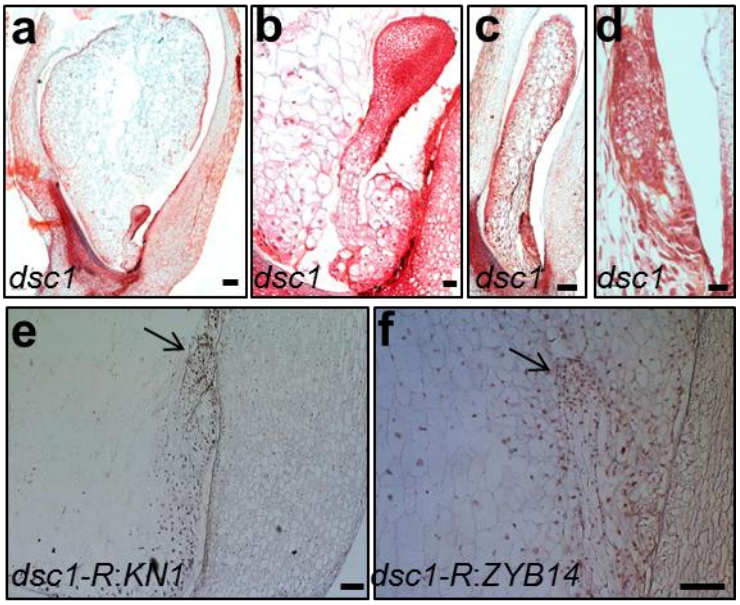

Figure 3.4 Severe *dsc1-R* mutants do not maintain a meristem and stop initiating lateral organs.

Two types of degenerate *dsc1-R* mutant embryos are identified at 20 DAP (a-b) and (c-d). The embryos in panels (b) and (d) are magnified from panels (a) and (c), respectively. *In situ* hybridizations using *KNOTTED1* (*KN1;* e) and *Zea mays YABBY14* (*ZYB14*; f) probes illustrate that transcripts do not accumulate in degenerate *dsc1-R* mutant embryos.

Arrows point to embryos. DAP, days after pollination.
Scale bars represent 500 um (a, c) or 100 um (b, d-f).

mutant embryo, differentiation of endosperm structures is delayed and eventually aborted in *dsc1-R* mutant kernels. At 8 DAP, endosperm structures are fully differentiated and anatomically distinct in non-mutant kernels. Aleurone cells assume their distinctive cuboidal shape, and are arranged into a layer surrounding the perimeter of the starchy endosperm (Figure 3.5a). Three layers of highly extended cells comprising the BETL develop in the base of the endosperm, immediately juxtaposed to the maternally-derived placenta (Figure 3.5b). In contrast, *dsc1-R* mutant aleurone cells are not differentiated at 8 DAP (Figure 3.5e), and just a single layer of BETL cells form at the base of the endosperm (Figure 3.5f). By 16 DAP however, *dsc1-R* mutant and non-mutant sibling kernels have fully differentiated endosperm structures, including an anatomically distinct aleurone layer surrounding enlarged and vacuolated cells of the starchy endosperm, and a BETL comprising three cell layers (Figure 3.5g, h; Figure 3.6a, b). At 20 DAP *dsc1-R* mutant endosperm development is again aberrant. Undifferentiated cell types arise within differentiated cell layers of the mutant aleurone and BETL, and other cells are completely degenerated (Figure 3.5i-l; Figure 3.6c, d).

dsc1 **encodes an ADP-RIBOSYLATION FACTOR-GTPase ACTIVATING PROTEIN (ARF-GAP)**

Previously, a 3,808 bp *Mu1*-inserted genomic fragment at the *DSC1* locus was obtained using transposon-tagging (Scanlon and Myers, 1998). Three additional *Mu*-insertion alleles obtained from the Trait Utility System for Corn (TUSC) generated *Mu* transposon-mutagenized population (*DSC1-H02*, *DSC1-C06*, and *DSC1-B09*) failed to complement the *DSC1-R* mutation (Figure 3.7a; Meeley and Briggs, 1995).

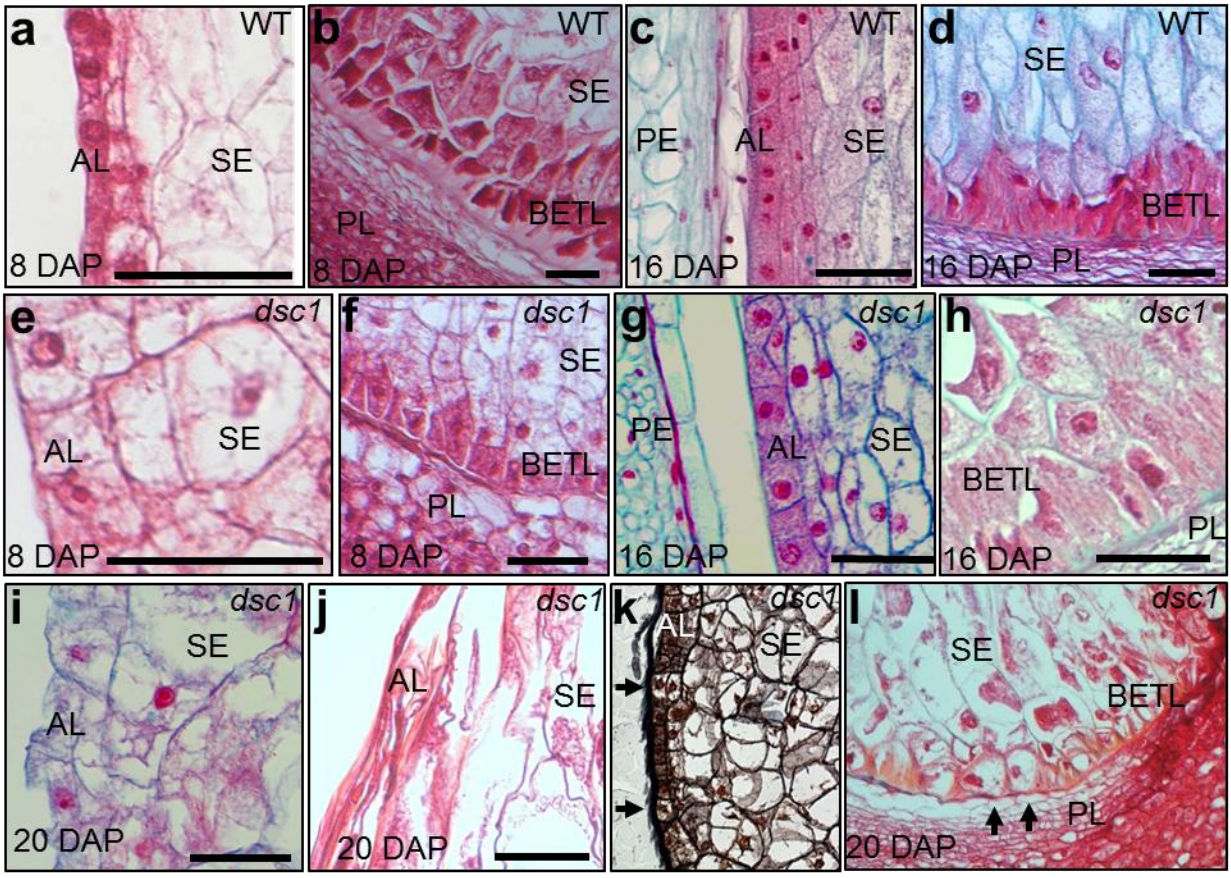

Figure 3.5 Development of endosperm structures is delayed in *dsc1-R* mutant endosperm before degeneration.

Sagittal sections of (a-d) non-mutant and (e-l) *dsc1-R* mutant kernels harvested at 8 DAP (a-b, e-f), 16 DAP (c-d, g-h), and 20 DAP (i-l).

Arrows point to undifferentiated cell types that arise in (k) the AL cell layer and (l) the BETL. AL, aleurone; BETL, basal endosperm transfer layer; DAP, days after pollination; PE, pericarp; PL, placenta; SE, starchy endosperm. Scale bars represent 100 μm.

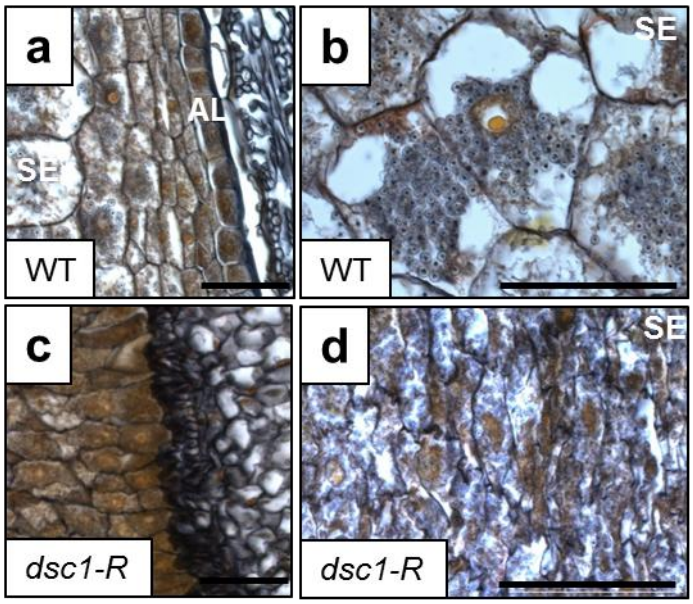

Figure 3.6 Additional *dsc1-R* mutant kernel defects.

Transverse sections of (a-b) non-mutant kernels and (c-d) *dsc1-R* mutant kernels stained with Safranin-O and Orange G. (a) In non-mutant kernels from right to left, there is a single file of AL cells, the sub-aleurone cell layer, and SE cells. (c) The AL cell layer is not distinct from SE in this *dsc1-R* mutant kernel. (b, d) SE cells are degenerate in *dsc1-R* mutants and ~3 times smaller than non-mutant SE cells.

Nuclei stain orange, starch grains are black, lignin stains red, and cell walls stain black. AL, aleurone; SE, starchy endosperm.
Scale bars represent 100 um.

Figure 3.7 *DSC1* encodes an ARF-GAP.

(a) The full length *DSC1* transcript is 3.194 kb. Position of *Mu* transposon insertions in *DSC1* mutant alleles are marked. Images of *dsc1* mutant kernels are from the failed complementation crosses. Hash marks indicate unknown length of genomic fragments. (b) DSC1 is 823 amino acids and is composed of a BAR, a PH, an ARF-GAP, and two ANKYRIN domains. (c) ARF-GAP domain-specific amino acid sequence alignments using ClustalW of DSC1, with the two maize paralogs on chromosomes 1 (GRMZM5G872204) and 7 (GRMZM2G059225), *Arabidopsis* VAN3/SFC/AGD3 (NP_196834), and *Homo sapiens* ACAP2 (AAH60767).

BAR, BIN-AMPHIPHYSIN-RVS; PH, PLECKSTRIN HOMOLOGY; ARF-GAP, ADP-RIBOSYLATION FACTOR-GTPase ACTIVATING PROTEIN; ANK, ANKYRIN.

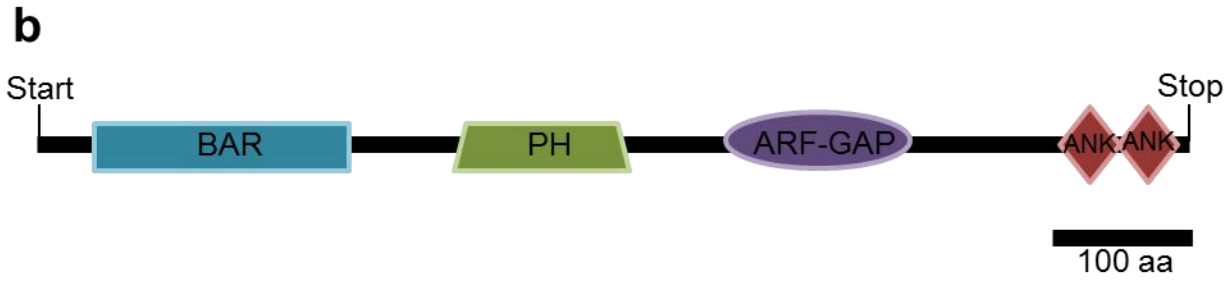

c

```
DSC1_ARF-GAP                EKPIDLLRKVDGNNMCADCGASEPDWASLNLGALLCIECSGVHRNLGVHI
DSC1_paralog_Chr1_ARF-GAP   EKPIDLLRKVDGNNMCADCGALEPDWASLNLGALLCIECSGVHRNLGVHI
DSC1_paralog_Chr7_ARF-GAP   DKPIDLLRKVAGNNCCADCGASEPDWASLNLGILLCIECSGVHRNMGVHI
VAN3/SFC/AGD3_ARF-GAP       EKPIDALRKVCGNDKCADCGAPEPDWASLNLGVLVCIECSGVHRNLGVHI
ACAP2_ARF-GAP               ESALQRVQCIPGNASCCDCGLADPRWASINLGITLCIECSGIHRSLGVHF
                            :..:: :: : **  *.***  :* ***:***  :******:**.:***:

DSC1_ARF-GAP                SKVRSLTLDVRVWEPSVINLFQSLGNMFVNSIWEETLPD-------DNSS
DSC1_paralog_Chr1_ARF-GAP   SKVRSLTLDVRVWEPSVINLFQSLGNMFVNNIWEDMLPD-------DNSS
DSC1_paralog_Chr7_ARF-GAP   SKVRSLTLDVRVWEQSVINLFQSIGNTFANSVWEEMLPSSSCVDHGDISR
VAN3/SFC/AGD3_ARF-GAP       SKVRSLTLDVKVWEPSVISLFQALGNTFANTVWEELLHSR---SAIHFDP
ACAP2_ARF-GAP               SKVRSLTLDT--WEPELLKLMCELGNDVINRVYEANVEKMG---------
                            *********.  ** .::.*:  :** . * ::*  : .

DSC1_ARF-GAP                ADGSD-TSQYLSVSKPKHKDVFSAKEKFIHAKYVNKEFLRNRS
DSC1_paralog_Chr1_ARF-GAP   ADGSD-TSQYLSVSKPKHKDVFSAKEKFIHAKYVDKEFIRKR-
DSC1_paralog_Chr7_ARF-GAP   ADGLENMSHGFAPKKPKQSDSIAVKEKFIHAKYAEKDFVRKH-
VAN3/SFC/AGD3_ARF-GAP       GLTVSDKSRVMVTGKPSYADMISIKEKYIQAKYAEKLFVRRS-
ACAP2_ARF-GAP               ------------IKKPQPGQRQEKEAYIRAKYVERKFVDKYS
                                        *    .    ** :*:***.:: *: .
```

The *Mu1*-inserted genomic fragment was aligned to maize EST libraries using BLAST (NCBI) to predict the full length *Dsc1* transcript. RT-PCR using primers designed in the ESTs identified from these alignments amplified a 2,472 bp *DSC1* transcript. Alignments of the *DSC1* transcript to BAC AC197554 were subsequently used to predict intron/exon boundaries. The full length *DSC1* transcript has 18 exons and encodes an ARF-GAP (Figure 3.7a, b). The *DSC1-H02* allele has a *Mu* insertion 283 bp upstream of the start codon only 50 bp downstream from the *Mu1* insertion of the *DSC1-R* allele (Figure 3.7a). Both the *DSC1-C06* and *DSC1-B09* alleles have *Mu* insertions in the first intron 284 bp and 250 bp downstream of the start codon, respectively (Figure 3.7a).

The predicted 823 amino acid DSC1 protein encodes the following domains: BIN-AMPHIPHYSIN-RVS (BAR); PLECKSTRIN HOMOLOGY; ARF-GAP; and two ANKYRIN repeats. BAR and PLECKSTRIN HOMOLOGY domains are both implicated in membrane interactions (Figure 3.7b); BAR domains sense membrane curvature and PLECKSTRIN HOMOLOGY domains bind lipids within membranes (Hurley, 2006). As described above, ARF-GAPs regulate ARF-GTPase activity, whereas ANKYRIN repeats function in protein-protein interactions (Inoue and Randazzo, 2007; Mosavi *et al.*, 2004). Taken together, the DSC1 protein is predicted to function during endomembrane trafficking.

ARF-GAPs are a conserved group of proteins identified in *Homo sapiens* (24), *Drosophila melanogaster* (7), *Saccharomyces cerevisiae* (9), *Oryza sativa* (23), and *Arabidopsis* (15; Inoue and Randazzo, 2007; Jiang and Ramachandran, 2006; Vernoud *et al.,* 2003). In maize, a total of 43 genes are predicted to encode an ARF-GAP domain including *dsc1* and a *dsc1* paralog located on chromosome 1 (DSC1*b;

GRMZM5G872204; Schnable *et al.,* 2009; RefGen version 2, http://www.maizesequence.org). According to the classification system in mammals, nine maize ARF-GAPs including DSC1 and DSC1b belong to the subgroup ACAP of the AZAP type ARF-GAPs that function in post-Golgi transport pathways (Randazzo and Hirsch, 2004; Jackson, 2000; Nie *et al.,* 2003; Miura *et al.,* 2002). ClustalW amino acid sequence alignments show that DSC1 is 95% identical (98% amino acid similarity) to DSC1b (Figure 3.7c; Figure 3.8a-c). DSC1 is homologous to the ARF-GAP VAN3 in *Arabidopsis*, which regulates endomembrane trafficking of the auxin efflux protein PIN1 (Koizumi *et al.,* 2005; Seiburth *et al.,* 2006). ClustalW alignments of the ARF-GAP domains DSC1, DSC1b, VAN3, and a human ACAP-type ARF-GAP (ACAP2) are shown in Figure 3.7c; DSC1 has 66% identity/77% similarity to VAN3, although another maize ARF-GAP (GRMZM2G059225) is more similar to VAN3 (69% identity/80%similarity).

To determine the *DSC1* expression profile, RT-PCR of dissected embryo and endosperm from kernels harvested at different time-points (6 DAP, 8 DAP, 12 DAP, 14 DAP, 16 DAP, and 18 DAP), the above ground shoot structures from fourteen day old seedlings grown in soil, and roots from plants grown on agar plates for fourteen days (Figure 3.9). The analysis reveals that *DSC1* transcripts accumulate during kernel development, in whole seedlings, and in roots.

YFP-tagged DSC1 co-localizes with the *trans*-Golgi network/early endosomes and the plasma membrane

Transient expression assays were performed in a heterologous plant system, the

Figure 3.8 Conservation of DSC1 domains in *Zea mays*, *Arabidopsis thaliana,* and *Homo sapiens.*

(a) BAR domain-, (b) PH domain-, and (c) ANK domain-specific amino acid sequence alignments using ClustalW of DSC1, with the two maize paralogs on chromosomes 1 (GRMZM5G72204) and 7 (GRMZM2G059225), *Arabidopsis* VAN3/SFC/AGD3 (NP_196834), and *Homo sapiens* ACAP2 (AAH60767).

BAR, BIN-AMPHIPHYSIN-RVS; PH, PLECKSTRIN HOMOLOGY; ARF-GAP, ADP-RIBOSYLATION FACTOR-GTPase ACTIVATING PROTEIN; ANK, ANKYRIN; Chr, chromosome.

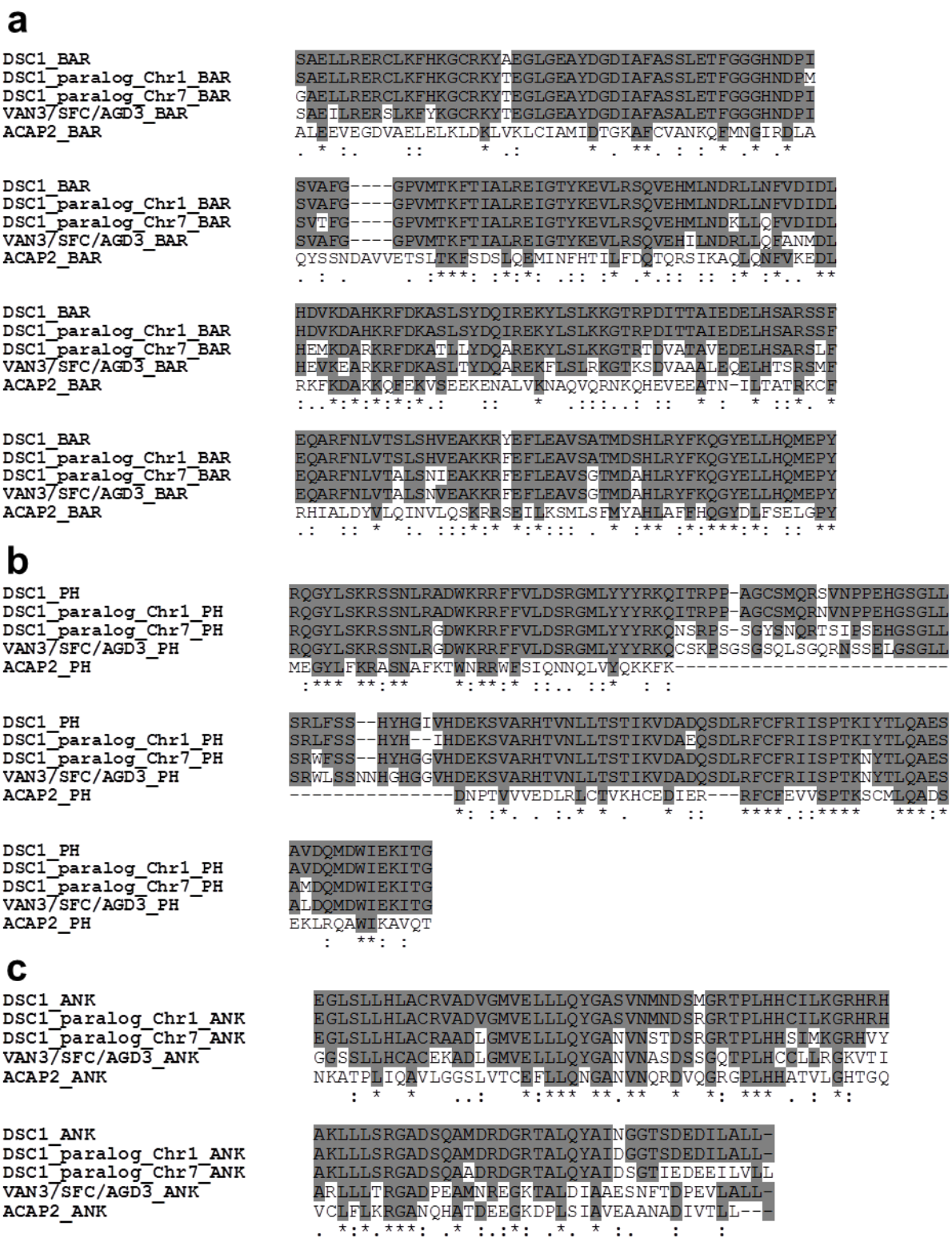
a
DSC1_BAR
DSC1_paralog_Chr1_BAR
DSC1_paralog_Chr7_BAR
VAN3/SFC/AGD3_BAR
ACAP2_BAR
b
DSC1_PH
DSC1_paralog_Chr1_PH
DSC1_paralog_Chr7_PH
VAN3/SFC/AGD3_PH
ACAP2_PH
c
DSC1_ANK
DSC1_paralog_Chr1_ANK
DSC1_paralog_Chr7_ANK
VAN3/SFC/AGD3_ANK
ACAP2_ANK

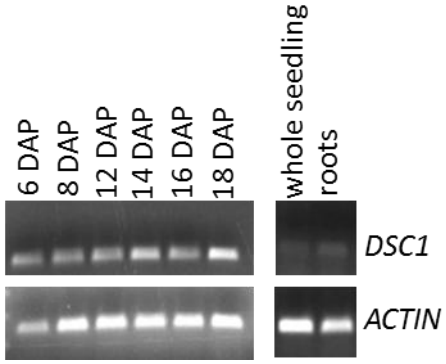

Figure 3.9 Transcript accumulation of *DSC1*.

RT-PCR of *DSC1* during kernel development (6 DAP-18 DAP), 14 day old seedling shoots and roots.

N. benthamiana leaf, with an N-terminal YELLOW FLUORESCENT PROTEIN (YFP)-tagged DSC1 construct to determine the subcellular localization of DSC1 (Earley *et al.,* 2006). A control construct lacking the DSC1 ORF was also generated (Earley *et al.,* 2006). Using both epifluorescence and confocal microscopy, infiltrated leaf sectors were imaged and show that YFP::DSC1 accumulates in distinct intracellular compartments or as foci at the plasma membrane (Figure 3.10a, d, g, j, m; Figure 3.11a, c). In contrast, the control 35s-YFP localizes to the nucleus or cytoplasm (Figure 3.11e, g). YFP::DSC1 labeled bodies also actively move around the cell (Figure 3.12a, b). The actively moving YFP::DSC1 labeled bodies can be detected by cytoplasmic streaming (i.e., the appearance of strands stretching laterally from the apical to the basal side of the plasma membrane; Figure 3.10m; Figure 3.12b). Furthermore, time series photography illustrates the intracellular movement of YFP::DSC1 bodies (Figure 3.12a, b).

FM4-64 (Invitrogen) is a lipophilic styryl dye that fluoresces in a hydrophobic environment, and traces endocytosis from the plasma membrane into the cell (Bolte *et al.,* 2004). Once internalized, FM4-64 labeled membranes successively co-localize with the *trans*-Golgi network/early endosomes, prevacuolar compartments, and ultimately the tonoplast (vacuolar membrane; Bolte *et al.,* 2004; Geldner *et al.,* 2009). Co-localization assays with several organelle-specific markers and the endocytic tracer FM4-64 were performed to identify more precisely the intracellular localization of YFP-tagged DSC1 bodies. YFP-tagged DSC1 does not co-localize with the mitochondrial marker COXIV::GFP, the peroxisome marker DsRed::catalase, auto-fluorescent chloroplasts, the *cis*-Golgi marker ERD2::GFP; or the Golgi stacks marker

Figure 3.10 YFP-tagged DSC1 in transient expression assays in *N. benthamiana* leaves.

(a,d, g) YFP::DSC1 bodies do not co-localize with (b) chlorophyll auto-fluorescence (c, merged image), (e) *cis*-Golgi marker ERD2::GFP (f, merged), or (h) the Golgi stacks marker mCherry::Got1p (I, merged). (j, m) YFP::DSC1 bodies do co-localize with some of the intracellular compartments labeled with the (k, n) endocytic tracer FM4-64 in mesophyll and epidermal cells (l and o, merged).

Arrows point to compartments that co-localize with YFP-tagged DSC1.
Arrowheads point to YFP-tagged DSC1 compartments a the plasma membrane.
Scale bars represent 50 µm.

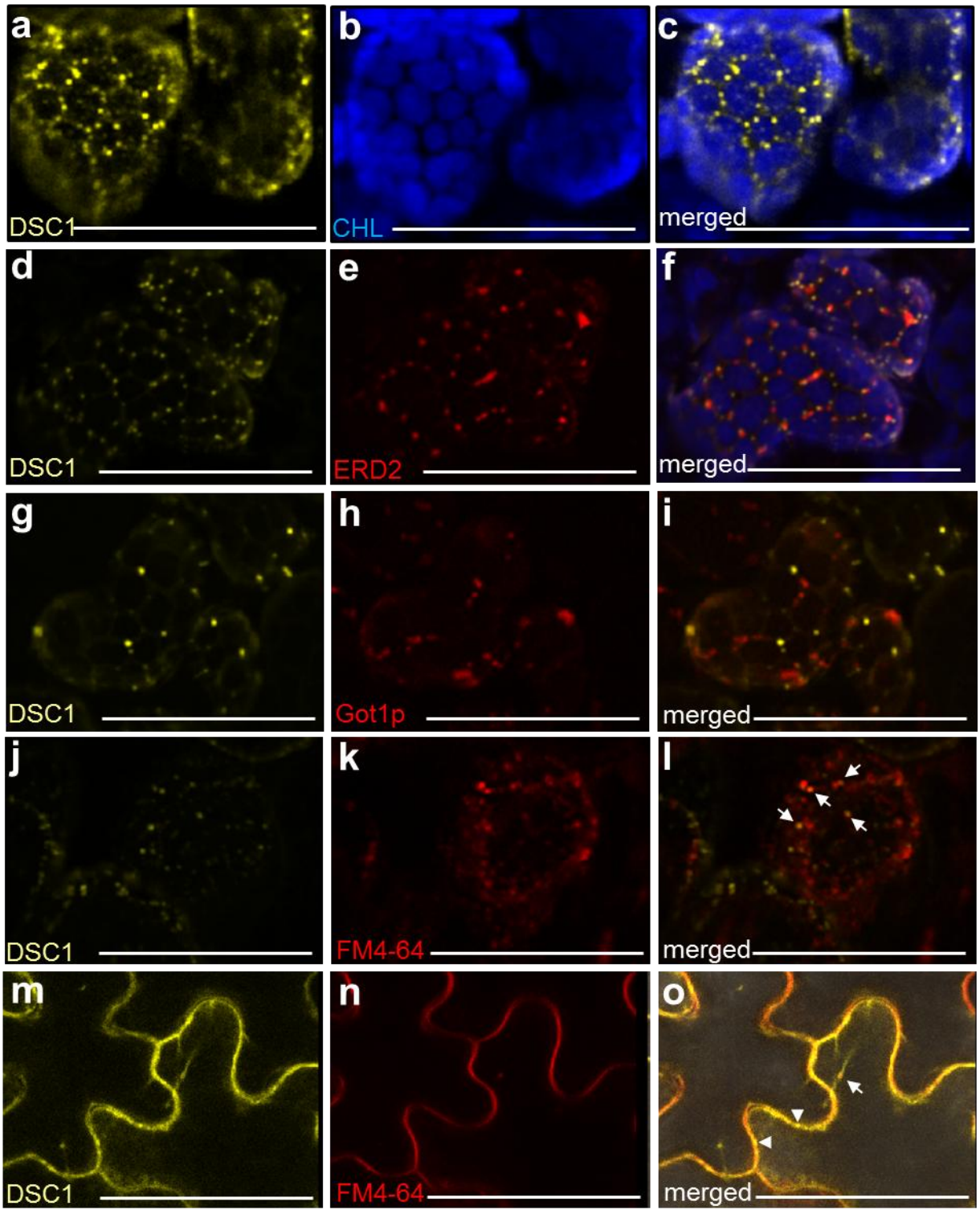
a
DSC1
b
CHL
c
merged
d
DSC1
e
ERD2
f
merged
g
DSC1
h
Got1p
i
merged
j
DSC1
k
FM4-64
l
merged
m
DSC1
n
FM4-64
o
merged

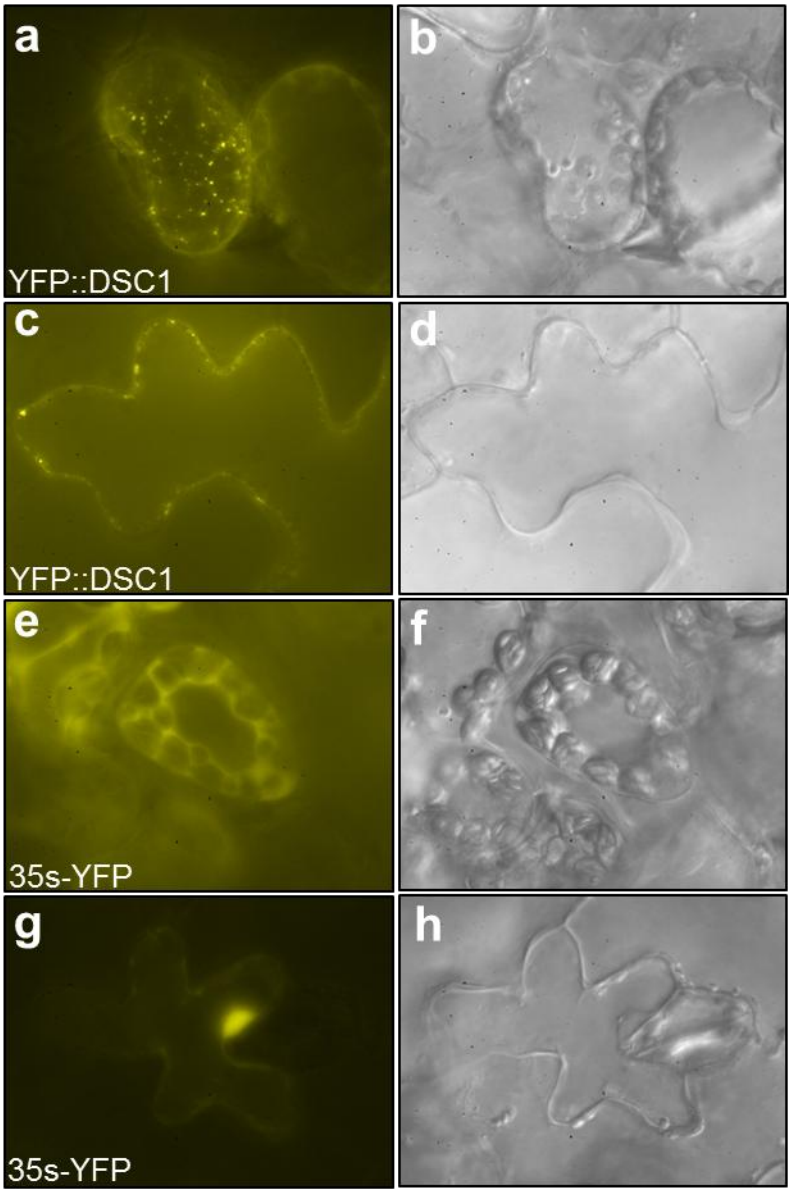

Figure 3.11 Subcellular localization of YFP-tagged DSC1 and YFP control construct.

YFP-tagged DSC1 localizes to punctate structures in (a) mesophyll and (b) epidermal cells. The control construct has nucleo-cytoplasmic localization in (e) mesophyll and (b) epidermal cells. (b, d, f, and h) Bright field images were taken of the cells located directly to the left.

Images were obtained using epifluorescence microscopy.

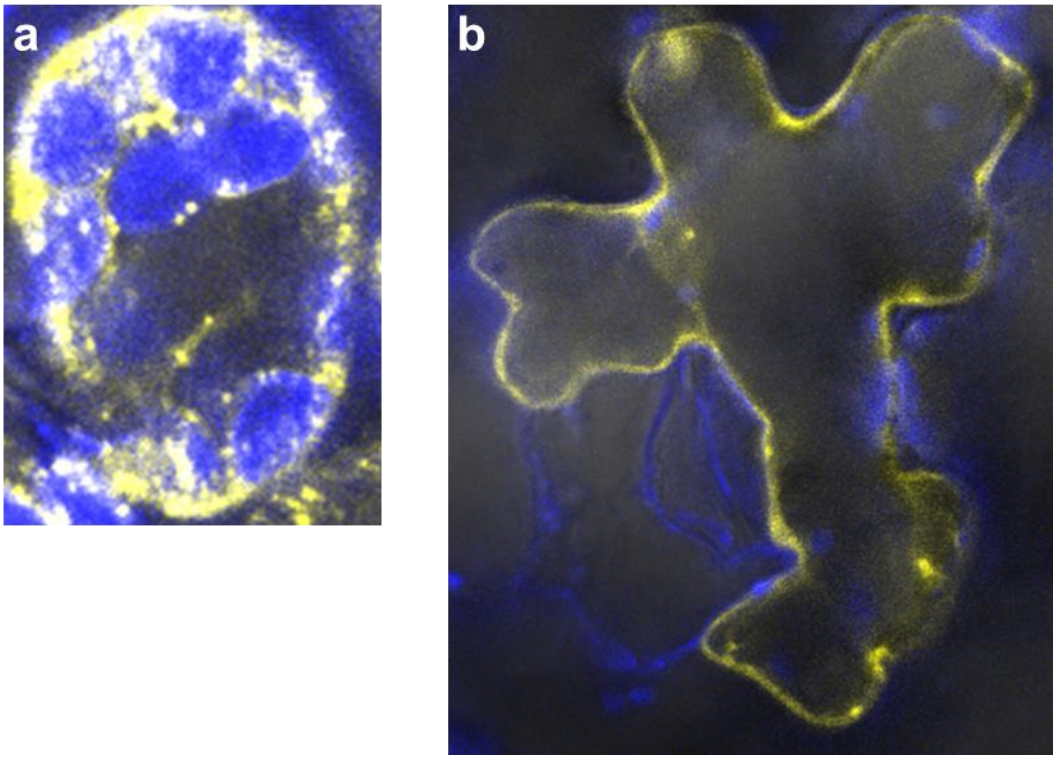

Figure 3.12 YFP::DSC1 labeled bodies actively move around the cell.

Transient expression of YFP::DSC1 in *N. benthamiana* leaf (a) mesophyll and (b) epidermal cells.

mCherry::Got1p (Figure 3.10a-l; Figure 3.13a-f; Kohler *et al.,* 1997; Reisen and Hanson, 2007; Boevink *et al.,* 1998; Geldner *et al.,* 2009). YFP::DSC1 labeled bodies co-localize with FM4-64 labeled intracellular compartments and the *trans*-Golgi network/early endosome marker mCherry::VTI12 (Figure 3.10j-o; Figure 3.13g-l; Geldner *et al.,* 2009). Furthermore, YFP-tagged DSC1 compartments also co-localize with FM4-64 at the plasma membrane (Figure 3.10m-o). Both the active movement of these YFP-tagged DSC1 labeled compartments and their co-localization with FM4-64 and the *trans*-Golgi network/early endosome marker illustrate that DSC1 functions in endomembrane trafficking.

PIN1a endomembrane transport is not disrupted in dsc1-R mutant embryos

In *Arabidopsis*, the ARF-GAP VAN3 functions in the transport of PIN1 from the plasma membrane to the recycling endosome (Seiburth *et al.,* 2006). YFP-tagged PIN1a was observed in *dsc1-R* mutant embryos to determine if the endomembrane transport of PIN1a is disrupted in maize. In both non-mutant and *dsc1-R* mutant embryos, YFP-tagged PIN1a localizes to the plasma membrane (Figure 3.14a-d). Non-mutant and *dsc1-R* mutant embryos were treated with Brefeldin A (BFA; Sigma-Aldrich) to inhibit the transport of PIN1a from the recycling endosome to the plasma membrane (Steinmann *et al.,* 1999; Geldner *et al.,* 2001). Here, PIN1a accumulates in endosomal compartments in both non-mutant and *dsc1-R* mutant embryos (Figure 3.14e, f). No difference in the size or number of these endosomal compartments is observed between non-mutant and *dsc1-R* mutant embryos. Therefore, the endomembrane transport of PIN1a in maize embryos is not disrupted by the *DSC1-R* mutation.

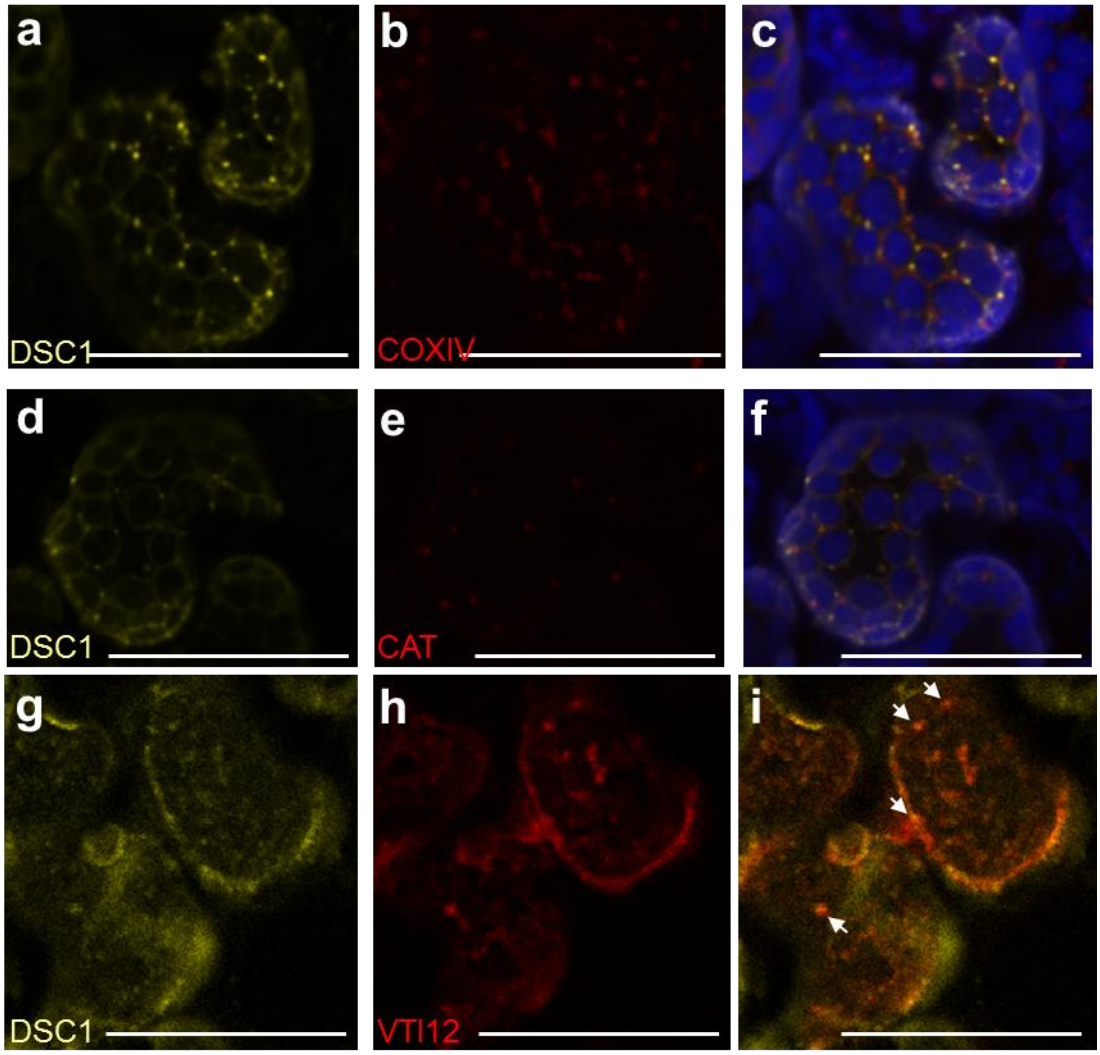

Figure 3.13 YFP-tagged DSC1 bodies in transient expression assays in *N. benthamiana* leaves.

(a) YFP::DSC1 bodies do not co-localize with (b) mitochondria (COXIV::GFP; c, merged image). (d) YFP::DSC1 bodies do not co-localize with (e) peroxisomes (DsRed::catalase; f, merged). (g) YFP::DSC1 bodies do co-localize with the (h) *trans*-Golgi network/early endosomes (mCherry::VTI12; I, merged).

Arrows point to compartments that co-localize with YFP-tagged DSC1.
Scale bars represent 50 µm.

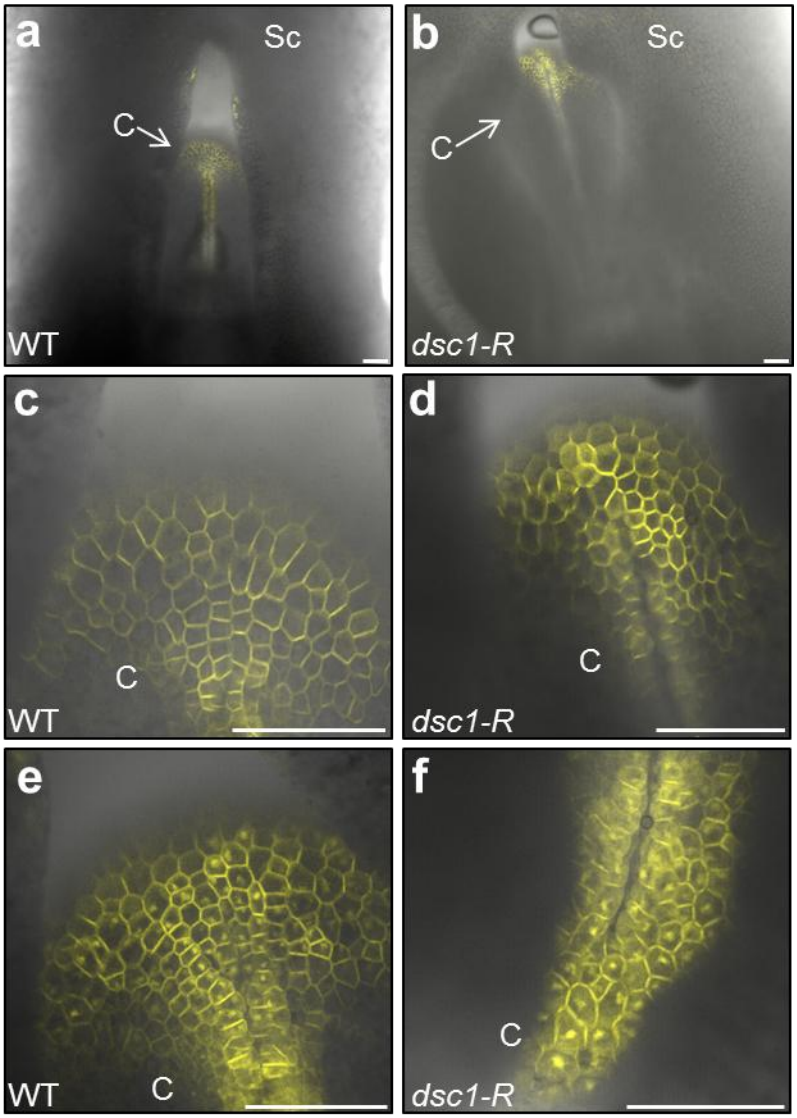

Figure 3.14 PINFORMED1a (PIN1a) endomembrane transport is not disrupted in *dsc1-R* mutant embryos.

(a) YFP-tagged PIN1a preferentially localizes at the plasma membrane in mock-treated (a, c) non-mutant and (b, d) *dsc1-R* mutant embryos. The coleoptiles imaged in (c) and (d) are magnified from (a) and (b), respectively. YFP-tagged PIN1a accumulates internally after Brefeldin A (BFA) treatment of embryos in both (e) non-mutant and (f) *dsc1-R* mutant embryos. No difference in the shape or number of endosomal compartments in non-mutant and *dsc1-R* mutant embryos is observed.

DAP, days after pollination; C, coleoptile; Sc, scutellum; BFA, Brefeldin A. Scale bars represent 100 µm.

Discussion

As a *dek* mutant, the *dsc1-R* mutant kernel phenotype has aberrations in both the embryo and the endosperm (Scanlon *et al.,* 1994; Scanlon and Myers, 1998). At first the development of *dsc1-R* mutant embryos and endosperm is normal, albeit delayed. Corresponding to this normal development, *dsc1-R* mutant embryos establish a meristem, have vasculature, and initiate the scutellum. In some cases, mutant embryos also initiate the coleoptile and/or the first foliar leaf, before further development is aborted and embryo structures completely degenerate. Like *dsc1-R* mutant embryos, the *dsc1-R* mutant endosperm structures fully differentiate despite a delay in development. Phenotypic variability is common in *DEK* mutations and could be a result of genetic redundancy because of the *DSC1* paralog in the maize genome. Both *DSC1* and *DSC1b* have similar transcript accumulation patterns in both NimbleGen array and RNA-sequencing analyses (Sen *et al.,* 2009; Sekhon *et al.,* 2011). As a result, a DSC1 paralog could potentially compensate for DSC1 function during the early stages of kernel development.

YFP-tagged DSC1 co-localizes with the endocytic tracer FM4-64 and the *trans*-Golgi network/early endosome marker mCherry::VTI12, but does not co-localize with the Golgi marker mCherry::Got1p. As previously described, mCherry::Got1p labeled Golgi does not associate with the endocytic tracer FM4-64, which is consistent with YFP::DSC1 labeled bodies co-localizing with FM4-64 but not mCherry::Got1p (Geldner *et al.,* 2009). Also described previously, the *trans*-Golgi network/early endosome marker mCherry::VTI12 partially co-localizes with FM4-64 (Geldner *et al.,* 2009). Again this is congruent with YFP-tagged DSC1 labeled bodies co-localizing with some but not

all FM4-64 and mCherry::VTI12 labeled intracellular compartments. Additionally, YFP-tagged DSC1 labeled bodies co-localize with FM4-64 at the plasma membrane. Therefore, DSC1 functions intracellularly at the *trans*-Golgi network/early endosome and at the plasma membrane.

The transport of YFP-tagged PIN1a from the plasma membrane to the recycling endosome is not disrupted in BFA-treated *dsc1-R* mutants. As a result, DSC1 function does not affect PIN1a trafficking. Although DSC1 functions to transport an unknown cargo, DSC1 is required to maintain kernel differentiation. As previously described, DEK1, CR4, and SAL1 function in a cell-to-cell signaling pathway that is necessary to regulate aleurone cell identity (Becraft *et al.,* 1996; Lid *et al.,* 2002; Shen *et al.,* 2003). Likewise, DSC1 may function to transport a cargo that is required for this intercellular signaling pathway.

Materials and Methods

Plant Materials

The *dsc1-R* mutation arose from a *Mu* transposon line and was introgressed into a B73 background for at least five generations before harvesting kernels to use in phenotypic and gene expression analyses (Scanlon and Myers, 1998). The *dsc1-C06*, *dsc1-H02*, and *dsc1-B09* alleles were identified after screening the Trait Utility System for Corn (TUSC), a *Mu* transposon-mutagenized population (Meeley and Briggs, 1995). Primers for this screen can be found in Table 3.1.

Histological Analyses and *in situ* hybridizations

For histological analyses, non-mutant and dsc1-R mutant kernels were harvested 6 DAP to 20 DAP and fixed overnight in 3.7% FAA. The kernels were dehydrated in an

EtOH/TBA series, embedded in paraplast, and 10 µm thick sections were stained with either Safranin O-Fast Green or Safranin O-Orange G as described in Ruzin (1999). For *in situ* hybridizations, non-mutant and dsc1-R mutant kernels were harvested 6 DAP to 20 DAP, fixed in 3.7% FAA, dehydrated, embedded in paraplast, sectioned, and hybridized with gene specific probes as described by Jackson (1991). Primers used to make probes can be found in Table 3.1. All samples were imaged using the Zeiss Axio Imager Z1-Apotome microscope (Thornwood, New York) and Zeiss Axiovision release 4.6 software.

Identification of the full length *dsc1* transcript and gene expression analysis

The Invitrogen Superscript III One Step RT-PCR Platinum Taq HiFi kit was used to clone *dsc1.* Briefly, poly(A) RNA was isolated from B73 enriched seedlings, primers were designed in the 5' and 3' ends of the predicted full length transcript, and RT-PCR was performed. For RT-PCR and quantitative RT-PCR, total RNA was isolated from harvested non-mutant kernels (6 DAP, 8 DAP, 12 DAP, 14 DAP, 16 DAP, 18 DAP) and dsc1-R mutant kernels (16 DAP) using SDS extraction as previously described in (Prescott and Martin, 1987) in combination with TRIzol (Invitrogen). Total RNA was extracted from whole fourteen day old seedlings grown on soil, and roots from fourteen day old seedlings grown on 0.02% agar using TRIzol (Invitrogen). Superscript III (Invitrogen) was used to synthesize cDNA from 1 µg of RNA treated with DNaseI (Invitrogen).

Transient expression assays

The Gateway Recombination Cloning System (Invitrogen) was used to clone the DSC1 ORF into the pEarleyGate104 destination vector as described (Earley *et al.,* 2006).

Table 3.1 Primers used in this study

***In situ* hybridization probes**			
Gene name	**Accession**	**Forward primer**	**Reverse primer**
KNOTTED1	GRMZM2G017087	ACAAGGTGGGGGCACCA	TCGGTCTCTCCTCCGCTA
Zea mays YABBY14	GRMZM2G005353	CGACCTCACCGCACGGTCT	GAGCTCCCTCCTGAGTTTGC
RAN BINDING PROTEIN2	GRMZM2G094353	GAACAGGAAGCCAGGAGACT	CAGTGCAAGTAGTTTTCGTAGGT

Primers used to screen *TUSC*	
Primer name	**Primer sequence**
*Mu*TIR	AGAGAAGCCAACGCCAWCGCCTCY
DO146621	TCAACGCCTCAACCATACTCCCAGTTAC
DO146618	CTTCTTCTTCCCTCCCCGAACGAAG

RT-PCR/qRT-PCR primers		
Gene name	**Forward primer**	**Reverse primer**
DSC1-RT-PCR	CTTCACCACCTGTTGGAAGTCCTAGA	TGCCATCTCTGCATGAACTCGTGCTA
ACTIN	TGTCAGGGACATCAAGGAA	TGGCTGGAATAGAACCTCA

DSC1 subcellular localization primers		
Gene name	**Forward primer**	**Reverse primer**
DSC1	CACCATGCATTTCGCCAAGATCGAT	TCTACTATGATCCTGTAATAACGCAAG

Electroporation was used to transform *Agrobacterium* strain C58C1 with the N-terminal YFP::DSC1 fusion construct, the control construct (empty pEarleyGate104 vector), and the organelle marker constructs (ERD2::GFP, COXIV::GFP, DsRed::CAT, mCherry::VTI12, mCherry::Got1p; Kohler *et al.,* 1997; Reisen and Hanson, 2007; Boevink *et al.,* 1998; Geldner *et al.,* 2009). Transformants from individual construct lines were grown overnight at 28°C in 2 mL of LB medium containing 50 µg/mL kanamycin and 5 µg/mL tetracycline. After precipitation, the cells were resuspended in 10 mM $MgCl_2$ to an OD of 0.5 and incubated at room temperature for 2-4 hours. For co-localization assays, equal parts of the suspensions transformed with each one of the five organelle markers were individually mixed with the suspension transformed with YFP-tagged DSC1 prior to incubation at room temperature. *N. benthamiana* leaves were infiltrated as described (Goodin *et al.,* 2002) and observed using confocal microscopy or epifluorescence microscopy between 48 and 72 hours later. If epifluorescence microscopy was used, images were obtained on the Zeiss Axio Imager Z1-Apotome microscope (Thornwood, New York) and Zeiss Axiovision release 4.6 software.

PIN1a transport assays

Plants heterozygous for *dsc1-R* were crossed with *Zm*PIN1a-YFP transgenic individuals (Mohanty *et al.,* 2009). The resulting progeny were planted, screened for the *dsc1-R* allele and YFP, grown to maturity, and self-pollinated. Ears were harvested the same day kernels were removed for live imaging. Embryos were dissected and put on culture media as described (Scanlon *et al.,* 1997). A BFA (Sigma-Aldrich) stock solution was diluted in DMSO and added to liquid culture media to make a final concentration of 100

Table 3.2 Confocal microscopy parameters.

Fluorescent protein	Laser	Excitation (nm)	Emission range (nm)	Additional fluoresent proteins used in assay	Assay
GFP	Ar	488	496 to 513	YFP/chlorophyll	Transient expression
chlorophyll	Ar	488	672 to 690	GFP/YFP/DsRed	Transient expression
chlorophyll	Ar	488	664 to 718	mCherry/FM4-64/YFP	Transient expression
YFP	Ar	488	526 to 609	GFP/chlorophyll	Transient expression
YFP	Ar	488	525 to 536	DsRed/chlorophyll	Transient expression
YFP	Ar	488	522 to 555	mCherry/FM4-64/chlorophyll	Transient expression
YFP	Ar	488	524 to 583	N/A	PIN1a transport
DsRed	Ar	514	589 to 620	YFP/chlorophyll	Transient expression
mCherry	DPSS	561	582 to 632	YFP/chlorophyll	Transient expression
FM4-64	DPSS	561	582 to 632	YFP/chlorophyll	Transient expression

μM BFA. Mock treatments were made by adding the same amount of DMSO (minus BFA) to liquid culture media. Harvested embryos were incubated in culture media containing BFA or the mock treatment for at least four hours before confocal microscopy image analysis.

Confocal Laser Scanning Microscopy

All imaging of fluorescent proteins was performed using a Leica TCS-SP5 confocal microscope (Leica Microsystems, Exton, PA, USA). Images were taken using either 10X or 40X objectives (NA 0.4 or 0.85, respectively). For the transient assays, images were obtained sequentially to separate signal from the two channels and were later superimposed. Time lapse series and images from transport assays were collected non-sequentially. All images were taken using either a blue argon ion laser (Ar) or a diode pumped solid state laser (DPSS). Excitation and emission parameters are presented in Table 3.2. Leica LAS-AF software (version 1.8.2) was used to process all images.

Acknowledgements

We thank Maureen Hanson for providing us with the mitochondria, peroxisome, and *cis*-Golgi markers for our transient expression assays. We also thank the Plant Cell Imaging Center at the Boyce Thompson Institute for Plant Research (Ithaca, New York) for use of the Leica TCS-SP5 confocal microscope, which was purchased with funds provided by the National Science Foundation Major Research Instrumentation Program (NSF DBI-0618969).

REFERENCES

Abbe, E.C. and Stein, O.L. The growth of the shoot apex in maize: embyrogeny. *Am. J. Bot.* **41**(4), 285-293 (1954).

Adams, K.L., and Wendel, J.F. Polyploidy and genome evolution in plants. *Curr. Opinion Plant Biol.* **8**, 135-141 (2005).

Becraft, P.W. and Asuncion-Crabb, Y. Positional cues specify and maintain aleurone cell fate in maize endosperm development (2000).

Becraft, P.W., Stinard, P.S., and McCarty, D.R. CRINKLY4: a TNFR-like receptor kinase involved in maize epidermal differentiation. *Science* 273, 1406-1409 (1996).

Becraft, P.W., Li, K., Dey, N., and Asuncion-Crabb, Y. The maize *dek1* gene functions in embryonic pattern formation and cell fate specification. *Development* **129**, 5217-5225 (2002).

Boevink, P., Opraka, K., Santa Cruz, S., Martin, B., Betteridge, A., and Hawes, C. Stacks on tracks: the plant Golgi apparatus traffics on an actin/ER network. *Plant J.* **15**(3), 441-447 (1998).

Bolte, S., Talbot, C., Boutted, Y., Catrice, O., Read, N.D., and Satiat-Jeunemaitre, B. FM-dyes as experimental probes for dissecting vesicle trafficking in living plant cells. *J. Microscopy* **214**, 159-173 (2004).

Brink, R.A., and Cooper, D.C. The endosperm in seed development. *Bot. Rev.* 13(9), 479-541 (1947).

Chardin, P., Paris, S., Antonny, B., Robinueau, S., Beroud-Dufour, S., Jackson, C.L., and Charbe, M. A human exchange factor for ARF contains Sec7 and pleckstrin-homology domains. *Nature* **384**, 481-484 (1996).

Cosgrove, D.J., Assembly and enlargement of the primary cell wall in plants. *Annu. Rev. Dev. Biol.* **13**, 171-201 (1997).

Duvik, D.N. Protein granules of maize endosperm cells. *Cereal Chem.* **38**, 374-385 (1961).

Earley, K.W., Haag, J.R., Pontes, O., Opper, K., Juehne, T., Song, K., and Pikaard, C.S. Gateway-compatible vectors for plant functional genomics and proteomics. *Plant J.* **45**, 616-629 (2006).

Feraru, E., and Friml, J. PIN polar targeting. Plant Physiol. **147**, 1553-1559 (2008).

Friml, J., Vieten, A., Sauer, M., Weijers, D., Schwarz, H., Hamann, T., Offringa, R., and Jurgens, G. Efflux-dependent auxin gradients establish the apical-basal axis of Arabidopsis. *Nature* **426**, 147-153, (2003).

Gallavotti, A., Yang, Y., Schmidt, R.J., and Jackson, D. The relationship between auxin transport and maize branching. *Plant Physiol.* **147**, 1913-1923 (2008).

Geldner, N., Devervaud-Tendon, V., Hyman, D.L., Mayer, U., Stierhof, Y-D., and Chory, J. Rapid, combinatorial analysis of membrane compartments in intact plants with a multicolor marker set. *Plant J.* **59**, 169-178 (2009).

Geldner, N., Anders, N., Wolters, H., Keicher, J., Kornberger, W., Muller, P., Delbarre, A., Ueda, T., Nakano, A., and Jurgens, G. The Arabidopsis GNOM ARF-GEF mediates endosomal recycling, auxin transport, and auxin-dependent plant growth. *Cell* **11**(2), 219-230 (2003).

Geldner, N., Friml, J., Stierhofm Y-D, Jurgensm, G., and Palme, K. Auxin transport inhibitors block PIN1 cycling and vesicle trafficking. *Nature* **413**, 425-428 (2001).

Goldberg, J. Structural and functional analysis of the ARF1-ARFGAP complex reveals a role for coatmer in GTP hydrolysis. *Cell* **96**, 893-902 (1999).

Goodin, M.M., Dietzgen, R.G., Schichnes, D., Ruzin, S., and Jackson, A.O. pGD vectors: versatile tools for the expression of green and red fluorescent protein fusions in agroinfiltrated plant leaves. *Plant J.* **31**(3), 375-383 (2002).

Hurley, J.H. Membrane binding domains. *Biochem. Biophys. Acta* **1761**, 805-811 (2006).

Inoue, H., and Randazzo, P.A. Arf GAPs and their interacting proteins. *Traffic* **8**(11), 1465-1475 (2007).

Jackson, T.R., Brown, F.D., Nie, Z., Miura, K., Foroni, L., Sun, J., Hsu, V.W., Donaldson, J.G., and Randazzo, P.A. ACAPs are Arf6 GTPase-activating proteins that function in the cell periphery. *J. Cell Biol.* **151**(3), 627-638 (2000).

Jackson, D. *In situ* hybridization in plants. In *Molecular Plant Pathology: A Practical Approach*, D.J. Bowles, S.J. Gurr, and M. McPherson, eds. Oxford University Press, Oxford, UK, 1991.

Jackson, D., Veit, B., and Hake, S. Expression of maize KNOTTED1 related homeobox genes in the shoot apical meristem predicts patterns of morphogenesis in the vegetative shoot. *Development* **120**, 405-413 (1994).

Jiang, S-Y., and Ramachandran, S. Comparative and evolutionary analysis of genes encoding small GTPases and their activating proteins in eukaryotic genomes. *Physiol. Genomics* **24**, 235-251 (2006).

Juarez, M.T., Twigg, R.W., and Timmermans, M.C.P. Specification of adaxial cell fate during maize leaf development. *Development* **131**, 4533-4544 (2004).

Kaplan, D.R., and Cooke, T.J. Fundamental concepts in the embryogenesis of dicotyledons: a morphological interpretation of embryo mutants. *Plant Cell* **9**, 1903-1919 (1997).

Kessler, S., Seiki, S., and Sinha, N. *Xcl1* causes delayed oblique periclinal cell division in developing maize leaves, leading to cellular differentiation by lineage instead of position. *Development* **129**, 1859-1869 (2002).

Kiesselbach, T.A., and Walker, E.R. Structure of certain specialized tissue in the kernel of corn. *Amer. J. Bot.* 39(8), 561-569 (1952).

Kohler, R.H., Zipfel, W.R., Webb, W.W., and Hanson, M.R. The green fluorescent protein as a marker to visualize plant mitochondria in vivo. *Plant J.* **11**(3), 613-621 (1997).

Koizumi, K., Naramoto, S., Sawa, S., Yahara, N., Uedo, T., Nakano, A., Suglyama, M., and Fukuda, H. VAN3 ARF-GAP-mediated vesicle transport is involved in leaf vascular network formation. *Development* **132**, 1699-1711 (2005).

Lid, S.E., Gruis, D., Jung, R., Lorentzen, J.A., Ananiev, E., Chamberlin, M., Niu, X., Meeley, R., Nichols, S.E., and Olsen, O-A. The *defective kernel1* (*dek1*) gene required for aleurone cell development in the endosperm of maize grains encodes a membrane protein of the calpain gene superfamily. *Proc. Natl. Acad. Sci. USA* **99,** 5460-5465 (2002).

Meeley, R., and Briggs, S. Reverse genetics for maize. *Maize Genetics News Letter* **69**, 67-82 (1995).

Memon, A.R. The role of ADP-ribosylation factor and SAR1 in vesicular trafficking in plants. *Biochem. Biophys. Acta* **1664**, 9-30 (2004).

Miura, K., Jacques, K.M., Stauffer, S., Kubosaki, A., Zhu, K., Hirsch, D.S., Resau, J., Zheng, Y., and Randazzo, P.A. ARAP1: a point of convergence for Arf and Pho signaling. *Mol. Cell* **9**, 109-119 (2002).

Mohanty, A., Luo, A., DeBlasio, S., Ling, X., Yang, Y., Tuthill, D.E., Williams, K.E., Hill, D., Zadrozny, T., Chan, A., Sylvester, A., and Jackson, D. Advancing cell biology and

functional genomics in maize using fluoresecent protein-tagged lines. *Plant Physiol.* **149**, 601-605 (2009).

Mosavi, L.K., Cammett, T.J., Desrosiers, D.C., and Peng, Z-Y. The ankyrin repeat as molecular architecture for protein recognition. *Protein Sci.* **13**, 1435-1448 (2004).

Neuffer, M.G., and Sheridan, W.F. Defective kernel mutants of maize. *I. Genetic and lethality studies*. *Genetics* **95**, 929-944 (1980).

Nie, Z., Boehm, M., Boja, E.S., Vass, W.C., Bonifacino, J.S., Fales, H.M., and Randazzo, P.A. Specific regulation of the adaptor protein complex AP-3 by the Arf GAP AGAP1. *Dev. Cell* **5**, 455-463 (2003).

Nie, Z., and Randazzo, P.A. Arf GAPs and membrane traffic. *J. Cell Sci.* **119**, 1203-1211 (2006).

Olsen, O-A. Endosperm development: cellularization and cell fate specification. *Annu. Rev. Plant Physiol. Plant Mol. Biol.* **52**, 233-267 (2001).

Opsahl-Ferstad, H-G., Le Deunff, E., Dumas, C., and Rogowsky, P.M. *ZmEsr*, a novel endosperm-specific gene expressed in a restricted region around the maize embryo. *Plant J.* **12**(1)**,** 235-246 (1997).

Poethig, R.S., Coe Jr., E.H., and Johri, M.M. Cell lineage patterns in maize embryogenesis: A clonal analysis. *Developmental Biol.* **117**, 392-404 (1986).

Prescott, A., and Martin, C. A rapid method for the quantitative assessment of levels of specific mRNAs in plants. *Plant Mol. Biol. Reporter* **4**(4), 219-224 (1987).

Randazzo, P.A., and Hirsch, D.S. Arf GAPs: multifunctional proteins that regulate membrane traffic and actin remodeling. *Cell Signal* **16**, 401-413 (2004).

Reisen, D., and Hanson, M.R. Association of six YFP-myosin XI-tail fusions with mobile plant cell organelles. *BMC Plant Biol* **7**, (2007).

Robertson, D.S. Characterization of a Mutator system in maize. *Mutat. Res.* **51**, 21-28 (1978).

Ruzin, S.E. Plant Microtechnique and microscopy. Oxford University Press, New York, New York, USA, 1999.

Samaj, J., Readm N.D., Volkmann, D., Menzel, D., and Baluska, F. The endocytic network in plants. *Trends Cell Biol.* **15**(8), 425-433 (2005).

Scanlon, M.J., Stinard, P.S., James, M.G., Myers, A.M., and Robertson, D.S. Genetic analysis of 63 mutations affecting maize kernel development isolated from Mutator stocks. *Genetics* **136**, 281-294 (1994).

Scanlon, M.J. and Myers, A.M. Phenotypic analysis and molecular cloning of *discolored-1* (*dsc1*) a maize gene required for early kernel development. *Plant Mol. Biol.* **37**, 483-493 (1998).

Scheffzek, K., Ahmadian, M.R., and Wittinghofer, A. GTPase-activating proteins: helping hands to complement an active site. *Trends Biochem. Sci.* **23**(7), 257-262 (1998).

Schel, J.H.N., Kieft, H., and Van Lammeren A.A.M. Interactions between embryo and endosperm during early developmental stages of maize caryopses (*Zea mays*). *Can. J. Bot.* **62**, 2842-2853 (1984).

Schnable, P.S., *et al.,* The B73 maize genome: complexity, diversity, and dynamics. *Science* **326**, 1112-1115 (2009).

Sekhon, R.S., Haining, L., Childs, K.L., Hansey, C.N., Buell, C.R., de Leon, N., and Kaeppler, S.M. Genome-wide atlas of transcription during maize development. *Plant J.* **66**, 553-563 (2011).

Sen, T.Z. *et al.,* MaizeGDB becomes 'sequence-centric' *Database.* 2009:Vol. 2009:bap020.

Shen, B. *et al.,* Expression of *ZmLEC1* and *WRI1* increases oil production in maize. *Plant Phys.* **153**, 980-987 (2010).

Sieburth, L.E., Muday, G.K., King, E.J., Benton, G., Kim, S., Metcalf, K.E., Myers, L., Seamen, E., and Van Norman, J.M. SCARFACE encodes an ARF-GAP that is required form normal auxin efflux and vein patterning in Arabidopsis. *Plant Cell* **18**(6), 1396-1411 (2006).

Smith, L.G., Greene, B., Veit, B., and Hake, S. A dominant mutation in the maize homeobox gene, Knotted-1, causes its ectopic expression in leaf cells with altered fates. *Development* **116**, 21-30 (1992).

Smith, L.G., Jackson, D., and Hake, S. Expression of *knotted1* marks shoot meristem formation during maize embryogenesis. *Developmental Genet.* **16**, 344-348 (1995).

Steinmann, T., Geldner, N., Grebe, M., Mangold, S., Jackson, C.L., Paris, S., Galweiler, L., Palme, K., Jurgens, G. Coordinated polar localization of auxin efflux carrier PIN1 by GNOM ARF GEF. *Science* **286**, 316-318 (1999).

Takai, Y., Sasaki, T., and Matozaki, T. Small GTP-binding proteins. *Physiol. Rev.* **81**, 153-208(2001).

Thompson, R.D., Hueros, G., Becker, H., and Maitz, M. Development and functions of seed transfer cells. *Plant Sci.* 160, 775-783 (2001).

Vernoud, V., Horton, A.C., Yang, Z., and Nielsen, E. Analysis of the small GTPase gene superfamily of Arabidopsis. *Plant Physiol.* **131**, 1191-1208 (2003).

Wisniewska, J., Xu, J., Seifertova, D., Brewer, P.B., Ruzixka, K., Blilou, I., Rouquie, D., Benkova, E., Schere, B., Friml, J. Polar PIN localization directs auxin flow in plants. *Science* **312**, 883 (2006).

Young, T.E., and Gallie, D.R. Programmed cell death during endosperm development. *Plant Mol. Biol.* **44**, 283-301 (2000).

Zhang, X. *et al.,* Laser microdissection of narrow sheath mutant maize uncovers novel gene expression in the shoot apical meristem. *PLoS Genet.* **3**(6), e101 (2007).

CHAPTER 4

Summary

The mature maize kernel is a single-seeded fruit that contains the following structures: the embryo, which will give rise to all vegetative structures of the seedling; the endosperm, which constitutes the bulk of the kernel (~85%); and three maternally derived structures (the pericarp, the pedicel, and the placenta), which are necessary for kernel development. Performing both genomic and genetic analyses contributes toward advances in kernel development.

Transcriptomic analyses of shoot apical meristem (SAM) ontogeny were performed to gain an understanding of how a meristem forms during the landmark stages in mazie embryo development. The SAM, which is responsible for producing all above-ground vegetative structures of the plant, has two functions: (1) to maintain a stem cell population; and (2) to initiate lateral organs. Analysis of transcript accumulation before and after a meristem forms identified *Zea mays YABBY16* (*ZYB16*), a gene implicated to function in lateral organ initiation that was first described and analyzed during this dissertation research. Accumulation of *ZYB16* transcripts before accumulation of those for the meristem marker *KNOTTED1* (*KN1*; Smith *et al.,* 1992; Smith *et al.,* 1995; Jackson *et al.*, 1994) suggests that in the maize SAM lateral organ initiation precedes the onset of stem cell maintenance. Transcriptomic analysis of a newly formed transition-staged SAM reveals that the embryo is still establishing apical and basal domains, and is predominantly involved in protein and DNA synthesis and metabolite production, preceding the proliferative growth that characterizes later stages of embryogenesis. In contrast, a mature L14 stage meristem initiating foliar leaves accumulates additional transcripts that function in transcriptional regulation; hormone signaling and metabolism; and transport. Examination of transcript

accumulation in the first three lateral organs elaborated during embryogenesis (the scutellum, the coleoptile, and the first foliar leaf) provides support that the maize cotyledon is a leaf-like bimodal structure comprising both the scutellum and the coleoptile, as previously hypothesized by Kaplan (1996). Finally, the three-way comparison between the initiation of juvenile, adult, and husk leaves indicate distinctive differences in the primordial stages of development for these three lateral organ types. Furthermore, this comparison reveals that genetic mechanisms operate between the SAM and the lateral meristem. The transcriptional data from the six stages of maize SAM development are publicly released for use in future studies (Sen *et al.,* 2009).

This study also identified novel transcriptional markers of the key events in maize embryogenesis. Two previously undescribed transcripts of unknown function, in addition to *ZYB16*, are specific for lateral organs. Cotyledon-specific (*Zea mays LEAFY COTYLEDON1*), scutellum-specific (*TAPETUM DETERMINANT1-LIKE*), coleorhiza-specific (*POLLEN OLE E I-like*), and vasculature-specific (*RAN-BINDING PROTEIN2*) markers are also identified in this study. Furthermore, three lipid transfer protein transcripts provide molecular markers for the protoderm and protoderm-derived tissues in the embryo and seedling. Finally, two new transcripts are described (*Arabidopsis LIGHT-DEPENDENT SHORT HYPOCOTYLS1* and *Oryza LONG STERILE LEMMA1*) that demarcate the boundaries between the SAM and initiating lateral organs.

The transcriptomic survey of maize SAM ontogeny is the first step toward identifying genes that function in SAM formation during the elaboration of embryonic lateral organs, in phase-specific leaf initiation, and during meristem-specific stem cell maintenance and lateral organ initiation. One caveat to this transcriptional data set is

that is does not measure accumulation of non-coding small RNAs because a poly(A) RNA amplification method is utilized. Additionally, this method does not provide functional analysis, in that changes in transcription are not always correlated with changes in protein accumulation or function. Therefore, reverse genetics of selected genes that have dynamic transcript accumulation patterns during SAM ontogeny could help to verify predicted and unknown gene functions. Uniform *Mu* and Ac/Ds populations are available to screen for mutations in candidate genes (McCarty *et al.,* 2005; Volbrecht *et al.*, 2010), and stocks are available at the Maize Cooperation Stock Center. Phenotypic analyses of plants with mutations in some of these candidate genes may help to correlate transcript accumulation with protein function during SAM ontogeny.

Genetic analysis of the *defective kernel (dek*) mutant *discolored* (*dsc1*) was performed to understand the contribution of DSC1 function to existing models for embryo and endosperm development. Previous analyses of the recessive *DSC1-R* mutation revealed that in addition to defects in embryo and endosperm development, mutant kernels are embryo lethal (Scanlon *et al.*, 1994; Scanlon and Myers, 1998). Here, phenotypic analyses illustrate that DSC1 is required to maintain differentiated embryo and endosperm structures. Interestingly, despite a delay in development, *dsc1-R* mutant embryo and endosperm structures develop normally prior to tissue degeneration and kernel abortion. Previously, transposon-tagging identified a genomic fragment of the *DSC1* locus (Scanlon and Myers, 1998), and was subsequently used in this study to determine the full length *DSC1* transcript. The *DSC1* full length transcript encodes an ACAP-type ADP-RIBOSYLATION FACTOR GTPase ACTIVATING

PROTEIN (ARF-GAP) implicated in vesicle membrane trafficking. In transient expression assays in *N. benthamiana* leaves, DSC1 co-localizes with the endocytic tracer FM4-64 and the *trans*-Golgi network/early endosome marker mCherry::VTI12 (Geldner *et al.* 2009), and thus is implicated to function in trafficking from the plasma membrane to the *trans*-Golgi network/early endosomes.

Genes that function in cell-to-cell signaling to maintain epidermal patterning of the embryo and the aleurone cell layer of the endosperm include *DEFECTIVE KERNEL1* (*DEK1*); *CRINKLY1* (*CR4*); and *SUPERNUMERY1* (*SAL1*; Becraft *et al.*, 1996; Lid *et al.*, 2002; and Shen *et al.*, 2003). Both *DEK1* and *CR4* encode receptors anchored at the plasma membrane and *SAL1* encodes an E vacuolar sorting protein that functions in vesicle trafficking (Becraft *et al.*, 1996; Lid *et al.*, 2002; and Shen *et al.*, 2003). Given its function in endomembrane trafficking, DSC1 may function downstream of this intercellular signaling pathway, delivering an as yet unknown cargo(s) required to maintain differentiation of embryo and endosperm structures. Future co-localization assays and phenotypic analysis of *dsc1 sal1* double mutants should determine whether or not DSC1 and SAL1 interact in the same endomembrane trafficking pathways.

Several DSC1 paralogs are reported, although it is not yet known if these paralogs perform overlapping functions with DSC1. Genetic analyses of these paralogs may determine whether or not they perform redundant functions during maize kernel development. Furthermore, *dsc1* paralog mutant alleles could be introgressed into the YFP-tagged PIN1a background to determine whether they are required for PIN1a transport. Additionally, co-localization experiments with DSC1 and DSC1 paralogs will determine if they are present in the same membrane compartments. These additional

analyses may determine if DSC1 function is unique during kernel development, or if other ACAP-type ARF-GAPs perform redundant functions with respect to DSC1.

REFERENCES

Becraft, P.W., Stinard, P.S., and McCarty, D.R. CRINKLY4: a TNFR-like receptor kinase involved in maize epidermal differentiation. *Science* 273, 1406-1409 (1996).

Geldner, N., Devervaud-Tendon, V., Hyman, D.L., Mayer, U., Stierhof, Y-D., and Chory, J. Rapid, combinatorial analysis of membrane compartments in intact plants with a multicolor marker set. *Plant J.* **59**, 169-178 (2009).

Jackson, D., Veit, B., and Hake, S. Expression of maize KNOTTED1 related homeobox genes in the shoot apical meristem predicts patterns of morphogenesis in the vegetative shoot. *Development* **120**, 405-413 (1994).

Kaplan, D.R. Early plant development: from seed to seedling to established plant. In *Principles of Plant Morphology, Chapter 5.* Berkeley, CA: Copy Central, University of California, Berkeley, 1996.

Lid, S.E., Gruis, D., Jung, R., Lorentzen, J.A., Ananiev, E., Chamberlin, M., Niu, X., Meeley, R., Nichols, S.E., and Olsen, O-A. The *defective kernel1* (*dek1*) gene required for aleurone cell development in the endosperm of maize grains encodes a membrane protein of the calpain gene superfamily. *Proc. Natl. Acad. Sci. USA* **99,** 5460-5465 (2002).

McCarty, D.R., Settles, A.M., Suzuki, M., Tan, B.C., Latshaw, S., Porch, T., Robin, K., Baier, J., Avigne, W., Lai, J., Messing, J., Koch, K.E., and Hannah, L.C. Steady-state transposon mutagenesis in inbred maize. *Plant J.* **44**, 52-61 (2005).

Scanlon, M.J., Stinard, P.S., James, M.G., Myers, A.M., and Robertson, D.S. Genetic analysis of 63 mutations affecting maize kernel development isolated from Mutator stocks. *Genetics* **136**, 281-294 (1994).

Scanlon, M.J. and Myers, A.M. Phenotypic analysis and molecular cloning of *discolored-1* (*dsc1*) a maize gene required for early kernel development. *Plant Mol. Biol.* **37**, 483-493 (1998).

Sen, T.Z. *et al.,* MaizeGDB becomes 'sequence-centric' *Database.* 2009:Vol. 2009:bap020.

Shen, B., Li, C., Min, Z., Meeley, R.B., Tarczynski, M.C., and Olsen, O-A. *sal1* determines the number of aleurone cell layers in maize endosperm and encodes a class E vacuolar sorting protein. *Proc. Natl. Acad. Sci. USA* **100(**11), 6552-6557 (2003).

Smith, L.G., Greene, B., Veit, B., and Hake, S. A dominant mutation in the maize homeobox gene, Knotted-1, causes its ectopic expression in leaf cells with altered fates. *Development* **116**, 21-30 (1992).

Smith, L.G., Jackson, D., and Hake, S. Expression of *knotted1* marks shoot meristem formation during maize embryogenesis. *Developmental Genet.* **16**, 344-348 (1995).

Volbrecht, E., Duvick, J., Schares, J.P., Ahern, K.R., Deewatthanawong, P., Xu, L., Conrad, L.J., Kikuchi, K., Kubinec, T.A., Hall, B.D., Weeks, R., Unger-Wallace, E., Muszynski, M., Brendel, V.P., and Brutnell, T.P. Genome-wide distribution of transposed *Dissociation* elements in maize. *Plant Cell* **22**(6), 1,667-1,685 (2010).

GLOSSARY

aleurone: the outer most cell layer of the endosperm

alveolus: tube-like wall structure

basal endosperm transfer layer (BETL): endosperm structure that forms over the vasculature of the maternal chalazal zone

caryopsis: single-seeded fruit where the pericarp is fused to the seed coat

chalaza: the basal part of an ovule or a seed where the integuments are fused to the nucellus

coleoptile: a bi-keeled leaf-like organ that forms a sheath surrounding the shoot apical meristem and embryonic foliar leaves

coleorhiza: a sheath that surrounds the root

embryo surrounding region (ESR): endosperm structure that forms a cavity wherein the proembryo develops

endoreduplication: when cells replicate nuclear DNA without chromatin condensation, chromatid separation, or cytokinesis

pedicel: a stalk that supports a single inflorescence

phragmoplast: central region of the mitotic spindle where vesicles gather to form the cell plate

quiescent center: progenitor of root stem cells

quiescence: dormancy

scutellum: first lateral organ initiated during embryogenesis with controversial homology

starchy endosperm: endosperm structure that constitutes the bulk of the kernel and stores energy reserves in the form of starch and prolamin proteins

stereotypical patterns of cell divisions: defined cell divisions

syncytium: a single cell with multiple nuclei formed by mitotic divisions without cytokinesis